

Characterisation of Sustainable Materials for Can Making

Emily Holding

Swansea University

Submitted to Swansea University in fulfilment of the
requirements for the Degree of Doctor of Engineering

2025



Engineering and
Physical Sciences
Research Council



Declarations

This work has not previously been accepted in substance for any degree and is not being concurrently submitted in candidature for any degree.

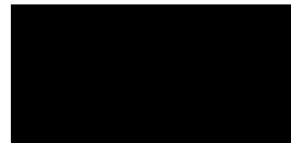
Signed:



Date: 15th January 2025

This thesis is the result of my own investigations, except where otherwise stated. Other sources are acknowledged by footnotes giving explicit references. A bibliography is appended.

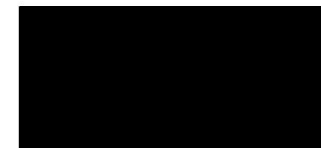
Signed:



Date: 15th January 2025

I hereby give consent for my thesis, if accepted, to be available for electronic sharing

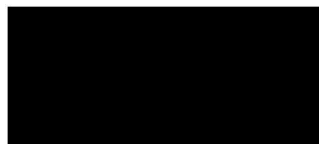
Signed:



Date: 15th January 2025

The University's ethical procedures have been followed and, where appropriate, that ethical approval has been granted.

Signed:



Date: 15th January 2025

Acknowledgements

I would like to sincerely thank everyone for their time, help and support throughout my research and academic work. Your contributions have helped me achieve something I never thought I would do.

Firstly, I would like to thank my academic supervisor Dr Eifion Jewell for all of your support, advice and knowledge during the last four years. Without your positive attitude and guidance, I don't think my research would be what it is today. You really are the best supervisor I could have asked for. Thank you!

To everyone at Baglan PMRC who has listened to me complain about being tired and de-motivated, given advice and provided training, thank you. I would also like to thank my industrial supervisors Samson Patole and Lynsey Jones for helping to guide my research and for reviewing countless presentations along the way.

Finally, I would like to thank my family and friends. In particular my husband Jon, my mum Sarah, Stepdad Mike and my in-laws Veronica and Mike for their support and help. Also, to my brother Sam for his constant jokes and dancing to lighten the mood. You have all helped keep me motivated and supported me in this long journey. I really appreciate how much you have helped to look after Grace while I took the time to complete my research and write this thesis. Your continuous support, guidance and praise has got me to this point in my career and I am so thankful for you all.

My thanks would not be completed without mentioning my daughter Grace whom has changed my life albeit made thesis writing a lot more difficult. If you had told me five years ago that I would be trying to juggle thesis writing, a new job and looking after a one-year-old I would have laughed and asked who would be crazy enough to attempt that.

Abstract

REACH legislation banning the use of Cr(VI) (hexavalent chromium) in can making initiated a drive to develop safer, more sustainable alternatives. TATA steel developed TCCT, as an alternative to ECCS (Electrolytic Chromium Coated Steel) substrates produced using Cr(VI) electroplating baths. The added requirement to remove BPA (Bisphenol A) from food contact materials means that the EP (Epoxy Phenolic) lacquer that is currently used must be replaced with a BPA free alternative, BPANI (Bisphenol A Non-Intent). Both TCCT and BPANI have been characterised using various mechanical and analytical techniques throughout this work.

Simulant concentration, substrate surface condition and CrOx (chromium oxide) weight are key influencers on material performance. A CrOx weight of 9-11 mg m⁻² is optimal. Water uptake by BPANI is a mechanical rather than chemical mechanism. EP and BPANI are both effective at providing corrosion protection for the underlying substrate.

Newer TCCT generations perform similarly to ECCS at lower uniaxial strain. The performance of all substrate types was similar at high strain. At high NaCl concentrations the simulant concentration is the primary influencer over material performance as opposed to strain. The change in surface condition due to strain was more significant for ECCS than TCCT.

A method was developed to induce and quantify biaxial strain and test lacquer adhesion. Biaxial strain is more detrimental to the substrate than uniaxial strain. Oxide pin hole identification confirmed that an increase in strain exposes more free metal. A correlation between an increase in copper percentage and a decrease in failure force confirmed that surface condition influences lacquer adhesion.

TCCT performance has improved with newer generations. It was concluded that based on the performance of TCCT being similar to ECCS under strain, that the novel TCCT substrate was suitable for use in the can shaping process. Retort and corrosion tests have also demonstrated the suitability of newer TCCT substrate generations for can making applications. The novel BPANI lacquer is heavily influenced by food simulant and retort conditions, more so than the commercially established EP lacquer.

Performance of newer generation TCCT generations is acceptable providing the lacquer covers any surface defects and an adequate CrOx layer is present.

Contents

| | |
|--|----|
| List of Figures..... | 10 |
| List of Tables | 14 |
| List of Equations | 15 |
| Nomenclature..... | 16 |
| 1 Introduction..... | 18 |
| 1.1 Project Background and Rationale..... | 18 |
| 1.2 Aims and Objectives | 19 |
| 1.3 Thesis Outline | 19 |
| 2 Literature Review..... | 22 |
| 2.1 Overview | 22 |
| 2.2 Steel packaging markets..... | 22 |
| 2.3 Impact of legislation on packaging | 23 |
| 2.4 Can making substrates..... | 24 |
| 2.4.1 Tinplate | 24 |
| 2.4.2 ECCS..... | 25 |
| 2.4.3 TCCT | 27 |
| 2.5 Organic Coatings..... | 28 |
| 2.5.1 Epoxy phenolic..... | 28 |
| 2.5.2 Polyester..... | 30 |
| 2.6 Can manufacture | 30 |
| 2.6.1 Metal cans | 30 |
| 2.6.2 Two-piece cans..... | 31 |
| 2.6.3 Three-piece cans..... | 31 |
| 2.6.4 Can Ends | 32 |
| 2.7 Theories of Adhesion | 33 |
| 2.7.1 Mechanical Adhesion Theory | 33 |
| 2.7.2 Adsorption Theory | 34 |
| 2.7.3 Chemical bonding | 34 |
| 2.7.4 Diffusion | 34 |
| 2.7.5 Electrostatic forces | 35 |
| 2.8 Adhesion of coated steel packaging..... | 35 |

| | | |
|--------|---|----|
| 2.8.1 | Wet and Dry Adhesion..... | 35 |
| 2.8.2 | Lacquer Performance | 36 |
| 2.8.3 | Scratch Testing..... | 37 |
| 2.8.4 | Spring-Loaded Pen Hardness Testing..... | 38 |
| 2.8.5 | Adhesive Tape Testing..... | 39 |
| 2.9 | Material properties | 40 |
| 2.9.1 | Hardness | 40 |
| 2.9.2 | Stress and Strain..... | 40 |
| 2.9.3 | Strain in Food Cans..... | 41 |
| 2.9.4 | Corrosion..... | 43 |
| 2.10 | Food Canning and Cooking | 44 |
| 2.10.1 | Food Canning | 44 |
| 2.10.2 | Heat treatment and sterilisation..... | 45 |
| 2.10.3 | Storage and Shelf-life..... | 45 |
| 2.10.4 | Recyclability | 46 |
| 2.11 | Lacquer Interface Failure Mechanisms..... | 46 |
| 2.11.1 | Migration Testing..... | 46 |
| 2.11.2 | Surface Topography | 47 |
| 2.12 | Conclusions | 48 |
| 3 | Materials and Methodology | 51 |
| 3.1 | Materials..... | 51 |
| 3.1.1 | Steel Substrates | 51 |
| 3.1.2 | Organic Lacquers | 52 |
| 3.1.3 | Simulant Solutions | 53 |
| 3.2 | Methodology | 54 |
| 3.2.1 | Substrate lacquering and curing..... | 54 |
| 3.2.2 | Sample Preparation | 56 |
| 3.2.3 | Retort..... | 57 |
| 3.2.4 | Scratch Testing..... | 59 |
| 3.3 | FTIR-ATR Spectroscopy | 61 |
| 3.4 | Filiform Corrosion Study | 63 |
| 3.4.1 | FFC Materials | 63 |
| 3.4.2 | FFC method..... | 65 |
| 3.4.3 | FFC Area Analysis..... | 66 |
| 3.5 | Uniaxial Strain | 67 |

| | | |
|-------|--|-----|
| 3.5.1 | Dog Bone Samples | 67 |
| 3.5.2 | Hounsfield Tensile Tester | 67 |
| 3.5.3 | SEM | 69 |
| 3.6 | Surface Metal Identification..... | 69 |
| 3.7 | Conclusion | 71 |
| 4 | The Influence of Food Simulant Concentration and CrOx Weight on Lacquer and Substrate Performance Pre- and Post-Retort | 73 |
| 4.1 | Introduction | 73 |
| 4.2 | Materials and Methodology | 76 |
| 4.3 | Multi-simulant testing | 76 |
| 4.3.1 | Dry Adhesion | 76 |
| 4.3.2 | DI Water | 78 |
| 4.3.3 | Citric Acid, Cysteine and NaCl..... | 78 |
| 4.3.4 | CrOx Weight | 79 |
| 4.4 | Varying Concentration of Salt Solution and CrOx Weight | 81 |
| 4.4.1 | DI Water/Salt | 82 |
| 4.4.2 | CrOx Coating Weight | 83 |
| 4.4.3 | Additional factors influencing adhesion | 84 |
| 4.5 | Spectroscopic Analysis of the Influence of Salt Concentration on the Level of Water Uptake in BPANI Lacquers | 85 |
| 4.5.1 | Simulant Influence | 87 |
| 4.5.2 | CrOx Weight | 89 |
| 4.5.3 | Other effects | 91 |
| 4.6 | FFC Study | 91 |
| 4.6.1 | Initiation of FFC using 2.5×10^{-3} FeCl ₂ | 92 |
| 4.6.2 | Initiation of FFC using 0.01M FeCl ₂ | 94 |
| 4.7 | Numerical analysis of FFC area | 96 |
| 4.7.1 | PVB | 96 |
| 4.7.2 | EP and BPANI | 99 |
| 4.7.3 | Cathodic delamination by Sodium Cations..... | 99 |
| 4.8 | Conclusion | 100 |
| 5 | The Impact of Uniaxial Strain on Chromium Coated Steel Substrates Used in Can Making..... | 103 |
| 5.1 | Introduction | 103 |
| 5.2 | Uniaxially Strained Substrates | 105 |
| 5.2.1 | Adhesion of Lacquers to Strained Samples Post-Retort | 105 |

| | | |
|-------|--|-----|
| 5.2.2 | TCCT | 106 |
| 5.2.3 | ECCS..... | 107 |
| 5.2.4 | The effect of a NaCl simulant on adhesion..... | 107 |
| 5.3 | SEM analysis of unlacquered TCCT and ECCS Samples at 0,5 and 15% Strain | 108 |
| 5.4 | Conclusion | 116 |
| 6 | Method Development and Analysis of Biaxially Strained Can Making Substrates | 118 |
| 6.1 | Introduction..... | 118 |
| 6.2 | Method Development..... | 120 |
| 6.2.1 | Reference Scale..... | 121 |
| 6.2.2 | Strain/Dome Height Calibration | 123 |
| 6.2.3 | Biaxial Strain Analysis..... | 124 |
| 6.3 | A Systematic Study Comparing Failure Forces Values Obtained from Scratch Testing and a Spring-Loaded Hardness Pen | 125 |
| 6.3.1 | Converting Hardness Pen Failure Force to Scratch Test Failure Force | 127 |
| 6.3.2 | Comparing Uniaxial versus Biaxial Failure Forces | 128 |
| 6.4 | Biaxial Strain..... | 132 |
| 6.4.1 | Dry Adhesion | 132 |
| 6.4.2 | Lacquer Adhesion Post-Retort in DI Water..... | 134 |
| 6.4.3 | Lacquer Adhesion Post-Retort in 0.1% NaCl | 135 |
| 6.5 | Oxide Pin Hole Identification using a Preece Test as a Way to Quantify Free Iron and Chromium on a Substrate Surface | 137 |
| 6.5.1 | Keyence Imaging and Area analysis..... | 137 |
| 6.5.2 | Failure Force and Non-CrOx Coated Area | 140 |
| 6.6 | Theory of Coating Inhomogeneity | 141 |
| 6.6.1 | Validating the Theory of Coating Inhomogeneity | 143 |
| 6.7 | Conclusions | 148 |
| 7 | Conclusions | 151 |
| 8 | Recommendations for Future Work..... | 156 |
| 9 | Appendix 1 - Publications..... | 159 |
| 10 | References | 161 |

List of Figures

| | |
|--|----|
| Figure 2.1 Structural diagram of ECCS (4,12) | 26 |
| Figure 2.2 Structural Diagram of TCCT (4,12) | 28 |
| Figure 2.3 A schematic to show the DRD and DWI processes for forming two-piece cans (57)..... | 31 |
| Figure 2.4 A schematic showing the three piece can manufacturing process used for tinplate (57)..... | 32 |
| Figure 2.5 A diagram of the end design of a food packaging can (60)..... | 32 |
| Figure 3.1 An RK-K Control bar coater used for lacquering steel | 55 |
| Figure 3.2 Labelled schematic of the bar/substrate/lacquer interaction that occurs during use of the Meyer bar coater (122)..... | 56 |
| Figure 3.3 THIEME KPX drying oven used for curing the BPANI and EP lacquers | 56 |
| Figure 3.4 a) A 120 x 40mm EP lacquered sample of TCCT b) Sample with epoxy coated edges | 57 |
| Figure 3.5 Labelled image of the Certoclav Multicontrol 2 autoclave used for retort processes | 57 |
| Figure 3.6 Temperature and pressure data for the validation of the Certoclav MultiControl 2 retort apparatus used for this research..... | 58 |
| Figure 3.7 Sample loading and inside of the retort apparatus..... | 59 |
| Figure 3.8 Labelled schematic of the inside of the retort vessel..... | 59 |
| Figure 3.9 Labelled image of the sheen automatic scratch tester BS3359 used to establish failure forces of the samples post-retort..... | 60 |
| Figure 3.10 Schematic showing how the scratch test is performed (123) | 61 |
| Figure 3.11 Labelled schematic showing total internal reflectance of an IR beam within an ATR crystal (129) | 62 |
| Figure 3.12 Perkin Elmer FTIR Spectrometer used for sample analysis..... | 63 |
| Figure 3.13 Diagram showing the set-up of a FFC experimental study | 65 |
| Figure 3.14 Example image showing the selection of the corroded sample area for numerical analysis using ImageJ..... | 66 |
| Figure 3.15 A dog bone sample with dimensions outlined..... | 67 |
| Figure 3.16 The Hounsfield tensile tester used for straining the TCCT/ECCS samples, maximum load of 25 kN | 68 |

| | |
|---|----|
| Figure 3.17 Filtered image of a TCCT sample showing how the surface copper was measured in Image J..... | 70 |
| Figure 4.1 Dry adhesion of BPANI and EP lacquers to ECCS and TCCT substrates | 76 |
| Figure 4.2 Failure force of EP coated TCCT after retort in various food simulants . | 77 |
| Figure 4.3 Failure force of BPANI coated TCCT after retort in various food simulants | 78 |
| Figure 4.4 Failure forces for EP lacquer on different CrOx weight TCCT and ECCS substrates in varying concentrations of salt solution..... | 81 |
| Figure 4.5 Failure forces for BPANI lacquer on different CrOx weight TCCT and ECCS substrates in varying concentrations of salt solution..... | 82 |
| Figure 4.6 FTIR spectrum for samples of 4.2 mg m ⁻² CrOx weight (Batch 74) TCCT Pre- and post-retort..... | 86 |
| Figure 4.7 FTIR spectrum for samples of 9.4 mg m ⁻² CrOx weight (Batch 56) TCCT Pre- and post-retort..... | 86 |
| Figure 4.8 FTIR spectrum for samples of 12.5 mgm ⁻² CrOx weight (Batch 64) TCCT Pre- and post-retort..... | 87 |
| Figure 4.9 Change in Transmittance of O-H Bending Peaks at 3600cm ⁻¹ with CrOx Weight and Salt Concentration for TCCT Substrates | 88 |
| Figure 4.10 Images comparing the visible differences in the coatings on 120 x 40mm samples post-retort on different CrOx weight batches of TCCT. | 89 |
| Figure 4.11 Lacquer Delamination for Low and High CrOx Weight Substrates..... | 90 |
| Figure 4.12 FFC images of EP coated samples over a 7-week period..... | 92 |
| Figure 4.13 FFC images of BPANI coated samples over a 7-week period | 93 |
| Figure 4.14 FFC images of corrosion of samples with 0.01M FeCl ₂ over a 10-week and 21-week period | 94 |
| Figure 4.15 Close-up images of PVB coated ECCS and TCCT after 22 weeks of FFC corrosion experiment..... | 95 |
| Figure 4.16 The change in FFC area over time for various EP/BPANI/PVB coated ECCS and TCCT substrate..... | 96 |
| Figure 4.17 The total corroded area of TCCT for each CrOx weight/coating combination after 22 weeks | 98 |
| Figure 4.18 The total corroded area of each TCCT substrate lacquered with EP and BPANI after 22 weeks | 98 |

| | |
|---|-----|
| Figure 5.1 The influence of strain on BPANI lacquer adhesion post-retort in water | 105 |
| Figure 5.2 The influence of strain on BPANI lacquer adhesion post-retort in 1% NaCl | 106 |
| Figure 5.3 SEM images of ECCS 9 mg m ⁻² CrOx weight surfaces from left to right: no strain, 5% strain, 15% strain. The green circle indicates Lüder bands | 108 |
| Figure 5.4 SEM images of TCCT 2019 13.2 mg m ⁻² CrOx weight surfaces from left to right: no strain, 5% strain, 15% strain. The green circle indicates Lüder bands.. | 109 |
| Figure 5.5 SEM images of TCCT 2019 4.2 mg m ⁻² CrOx weight surfaces from left to right: no strain, 5% strain, 15% strain..... | 110 |
| Figure 5.6 SEM images of TCCT 2019 9.5 mg m ⁻² CrOx weight surfaces from left to right: no strain, 5% strain, 15% strain. The yellow squares indicate the apparent change in depth of the Lüder bands as strain is increased. | 111 |
| Figure 5.7 SEM images of TCCT 2021 11.3 mg m ⁻² CrOx weight surfaces from left to right: no strain, 5% strain, 15% strain..... | 112 |
| Figure 5.8 Force-Displacement graph for 15% nominal strain of TCCT 2021 substrate..... | 113 |
| Figure 6.1 Erichsen cupping apparatus used for biaxially straining samples | 120 |
| Figure 6.2 Schematic of the Erichsen Cupping Apparatus Operation (160)..... | 121 |
| Figure 6.3 An example of the strained samples used with a reference grid..... | 122 |
| Figure 6.4 ImageJ measurements taken to calculate conversion factors | 122 |
| Figure 6.5 Calibration curve representing strain values that correspond to Erichsen dome heights | 124 |
| Figure 6.6 Spring-loaded hardness pen with components labelled (80) | 125 |
| Figure 6.7 A scatter plot of failure forces for scratch testing versus hardness pen.. | 127 |
| Figure 6.8 Uniaxial and biaxial failure forces for BPANI Coated ECCS and TCCT substrates a) pre-retort and b) post-retort in DI Water plotted against percentage strain..... | 128 |
| Figure 6.9 Comparing uniaxial and biaxial failure force results for BPANI coated TCCT Samples Pre-Retort | 130 |
| Figure 6.10 Biaxial strain versus failure force for EP coated TCCT and ECCS samples under dry conditions..... | 132 |
| Figure 6.11 Biaxial strain versus failure force for BPANI coated TCCT and ECCS samples under dry conditions..... | 133 |

| | |
|--|-----|
| Figure 6.12 A graph of biaxial strain versus failure force for EP coated TCCT and ECCS samples retorted in DI Water | 134 |
| Figure 6.13 A graph of biaxial strain versus failure force for BPANI coated TCCT and ECCS samples retorted in DI Water..... | 134 |
| Figure 6.14 Biaxial strain versus failure force for EP coated TCCT and ECCS samples retorted in 0.1% NaCl..... | 135 |
| Figure 6.15 Biaxial strain versus failure force for BPANI coated TCCT and ECCS samples retorted in 0.1% NaCl..... | 136 |
| Figure 6.16 a) to f) Keyence images of copper deposits on biaxially strained samples of unlacquered TCCT..... | 138 |
| Figure 6.17 The percentage area of copper deposits on a substrate surface at different strain values on various TCCT and ECCS substrates | 139 |
| Figure 6.18 Failure Force versus Copper% for BPANI Coated TCCT and ECCS Substrates | 140 |
| Figure 6.19 Diagrams showing the proposed mechanisms of coating inhomogeneity on steel can making substrates | 141 |

List of Tables

| | |
|--|-----|
| Table 3.1 Batch specific information for each substrate of TCCT or ECCS used throughout this research | 52 |
| Table 3.2 Food simulants use for this research, their composition and chemical information..... | 53 |
| Table 3.3 Chemicals used to produce materials for the FFC studies | 63 |
| Table 3.4 Instrument Calibration Parameters for Sample Straining | 67 |
| Table 3.5 Chemical constituents used to produce the Copper Sulfate solution | 70 |
| Table 6.1 Comparison of Analytical Techniques for Surface Analysis of Chromium Coated Steel Substrates | 144 |

List of Equations

| | |
|--|-----|
| (2.1) Newton's Second Law of Motion..... | 38 |
| (3.1) Standard Error | 60 |
| (6.1) Error in Strain Measurement | 122 |
| (6.2) Calculate Percentage Strain..... | 123 |
| (6.3) Convert Hardness Pen Failure Force into Scratch Test Failure Force | 128 |

Nomenclature

| Abbreviation | Definition |
|--------------|--|
| BPA | Bisphenol-A |
| BPANI | Bisphenol A Non-Intent |
| Cr(III) | Trivalent Chromium |
| Cr(VI) | Hexavalent Chromium |
| CrOx | Chromium Oxide |
| ECCS | Electro-Chromium Coated Steel |
| EP | Epoxy Phenolic |
| FFC | Filiform Corrosion |
| IE | Erichsen Index |
| NaCl | Sodium Chloride |
| REACH | Registration, Evaluation, Authorisation and restriction of Chemicals |
| SEM | Scanning Electron Microscopy |
| TCCT | Trivalent Chromium-Coating technology |

Chapter 1

Introduction

1 Introduction

1.1 Project Background and Rationale

The value of the worldwide metal packaging market in 2024 was £118 billion and is estimated to rise to £141 billion by 2029 (1). Metal food packaging has been in use since the early 1800's, when tin coated steel cans were patented and supplied to the navy for commercial use (2). Since their introduction commercially, the use of metal packaging has soared, currently accounting for 12% of the food packaging industry (3). Unlike other packaging types, metal packaging enables food to be stored without the need for refrigeration, due to the sterilisation process the food is subjected to after it has been sealed within the can.

There are various types of metal packaging in use, but two types predominate the steel packaging industry, ECCS (Electro-Chromium Coated Steel) and tinplate (4). Initially the use of tinplate dominated the metal packaging market but began to be phased out due to limited amount of tin resources (5). Its replacement was ECCS, a hexavalent chromium coated substrate. The introduction of the REACH (Registration, Evaluation, Authorisation and restriction of Chemicals) legislation, in 2003 which banned the use of hexavalent chromium in can making prompted the development of alternative packaging methods (6). TCCT (Trivalent Chromium Coating Technology) was developed by TATA Steel as an alternative to ECCS. Since the commencement of this research and the introduction of REACH legislation the UK left the EU and as such packaging materials supplied to the UK market do not have to be REACH compliant. Despite this food cans must still comply with this legislation if UK businesses are to continue supplying food cans to the EU. In addition to REACH there is also legislation requiring the removal of BPA (Bisphenol-A) from food contact materials. BPA is found in the EP (Epoxy Phenolic) lacquers that are currently used as a barrier between the internal side of the food can and the food. As such EP lacquers have been replaced by polyester lacquers.

TCCT has shown promise from initial studies but its performance, when subjected to abnormalities during can making, sterilisation and food storage, is unknown. In addition to this the BPANI lacquer as an alternative to EP has limited research into its use. The overall aim of this research is to characterise the substrate surface using various mechanical and analytical techniques to provide a comprehensive picture of

the lacquer and substrate performance of both commercially available and developmental materials. The intention is to characterise the substrate not only in its unstrained state but after uniaxial and biaxial deformation. This is so testing can more accurately reflect the behaviour of a food can during production and use.

1.2 Aims and Objectives

1. Quantify the performance of the latest generation of Cr(III) coated steels and contrast these to the performance of the incumbent Cr(IV) steels.
2. Evaluate the impact of can processing steps on the performance.
3. Understand the underlying mechanisms which relate the surface characteristics to can performance
4. Enhance the suite of tests which can be used to evaluate the likely performance of any Cr coated substrate prior to can making
5. Recommended limits of performance and likely can failure mechanisms with new materials

1.3 Thesis Outline

Following a review, the latest research is discussed in depth in *Chapter 2 ‘Literature Review’*. It gives an overview of the current and historical research in the field related to this thesis and a justification of the methods adopted throughout. *Chapter 3 ‘Materials and Methodology’* gives a description of the materials and method used throughout the study.

The first set of results is captured within *Chapter 4* which is titled ‘*The Influence of Food Simulant Concentration and CrOx Weight on Lacquer and Substrate Performance Pre- and Post-Retort*’. The aim of this section is to perform initial adhesion studies using common food simulants and investigate further the food stuff that has the greatest influence over lacquer adhesion. Additional studies such as water uptake and corrosion will be conducted to further understand how other factors such as humidity, temperature and pressure influence the lacquer/substrate.

Chapter 5 focuses on ‘*The Impact of Uniaxial Strain on Chromium Coated Steel Substrates Used in Can Making*’. The intention of this research is to study the effects of uniaxial strain on the substrate performance both pre- and post-retort when used in conjunction with a lacquer. Part of this experimentation will also be to study the surface in more detail to understand the surface changes resulting from uniaxial strain.

The final piece of research in Chapter 6 details '*Method Development and Analysis of Biaxially Strained Can Making Substrates*'. This chapter will contain an initial method development stage where the aim is to establish a method to biaxially strain coated TCCT and ECCS substrates and subsequently adhesion test them. It is important to establish if uniaxial and biaxial strain is equivalent at the same numerical value and to see if these can be interchanged. The final part of the chapter will look at using an oxide pin hole identification technique for quantifying free metal on the substrate surface.

The intention of this research is to conclude whether TCCT and BPANI are suitable replacements for ECCS and EP in can making. The work to be conducted based on unstrained, uniaxial and biaxial performance in addition to changing other processing parameters should provide a comprehensive picture of the materials performance under can making and food sterilisation processes.

Chapter 2

Literature Review

2 Literature Review

2.1 Overview

Extensive literature exists detailing research into the extent and effects of leaching from can coatings into the foodstuffs stored within them, however, little research has been conducted to analyse the consequence that the foodstuff can have on the chemistry of the can. (7–11) Examples of existing research on the effect of foodstuffs on the chemistry of the can include: BPANI lacquer performance post-retort (12); pre- and post-retort performance of ECCS and TCCT and organic lacquers (8) and the impact of different foodstuffs on lacquer adhesion (9). This literature review aims to give an overview of the packaging materials available on the market; how they are manufactured; and their uses. Their advantages and disadvantages will also be compared and contrasted, and alternative packaging materials will be discussed in depth. In addition to this the current and developmental lacquer material will be explored. Physical and analytical testing methods for assessing the performance of the developmental materials against the approved market materials will be extensively reviewed.

2.2 Steel packaging markets

The value of the metal packaging market in 2024 was £60.5 billion and is estimated to rise to £73.1 billion by 2026 (1). Metal packaging is desirable for food storage applications due to it being recyclable in addition to its long-term food storage capabilities. There are two types of coated steel that predominate the steel packaging industry, ECCS and tinplate (4). Tinplate, one of the first packaging materials, was developed in the 1800s as a method for food preservation (13). Initially, tinplate dominated the food packaging industry, however, it was and is still not known how long the finite resources will last (5). There are also higher costs associated with tinplate production compared with alternative coating materials as several micron thick tin deposits are required (14). Therefore, it was deemed necessary to develop an alternative to tinplate that was able to withstand all the manufacturing conditions to which it would be subjected, in addition to having suitable properties for food processing and long term storage (4).

ECCS was originally produced as an alternative to tinplate in order to overcome the adverse reactions observed when using tinplate to package sulfur releasing food

compounds. It should be noted that in order to use ECCS for a food packaging application an additional protective organic coating is required to prevent corrosion, which is not necessary when using tinplate (15).

Currently there is ongoing development within the steel packaging market due to the introduction of the REACH legislation requiring the removal of Cr(VI) (Hexavalent Chromium) from the substrate coating process when producing cans for the food packaging industry. This is as a result of its carcinogenicity and the health concerns it poses to the extensive amount of people that are exposed to Cr(VI) in the can manufacturing process (16). The major reason for removing Cr(VI) was the need to meet EU guidelines in order to be able to supply packaging to customers outside of the UK. The deadline to replace Cr(VI) in the electroplating process for coating steel was initially extended from 2017 to 2021 and has now been extended to 2024 as no suitable alternative has been developed to the desired performance level (17,18). There is also the additional requirement to remove BPA from the protective lacquer due to concerns surrounding its use. Studies have shown an increase in detectable BPA levels related to an increase in canned food consumption. This has influenced the decision of several countries to require its removal from the can making process (19).

2.3 Impact of legislation on packaging

The introduction of the REACH regulation has prompted development of an alternative method to produce protective coatings for steel food cans. It has been noted that trivalent chromium is a less toxic alternative to hexavalent chromium (20). TATA Steel have developed a Cr(III) (Trivalent Chromium) salt electroplating technique that eliminates Cr(VI) from the production process (21). This product, known as TCCT, shows promise but further work is needed to develop and stringently test it to ensure it can withstand the different conditions to which the can will be exposed (22).

BPA is used in the can manufacturing process as a precursor for epoxy phenolic-based coatings. In recent years there has been increasing concern relating to the use and exposure to BPA as a consequence of internal and external factors. This prompted research to be completed by the European Food Safety Authority into the dietary and aggregated exposure to BPA. Despite the conclusions that there was no health concern related to dietary exposure, there are still demands from several countries for it to be replaced in the can making process (23).

BPANI has been selected as an alternative to the EP lacquer currently used in the lacquering process. BPANI has been developed such that it does not have BPA intentionally added to it, however, BPA may be present in trace amounts. Unlike epoxy phenolic lacquers, which contain BPA, the BPANI lacquers being introduced are polyester based and therefore the concerns surrounding their toxicity is eliminated. Migration studies from polyester coatings into foodstuff has shown there is a minimal risk to those who consume the product (11).

A report published in 2005 prepared for Department of Environment, Food and Rural affairs outlined the risks associated with the use of Cr(VI) in manufacturing (15). It found the risks posed to aquatic and terrestrial environments by emissions in the UK was negligible when producing ECCS and tinfoil. It took into consideration the difficulties associated with removing it from the electroplating processes and outlined that although Cr(III) would be a safer and suitable alternative, it was not necessary to remove it from the production process due to the minimal risk posed. It was also noted that Cr(VI) is so far the only suitable coating available for tinfoil passivation (15).

2.4 Can making substrates

2.4.1 Tinplate

Tinplate is one of the most commonly used materials in the food packaging industry due to its formability, strength and corrosion resistance properties (24). Tinplate is produced by electrolytically depositing a layer of tin onto a sheet of steel that is 0.15 – 0.5mm thick (25). Tin deposition is performed using an acidic bath containing stannous ions, the resulting tin layer is approximately 0.2 – 1.6 μm thick. There are several commercial processes that are adopted for tinplate production, these are: the Ferrostan process; the Halogen process; the Fluoroborate method, and the alkaline stannate bath (26). Flow melting is used after the tin layer has been deposited to form an interfacial layer of iron distannide approximately 0.15 μm thick. This layer improves the adhesion of the tin to the steel surface and also aids in improving corrosion resistance through being chemically inert (27).

Tinplate passivation following deposition is commonly used to improve adhesion of the lacquer to the surface of the substrate and prevent growth of tin oxide. Tinplate

passivation is typically conducted using a chromate bath. The passivated metal layer consists of an extremely thin chromium oxide layer that is less than a micron thick (25). Passivation is used for several reasons, including: removing surface oxides produced during flow melting and water quenching, and to produce an oxide film that is resistant to sulfur staining (28). There is an increased health concern when using tinplate because the chromate layer is in direct contact with the foodstuff stored within the can (29). Therefore, after passivation it is common for a lacquer to be applied to tinplate when it is being used for food storage applications.

Tin provides excellent corrosion resistance in anaerobic environments whereas these environments accelerate the corrosion of iron. As a result of the reactivity of the iron there is concern if the tin layer is dissolved, the steel will corrode very quickly and compromise the contents of the can. This signifies the end of the can's lifetime (30). Electrochemical impedance spectroscopy is commonly used to detect the electrochemical signal that tinplate produces when it corrodes. This can be used to quantify its corrosion resistance properties (24).

2.4.2 ECCS

ECCS, also known as tin-free steel, has: lower coating weights; higher temperature resistance, and improved adhesion compared with tinplate. ECCS is manufactured using a Cr(VI) electroplating technique by depositing a chromium layer onto a sheet of steel at 40 °C (4). A layer of chromium oxide then grows on the chromium layer, the growth of this oxide is improved through the use of an acid in the electroplating bath (22). The sheet of steel is transported through plating cells at speeds greater than 5 m s⁻¹. As a result of the high speed used, the electroplating process only takes seconds to complete. This is as a result of high current densities, in the region of 15 A/dm², being applied due to the high mass transfer rate created by the turbulent movement produced at this speed (31). The final coating consists of a chromium metal layer typically weighing 50-150 mg m⁻² and a trivalent chromium oxide layer which typically weighs 7-35 mg m⁻² (21). The combined layers of chromium metal and chromium oxide have a total thickness of approximately 30 nm. In the case of ECCS it also has a protective layer of an EP lacquer subsequently added to prevent any attack from the foodstuff that will be stored within the can. This lacquer aids in preventing

gas from forming and corrosion of the metal (7). A structural diagram of ECCS is shown in *Figure 2.1*.

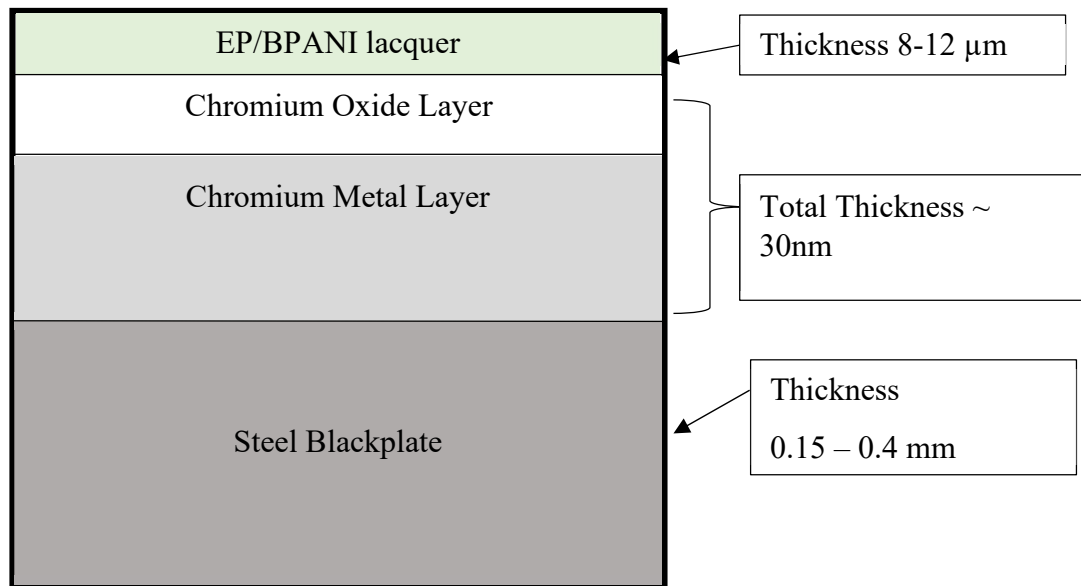


Figure 2.1 Structural diagram of ECCS (4,12)

Despite the advantages that ECCS provides to the can making industry, it also has its downsides. The major downside to ECCS, which has been discussed previously, is the health concern it poses to the manufacturer of the substrate. In addition to this, the aqueous electrolyte has its limitations such as gas formation that can cause hydrogen embrittlement and the need for hazardous additives like fluorides (16). Unlike chromium coated steels, hydrogen embrittlement is unlikely to occur on tinplate due to the baking step to which the substrate is subjected after electroplating. This process aids with the diffusion of hydrogen before significant embrittlement can occur (32). Customer preference for tinplate also plays a role in this due to its shinier visual appearance, and improved robustness making it preferred over ECCS (33). Aside from the aforementioned advantages of using tinplate it should be considered that tinplate cans are three piece, whereas ECCS cans can be two piece meaning the costs associated with ECCS production are often lower.

The current industrial requirement is to remove Cr(VI) from the can manufacturing process in order to reduce the environmental impact. There is the added difficulty that any alternative material must perform equivalent to or better than ECCS. Its intended application for use in the food packaging industry means that any developed material must be non-toxic and able to withstand the can forming and retort processes (34).

2.4.3 TCCT

Trivalent chromium baths have been used for decoration since the 1970s, however, research into their application for coating steel in the can making process, has been limited (35). With the aim to replace hexavalent chromium in the can electroplating process, the potential of trivalent chromium has been explored in depth due to the less toxic nature of Cr(III) electroplating baths (36). It is thought that this reduction in toxicity is as a result of the reduced oxidising power of Cr(III) compared with Cr(VI) (20). Whilst there are similarities in the electrodeposition of Cr(III) and Cr(VI) there are several issues faced with the deposition of Cr(III). Early research was met with several technical issues, including: a lack of control over the chromium coating thickness (37), and maintaining the bath due to complex bath chemistry (38).

The use of aqueous and non-aqueous solutions of Cr(III) salts has been explored. It was demonstrated that in an aqueous bath solution a high potential is required to reduce the Cr(III) hexahydrate ion which then results in hydrogen evolution. This hydrogen evolution results in poor chromium deposition on the surface of the metal (39). Several Cr(III) salts have been used to successfully deposit the chromium layer including chromium (III) chloride, chromium (III) nitrate and chromium (III) sulfate. It has been established that in order to enable electrodeposition of Cr(III) from a trivalent chromium bath, an organic complexing agent has to be present. These complexing agents such as formate, oxalate and acetate work by destabilising the Cr(III) hexahydrate ion. The complexing agents co-ordinate to the chromium ion, competing with water for these coordination sites which reduces the stability of the Cr(III) hexahydrate ion (36). The addition of the complexing agent enables the reaction to proceed via a single step reduction mechanism which enables the coating weight to be controlled and to near the weight of those produced by Cr(VI) (18).

It has been established that addition of organic complexing agents can result in the pH of the diffusion layer increasing which can lead to formation of polymeric forms of chromium oxide. This can result in a slow chromium deposition rate and can account for the inconsistencies in the chromium coating (40). More recent research has enabled control of the coating thickness through alteration of the bath chemistry composition and study of the mechanism of coating deposition. Despite these issues being overcome there still remains the issues of conductivity and uneven coating power (18).

There are several advantages of using TCCT. Firstly, The use of TCCT cans for food packaging reduces food waste and the cans are recyclable aiding in achieving a circular economy (41). TCCT can also be easily integrated into food can forming lines with minimal alterations to the current equipment used to produce ECCS cans (42). Lastly, studies have demonstrated that substrates which did not contain tin showed better adhesion due to tin oxide not being able to form on the surface during passivation. It is important to also consider that lower chromium content is associated with poorer adhesion (43). Particularly in the case of TCCT, a thicker Cr layer is required to achieve uniformity and similar performance levels to ECCS substrates. The difference between the structures of ECCS and TCCT can be seen in *Figure 2.1* and *Figure 2.2*.

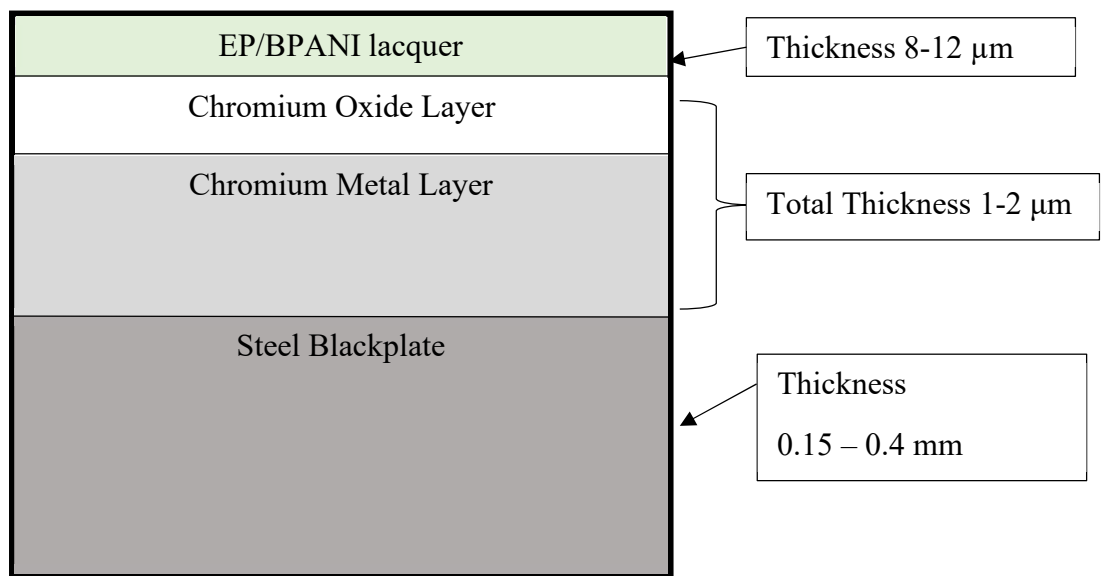


Figure 2.2 Structural Diagram of TCCT (4,12)

2.5 Organic Coatings

Can coatings have several uses including protection and decoration. The can coating selected depends on the application of the finished product and the conditions to which it will be subjected. Selection of a lacquer is important as its interaction with the substrate being used must also be considered. EP lacquers are often selected for use in the can industry due to the protection they afford the chromium layer on ECCS from chemical and thermal attack.

2.5.1 Epoxy phenolic

There are two types of phenolic lacquers that can be produced from phenol and formaldehyde, Novolac and Resol. The Novolac reaction mechanism proceeds via an acid catalysed reaction of formaldehyde in an excess of phenol. Resol resins are

produced by reacting phenol with an excess of formaldehyde under basic conditions. Both types of resin exhibit excellent chemical resistance and adhesion properties when cross-linked with an epoxy resin. Novalac provides additional properties of flexibility and film strength, while Resol is commonly selected for its high impact resistance (44).

EP resins consist of a high molecular weight BPA (bis-phenol A) diglycidyl ether type epoxy resin and a resol-type phenolic resin (44). Despite epoxy resins being chemically resistant to most food types they do not provide an acceptable level of protection against acidic attack. Under acidic conditions phenolic resins are much more resistant to degradation compared with epoxy resins as they are: chemically inert; thermally stable, and resistant to oxidation. (45) Despite this, when used alone phenolic resins do not have adequate flexibility or adhesion for sole use in can making (46). It is common practice for phenolic resins to be cross-linked with epoxy resins to achieve an adequate level of chemical resistance and desirable physical properties, thus optimising the performance of the lacquer for its use in food packaging (47).

EP lacquers have been shown to have good wet and dry adhesion. This adhesion is upheld before and after the sterilisation process using both heat and high pressure (48). A high impact resistance for EP lacquers is necessary to be able to withstand the can forming process during which it is subjected to deformation. EP lacquers have improved mechanical properties compared with epoxy lacquers alone. As they exhibit higher yield strengths they are more ductile and therefore more formable when subjected to can shaping processes. (49) The chemical resistance of EP lacquers is important both during the retort process and for long term food storage due to the varied nature of the foodstuffs contained within the cans. For these reasons Resol-type lacquers are usually selected for can coating applications (44).

Effective curing of lacquers has been shown to be important; the extent to which lacquers are cured has an impact on their chemistry and weight loss over time. Insufficient curing time and temperature results in a greater loss of solvent and water over time. (44) Water absorption into EP coatings has been observed despite them being considered highly resistant to chemical attack and is considered the first stage in coating degradation. Electrochemical impedance spectroscopy has been used to estimate the volume of water absorbed by a coating due to the difference between the

dielectric constant of water and polymers. Water uptake studies test the coating performance for providing corrosion resistance whilst enabling a prediction of its use in food packaging to be established (50).

2.5.2 Polyester

Polyester lacquers are formed by condensation polymerisation which involves reacting a diol with a dicarboxylic acid. Each alcohol group forms an ester linkage with a carboxylic acid group and this reaction happens continuously, forming the polymer chain. When each ester linkage is formed a water molecule is lost as a by-product (51). Polyester linkages are weak making them prone to acid catalysed hydrolysis. In the presence of an acid, water and heat, the polyester linkage can be broken and reform the corresponding diol and dicarboxylic acid. An example of this is when a food can coated with BPANI is retorted in a jar containing an acetic acid food simulant solution. The polyester will absorb the water from the solution with the acetic acid acting as a catalyst for this reaction to proceed. This reaction is reversible however the excess of water present causes the equilibrium to favour formation of the alcohol and carboxylic acid. (52)

Polyester coatings are weaker than EP lacquers due to their higher diffusion coefficients enabling corrosive species such as oxygen and water to penetrate through the lacquer. Their lower cross-linked density enables corrosion to propagate and increases the speed at which delamination of the coating occurs (53). As the temperature to which the lacquer is exposed during the retort process increases so does the diffusion coefficient, exacerbating the rate by which water and corrosive species can diffuse through the coating. (54) Research into the adhesion properties of polyesters with Cr(III) coatings has shown their performance is reduced by 10% compared with EP coatings (7,10). It has been shown that additives are required in order to improve lacquer properties such as formability and thermal stability (53).

2.6 Can manufacture

2.6.1 Metal cans

Metal food cans are produced by lacquering flat sheets of coated stainless steel followed by heat curing and then forming into either two-piece or three-piece cans

depending on the coating material (7). The lacquer deposition process is performed using a roller coater which covers the surface with a thin, uniform layer of lacquer (55). The purpose of the coating is to prevent electrochemical reactions between the metal and foodstuff which would lead to corrosion of the can and leaching of the metal ions into the foodstuff (4). Currently, the two most commonly used metal packaging materials are ECCS and tinplate.

2.6.2 Two-piece cans

ECCS cans are two-piece cans which can be manufactured by two methods, these are draw re-draw (DRD) and draw and wall-ironing (DWI). The DRD process involves drawing a disc of steel into a cup shape and then re-drawing it into the final can shape. This process produces shorter cans compared to the DWI process. Line speeds for DRD can making are in the range of 50-1000 cans per minute (56). The DWI process involves the same initial steps as the DRD process, with the added final step of ironing the sides out to thin them and increase the overall height of the can. The final stage of forming both types of two piece cans is to mechanically attach the lid (57).

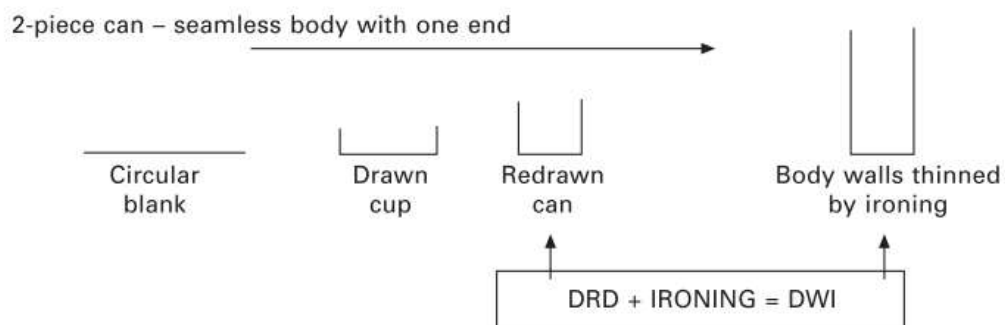


Figure 2.3 A schematic to show the DRD and DWI processes for forming two-piece cans (57)

2.6.3 Three-piece cans

Tinplate cans are three-piece cans produced from a coil of steel that has been coated with tin on both sides. The main cylinder is formed, and the bottom is attached via electrical resistance welding which forms a seam. Flanging is used to seal the ends to the main cylinder of the can. The open-top cans are supplied to the manufacturer for

filling with the required foodstuff and then the end is attached. The end can be made from tinplate, ECCS or aluminium (58). This manufacturing process is suitable for making cans of all sizes and is an efficient process for metal consumption (13). The production lines for three piece cans can manufacture up to 500 cans per minute (59).

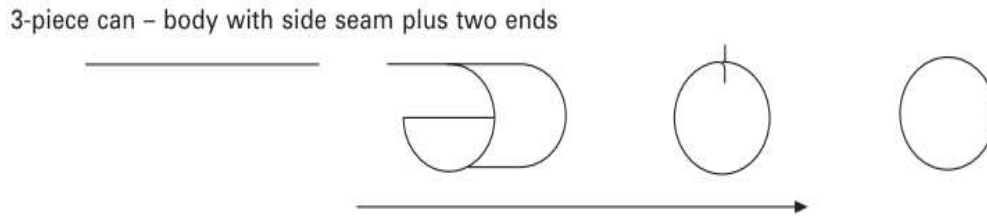


Figure 2.4 A schematic showing the three piece can manufacturing process used for tinplate (57)

2.6.4 Can Ends

Can ends are designed to be formable such that if they are subjected to internal pressure due to gas formation within the food can, they will return to their original shape without permanently deforming. Precision is required when producing can ends to ensure the shape of the end piece is correct to allow for internal and external stress and to form a hermetic seal. This is achieved through a sequence of presses, which are set to achieve the desired shape, this includes curling at the edges to aid in forming the seam between the main body of the cylinder and the end. The end piece can be both lacquered or unlacquered. In the case of lacquered ends a lubricant is applied prior to stamping in order to reduce lacquer breakage (60).

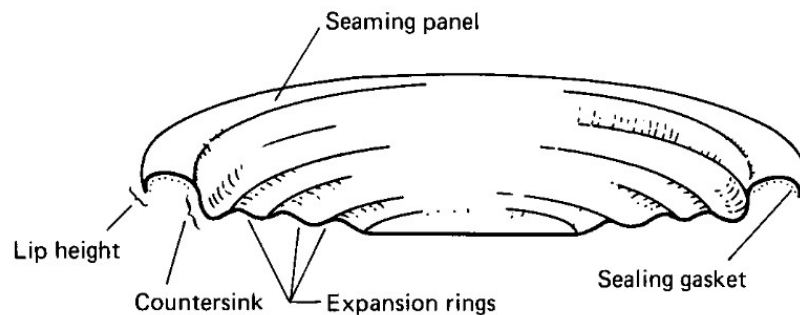


Figure 2.5 A diagram of the end design of a food packaging can (60)

2.7 Theories of Adhesion

Adhesion between a substrate and lacquer occurs through bonding on a fundamental level. Adhesion often cannot be attributed to a single mechanism but can be explained by several mechanisms occurring simultaneously. For each individual coating/substrate combination the mechanism(s) of adhesion will vary and the extent to which each occurs will also change. The following mechanisms have been proposed and are generally agreed upon:

- Mechanical adhesion
- Adsorption (Wetting) Theory
- Chemical bonding
- Diffusion
- Electrostatic Theory (61,62)

2.7.1 Mechanical Adhesion Theory

Mechanical adhesion theory states that the contact surface of the adhesive (lacquer) and adherend (substrate) is what determines the strength of mechanical interlocking. The substrate surface area and its roughness both influence mechanical adhesion (61). Surface roughness can be increased by mechanical abrasion, chemical or physical processes (63). It has been proposed that roughness improves mechanical interlocking due to the porous nature of the surface enabling the adhesive to penetrate it and improve contact between the lacquer and substrate (61). It is thought that an increase in surface area because of surface asperities results in an increase in surface energy which improves wetting and therefore adhesion (64).

Despite it having been demonstrated that surface asperities improve mechanical interlocking, good adhesion has also been demonstrated on flat, smooth surfaces (61). If the surfaces are smooth and flat then the wettability of the coating on the surface must also be considered (65). Chemical and physical properties may also be altered when the surface roughness is increased which may also improve adhesion. An increase in surface area likely improves chemical bonding and wettability of the surface (62).

2.7.2 Adsorption Theory

Adsorption theory states that molecular contact between two surfaces and the forces that are produced between them results in adhesion. The process whereby contact is formed between the substrate and adhesive is called wetting. For wetting to occur the surface free energy of the solid substrate must be greater than that of the lacquer being applied to it (62). The directly proportional relationship between surface energy and surface tension has been demonstrated, therefore, increasing the surface energy increases the surface tension of the substrate (66). There will be improved spreading of the lacquer upon application and also increased wettability which improves adhesion (64). If the wetting is insufficient, defects can be generated on the surface and result in a reduction in the bond strength and therefore the adhesion. A higher bond strength can be produced by complete wetting of the surface (61).

2.7.3 Chemical bonding

The chemical bonding theory attributes adhesion between a substrate and coating to chemical forces on their respective surfaces. Chemical bonding can result from intramolecular forces like covalent bonding or intermolecular forces such as hydrogen bonding. The strength of these bonds varies significantly, and their occurrence depends on the chemistry of the substrate and coating. The covalent and ionic intramolecular bonds are stronger than the secondary forces such as hydrogen bonding and account for stronger adhesion properties. Covalent bonding can also form across the interface providing equally reactive groups exist and are typically the strongest type of chemical bond. Electrostatic forces, diffusion and mechanical forces most likely contribute to the adhesion in addition to these chemical bonding forces. There are five types of intermolecular forces that exist, these are: Hydrogen bonding, Dipole (polar molecules only), Dipole-dipole, London dispersion forces and Polarizability (61). The type of intermolecular bonding that can occur depends on the chemical nature of the two bonding surfaces.

2.7.4 Diffusion

Diffusion theory suggests that adhesion occurs as a result of molecular diffusion within and between the substrate and coating. It is likely that diffusion is only

occurring when both the substrate and coating are polymers of similar properties (61). Diffusion occurs when the chain of one polymer material enters the other. The most common occurrence is interdiffusion where both the adhesive and adherend cross the substrate/coating interface and form an interphase (63). Molecular diffusion accounts for the bonding that occurs when thermoplastics are heat-welded (62). The bonding is strongest when the solubility of the adhesive and adherend is matched (61).

2.7.5 Electrostatic forces

Electrostatic theory states that an electrical double layer forms at the coating/substrate interface and accounts for the electrostatic forces that exist between them. The electrostatic forces that exist between the substrate and coating provide resistance to separation. This has been observed when a coating has been removed from a substrate and electrical discharge has occurred (62). Electrostatic forces support the theory of polymer adhesion to metal surfaces. Chemical bonding has been established as much more significant than electrostatic forces between non-metallic materials (61).

2.8 Adhesion of coated steel packaging

2.8.1 Wet and Dry Adhesion

There are several forces that need to be considered when studying lacquer adhesion, these include: electrostatic forces, Van der Waals forces and covalent bonds (48). Dry adhesion measurements are useful to understand the mechanism by which the lacquer bonds to the substrate after coating. It is also a useful method for quality control of each substrate/lacquer combination. If dry lacquer adhesion is poor then it is an indication that the lacquer will perform poorly during the retort process (10).

Although dry adhesion measurements are useful, they provide limited information about the adhesion properties of the lacquer post-retort. Canned food is cooked using an autoclave or retort which also sterilises the food by destroying bacteria. During the retort process the can and its contents are subjected to high pressure and temperatures exceeding 121°C in a wet environment for at least 15 minutes. Therefore, it is important to study the effects that moisture, temperature and pressure have on the lacquer and whether its adhesion is satisfactory post-retort (67).

De-ionised water is used as a retort solution to achieve a baseline measurement. This allows a value of adhesion to be determined for the performance of the lacquer in a simulant solution without any additives such as sodium chloride. It has been demonstrated by Allman *et. al.* that there is a definitive correlation between: the lacquer; its adhesion properties; the substrate, and the type of simulant solution (9). Therefore, the addition of additives introduces other potential reaction mechanisms and as such make adhesion studies more complex.

2.8.2 Lacquer Performance

Comparison of the performance of EP and BPANI lacquers has shown that EP lacquers perform better than BPANI. EP lacquers exhibit consistently higher failure forces and also show a smaller reduction in failure force post-retort compared with those of BPANI lacquers. Likewise, both of these lacquers perform better in conjunction with an ECCS substrate than a TCCT substrate (10).

It has been suggested that the delamination of polyester based BPANI lacquers is as a result of water absorption into the bulk of the lacquer. Water diffusion within the lacquer determines the time taken for delamination of the lacquer to occur. The rate of water diffusion within the lacquer is dependent on the thickness of the lacquer and also the speed and flow direction of the simulant solution in contact with the lacquer (68). At room temperature, diffusion coefficients for epoxy lacquers are of the order of 10^{-7} mm²/s, whereas, for polyester lacquers they are of the order of 10^{-6} mm²/s. (69,70) This means that water can penetrate through the BPANI lacquer 10x further than the EP in the same time period. This is significant due to the lacquers only being several micron thick this could be the difference between moisture only penetrating the top surface of the lacquer or reaching the CrOx/lacquer interface

The presence of oxygen within the simulant increases the rate of the oxygen reduction reaction on the metal substrate, which can lead to blistering of the lacquer (71). Removal of oxygen from the simulant solution using a nitrogen purge improves the lacquer adhesion post-retort. Certain compounds such as citric acid have been shown to improve lacquer adhesion due to passivation of the stainless steel surface (9). Passivation can create or preserve functional groups promoting chemical bonds with the lacquer while also improving its corrosion resistance through removal of

contaminants. The improved chemical and mechanical bonding between the lacquer and passivated surface can lead to long-term stability of the adhesion and reduce the likelihood of delamination due to environmental factors (72).

Lacquer adhesion post-retort has been shown to improve over time but does not return fully to its pre-retort state, showing there is a level of reversible adhesion. It should be noted that adhesion measurements do not account for any changes at the lacquer/substrate interface as adhesion measurements are taken near the surface.

Heat treatment prior to filling the cans and sterilisation has been shown to remove stresses within the material that are induced during can forming. The temperature increase can also improve mobility of polymer chains resulting in repair of lacquer/CrOx bonds. This increase in bonding will reduce the diffusion coefficient of the lacquer which in turn reduces the amount of water that reaches the metal/coating interface. Despite the heat treatment only reducing the size of defects, not the number of defects, there is still a measurable reduction in the amount of coating delamination (73).

The presence of oxygen during the food sterilisation process can cause corrosion of the food can. (74) When real food stuffs are packaged within the can making material it is able to consume any oxygen before it can detrimentally affect the can material. In experimental procedures where a salt simulant is used the oxygen is not absorbed and delamination of the lacquer can result (73).

2.8.3 Scratch Testing

Scratch testing is a standardised, quantitative method for measuring adhesion properties of coatings on substrates (75,76). Despite the apparent simplicity of the scratch testing technique, it has been established as a consistent and reliable method for testing failure force since its introduction in the 1950s. Planar sample testing is often conducted using a motorised scratch tester which is operated manually by adding increasing weight to the scratch tester up until a point where enough force is applied that the lacquer disbonds. The action of the tip under this applied force removes the lacquer and the tip makes contact with the metal surface. This is indicated by a spike in voltage, the weight at which this occurs is recorded as the critical load (77). It is common to quote the weight at which the coating fails as a failure force by converting weight to force using *Equation 2.1*.

$$F = ma \quad (2.1)$$

Sekler *et al.* defined the critical load to be ‘the minimum load at which the first damage occurs’ (78). The major factor in determining the critical load has been established as the adhesion between the substrate and the lacquer (77). Coating failure can either be adhesive or cohesive. Adhesive failure occurs when the coating peels away from the substrate at the interface, whereas cohesive failure occurs within the coating whereby part of the coating fragments. Fragmentation can occur due to internal or external factors and will result in a decrease in the failure force of the coating. Material stress can also impact the critical load. Stress can be induced by friction between the diamond tip and coating or as a result of poor elasticity of the coating or substrate. In practice adhesive and cohesive failure can occur individually or in tandem resulting in coating disbondment (75).

Hardness of the substrate and coating, in addition to the thickness of the coating, has been shown to influence the critical load value. A harder substrate or lacquer and also a thicker layer of lacquer will all result in a higher critical load being required to observe a failure in the coating (79). The scratch test technique unlike a hardness tester measures the resistance to scratching of a surface rather than its resistance to deformation. Even though scratch testers measure a materials resistance to surface damage, not its hardness, these properties are linked. Melvin *et al.* demonstrated that an increase in tin coating weight results in a more disorganised tin structure. As a result of the higher tin coating weight, a thicker tin oxide film is produced which reduces the adhesion properties (33).

2.8.4 Spring-Loaded Pen Hardness Testing

Scratch testing of curved surfaces poses more of a challenge and in these circumstances a spring-loaded pen hardness test is more suitable. Spring loaded pens are operated by setting a force and moving the pen across the coated surface. The force setting determines how far the tip can retract into the pen and this is independent of the amount of manual pressure that is applied. After scratching the pen across the surface, the coating is evaluated visually to check if it has been removed. The failure force is recorded to be the lowest load required to remove the coating (80). The

precision of the of the spring-loaded hardness pen depends on which spring is loaded, for forces below 3N it can be measured within $\pm 0.1\text{N}$, however for values up to 10N the precision is only $\pm 0.5\text{N}$ and for up to 30N it is $\pm 1.5\text{ N}$ (81). Therefore, the precision of this technique is only comparable in precision to automated scratch testing at low failure force values. The surface roughness should also be considered in instances where the lacquer may not be thick enough to compensate for the roughness and the tip of the pen may reach the surface beneath the lacquer. This would result in failure force measurements that combines both the lacquer and the substrate.

2.8.5 Adhesive Tape Testing

Adhesive tape testing is a qualitative only method for testing adhesion as it does not provide numerical results for the failure of a coating. The process involves applying a piece of tape to the surface of the coating and peeling the tape away from the surface in a consistent direction. If the coating peels away with the tape then it is considered a failure. It is rated on a 1-5 scale based on the perceived amount of coating that is removed by the tape. This leaves the outcome of the test open to interpretation and also does not distinguish between two substrates that fall into the same number range even if the amount of lacquer moved is different. As this method alone is not quantitative it does not allow the adhesion qualities of two coatings to be compared should both pass or fail this test.

This method would require additional steps to calibrate it in order to make it quantitative such as: ensuring the same tape is used each time; using a tape that meets a standard e.g. ASTM, and introducing a measuring scale for ensuring a consistent force is applied each time the test is undertaken (82). The disadvantages of this method are related to its manual operation and the tape used in the experiment. The quality and age of the tape being used as well as the speed and angle at which the tape is pulled can all influence the experimental results (65). This introduces several variables which become sources of error for this method of adhesion measurement.

2.9 Material properties

2.9.1 Hardness

One of many reasons why chromium is selected for use in coatings is due to its high hardness values (83). Hardness testing is a well-established method to test the strength of metals and their alloys. There are several testing approaches and measuring scales that are approved by ISO and various other organisations as methods for testing hardness (84). Knoop hardness has been used to confirm that chemical changes occur to the coating of BPANI lacquered ECCS during retort. It was demonstrated that not only does the retort process itself significantly reduce the hardness of the lacquer but that the introduction of a food simulant reduces it further. Increasing the concentration of the simulant has the effect of reducing the hardness even more (10).

A deposition mechanism for ECCS has been proposed by Wijenberg, whereby chromium-carbide can also be formed in addition to the Cr layer. This is dependent on the current density and other variables during the electroplating process. The coating weight and composition will vary depending on these variables. At low current densities, no deposit is produced and at high current densities chromium oxide is the predominant deposit (21). If chromium carbide is present in the plated layer, it can increase the hardness and wear resistance of the material, this can also make the layer more brittle and effect the overall performance of the can.

2.9.2 Stress and Strain

Stress is defined as the applied force per unit area. Strain is the deformation of a solid resulting from the applied stress, it is measured as a ratio of the elongation to the original length (85). If the elongation is positive, then the material is being tensioned and if it negative, then the material is being compressed. The process difficulties of quantifying the stress of tinplate cans have been noted due to the difference between experiment and theory arising from the non-uniform nature of the buckling of the cylinder. A study performed by Shah *et al.* using a universal compression plate apparatus found that liquid filled cans performed significantly better than empty cans under axial compression. This improved performance was only observed when there were no imperfections present that may cause the cylinder to shift horizontally and result in shear loading (86).

Residual strain is a useful way to determine the limit of a material based on the thermo-mechanical loads to which it has been subjected. Commonly selected methods for measuring strain include strain gauges and extensometers. For these instruments to take measurements they must be directly attached to the material and measure strain in the direction determined by their placement. Extensometers can measure strain in two directions and over a substantial extension length, whereas strain gauges operate best over small distances. Strain gauges have the advantage that they can be positioned anywhere and measure in any direction on the material, however, their small measuring cross-section can be unrepresentative of the bulk of the material if it is braided or woven.

Alternative methods such as digital image correlation and video extensometry are non-contact and can measure strain over the whole surface of the material. Their disadvantages include their large size and high initial purchase cost. Methods that do not measure strain directly such as tensile testers that read from the crosshead, are not suitable when accurate strain measurements are required. Temperature and humidity also influence the performance of strain gauges but have little effect on the other techniques discussed above (87).

2.9.3 Strain in Food Cans

A significant amount of the literature details techniques for measuring uniaxial strain, however, this is unrepresentative of most real food can systems as the strain is often multiaxial (87–89). Laboratory based techniques for inducing strain into thin sheets of steel are well-controlled and as such are reproducible (90). It has been shown by previous research that the areas of localised, high strain are consistent across sample sets (91). It is important to consider that food cans can also become deformed after the retort process is complete. If cans are dropped and dented, then deformation will occur, however, this will be inconsistent across samples and as such is hard to simulate.

The Erichsen Dome apparatus is a very useful tool to analyse coating properties such as adhesion, formability and ductility. Its ability to provide this level of analysis means that it can induce biaxial strains that are comparable to those that the substrate is subjected to during the can forming process (92). The downside of using the Erichsen Dome to induce strain is the difficulty presented in coating and adhesion testing a non-planar sample in a laboratory environment, whilst also ensuring reproducibility of results. Cruciform samples, also known as a Maltese cross, enable biaxial strain to be

induced while maintaining the flatness of the sample. The downside to this for most research and development of methods is that biaxial straining equipment is large and expensive and as such is not practical for most laboratory research (93).

Even though many methods exist to induce biaxial/multiaxial strain into sheet metals, the need to quantify the strain produces an additional hurdle for performing these experiments. Neutron diffraction has been successfully employed by several researches to analyse multiaxial strain of a bulk metal (94–96). The advantage of using neutrons to probe strain values is their non-destructive nature and their ability to measure beneath the surface of the material. In order to measure residual strain of cylinders, measurements must be taken of the circumference, axial and radial direction by rotating the neutron beam and detector (95). If a complex load is applied, shear strain may also be present and these three measurements will not fully represent principal strains (97).

DIC (Digital Image Correlation) has been proven as a robust and reproducible techniques for quantifying strain of sheet metals in real time (90,92,98). Although this method is well established, it also requires complex and expensive equipment in addition to this the capability to set up the equipment to monitor samples during a tensile test is needed. The drawback of this methods aside from cost and complexity is the accessibility of the equipment for small-scale research and development projects where the initial outlay and timescale cannot be justified.

Microgrids for strain area analysis can be printed using a multitude of techniques, including electron beam lithography (98), deposition (99) and electro-polishing (100). All of these techniques are used similarly as they enable the researcher to measure the elongation of the grid in correlation with the applied force. It is important to consider that several of these techniques produce a grid by etching or lasering a surface by removing the top layer. As such these techniques would be unsuitable for any application where the sheet metal is coated with a thin organic layer that must remain intact for analysis purposes.

Laser speckle interferometry is a technique that can measure strain and surface displacement with a high sensitivity and resolution (101). A laser beam is directed onto the substrate surface and the roughness of the surface scatters the light in many different directions. The scattered light waves interfere with other scattered light

waves and a pattern of this interference is created, known as a speckle pattern. The speckle patterns of the unstrained and strained surfaces can be compared and quantitatively analysed to give a value of strain. This technique is non-destructive and as such is suitable for applications where strain of lacquered substrates must be studied (102).

2.9.4 Corrosion

There are two important corrosion mechanisms that occur to steel packaging cans, these are wet corrosion and atmospheric corrosion. Wet corrosion occurs on the internal surface of a can where food material is in contact with the metal surface. Atmospheric corrosion occurs on the external surface of the can where it is in contact with air and any other chemicals that can initiate corrosion (103).

Chromium coatings can provide resistance against delamination of the protective lacquer on the surface, however, surface defects can occur during the can making process and are excellent sites for cathodic delamination to occur. The nature of food stuffs packaged within food cans initiate a reaction with the metal that is exposed by these defects and a cathodic oxygen reduction reaction can occur. This leads to cathodic disbondment and causes delamination of the lacquer (104). Koehler demonstrated that cathodic delamination could only occur when metal environments contained a group (I) alkali metal such as sodium to act as a counter ion to the hydroxide anion produced at the cathode (105). Meanwhile the metal surface acts as the anode and undergoes an anodic oxidation reaction which initiates corrosion and forms iron oxide (rust) (22).

FFC (Filiform Corrosion) is an example of anodic delamination whereby the lacquer delaminates as a result of an anodic oxidation reaction. Filiform corrosion appears as a 'worm' like feature and thus is concerning when observed on food packaging. Several conditions are required in order for FFC to be initiated on polymer coated metals (106). FFC propagates when there are high levels of humidity that exceed 60%, high temperatures and additional factors such as oxygen presence (106,107). It should be noted that defects must also be present to enable FFC to initiate and it has been demonstrated that the presence of defects on the surface influences the brittleness of a coating and how it is applied (106). Can substrates and lacquers are exposed to high levels of moisture and temperatures during the retort process in order to effectively

sterilise the food stuff. This combined with the oxygen present within the vessel and the food stuff can provide ample conditions for FFC to occur.

FFC propagates via a differential aeration mechanism whereby oxygen diffuses through the tail to the head. Due to the limited amount of oxygen reaching the front of the head this becomes the site for the anodic metal dissolution. The back of the head nearest the tail has a higher concentration of oxygen being supplied to it so becomes the cathodic site for oxygen reduction (108). Salts such as sodium chloride can act as a source of chloride anions that can initiate metal dissolution and form part of the ferrous chloride electrolyte. There is a potential difference present which causes the electrolyte ions within the filiform to propel forward in the head, increasing the surface area of the corrosion. A pH gradient also exists which indicates there are anodic and cathodic sites and confirms that there is a differential aeration corrosion cell present (107).

If the tin layer on the steel in tinplate is not continuous then the steel corrodes at an accelerated rate. The amount of corrosion as a result of electrochemical reactions is influenced by the foodstuff, the pH within the can and the oxygen level. In order to minimise leaching of tin and iron into the foodstuff a protective lacquer is used (109). It has been demonstrated that if the iron layer of ECCS is exposed during can forming then this acts as a site at which FFC can be initiated (73). As with tinplate, ECCS is coated with an organic lacquer to provide an additional layer of corrosion resistance for the iron layer (22).

2.10 Food Canning and Cooking

2.10.1 Food Canning

Canning of food involves several stages. Firstly, the raw food must be cleaned and prepared accordingly for storage within the can. The food is then blanched to reduce loss in quality while the food is stored for prolonged periods of time. Blanching involves scalding the food in boiling water for a short time and then subjecting it to cold water to prevent further cooking. The can is then filled with the food which is usually done under vacuum. The can is then closed and sealed as described previously in *Section 2.6.3 (2)*.

2.10.2 Heat treatment and sterilisation

Foodstuffs are often canned while raw and therefore require cooking and sterilisation prior to supplying to a customer. There are several advantages to heat treating food which includes the ability to store foods at room temperature where it is not possible to refrigerate them. It is important that the temperature selected is sufficient such that it will destroy harmful microorganisms, but not so high that it compromises the texture and flavour of the food. The quality of food is improved when high temperature food processing for a shorter time is used in place of longer, lower temperature heat treatment (34).

The most common approach for heat treating canned food is to retort the sealed can and its contents. The food is subjected to a high pressure and temperatures exceeding 121°C, for a prolonged period. In addition to cooking the food, this process also sterilises the environment within the can ensuring no harmful bacteria and microbes remain. The acidity of the foodstuff also influences the temperature at which sterilisation occurs. At acidic pH's below 4.5, bacteria cannot survive and therefore sterilisation can be achieved below 100°C. The type of food and the size and shape of the packaging also effect the time taken to sterilise the food (67). The final stage after sterilisation is for the food can to be labelled accordingly.

Round robin testing conducted in conjunction with TATA Steel and Crown Packaging established that the following conditions were suitable for the cooking and sterilisation of food stuffs: a temperature of 121°C, a retort time of 90 minutes and a pressure of 1.06 bar (110). In addition to the parameters outlined it should also be noted that water is added to the autoclave which produces steam during the retort process. Whilst this does not affect the foodstuff contained within the can it can affect the lacquer and external can surface.

2.10.3 Storage and Shelf-life

The rate at which foodstuffs perish depends on their storage conditions and the container in which they are stored. The shelf-life of food is measured by several factors including its safety, appearance and also nutritional value. Food is considered unsafe if it poses a hazard to the consumer such as something chemical or physical (111). Canned foods are often given shelf-lives of two years, after which changes in texture

and colour may be observed over time. In actuality, the food within the can last significantly longer, being safe from microbes providing it is stored at room temperature (67). The prolonged shelf-life afforded by metal packaging in comparison with other storage materials accounts for the significant value of the worldwide metal packaging market (112).

2.10.4 Recyclability

Metal food packaging has a significant advantage over other packaging materials due to its recyclability, which is approximately 60% in EU countries (113). The advantage of this is that a metal food can could be infinitely recycled without a loss in quality. This contributes to a circular economy in several ways. Firstly, through the reduction in the amount of finite resources such as tin being used (114). The recyclability of metal cans makes them ‘reusable’ meaning the initial production costs associated with producing a brand-new can are replaced by much lower re-processing costs. This not only reduces the cost impact on the supplier but is also passed onto the consumer. Finally, the environmental impact is reduced, as up to 75% less energy is required for recycling than new manufacturing which saves on average 1.7 tonnes of CO₂ per tonne of steel cans that are recycled (115). Producing food cans using other types of scrap steel by melting it in an electric arc furnace requires up to 94% less energy than making food cans from virgin material. This equates to up to 94% less CO₂ burden (116).

2.11 Lacquer Interface Failure Mechanisms

2.11.1 Migration Testing

The complex matrix involved in real foodstuffs mean it is uncommon to use the actual foodstuff in migration testing as no standards for comparative analysis exist. Simulants are used as an alternative in order to make testing reproducible. This enables small changes in composition of the simulant to be studied, as it has been found that these can have significant effects on the results obtained (117). Allman *et al.* used retort testing to demonstrate that there is a significant interaction between the foodstuff in the can and the novel lacquer/substrate combination of BPANI/TCCT. Several methods were used to identify this. Firstly, post-retort there were visible changes in the lacquer and substrate surface. The lacquer was peeled away from the surface and

also spots of corrosion were seen. This was confirmed through adhesion testing using the scratch testing method, hardness testing and a study of surface chemistry using XPS. Retort testing and the simulant have also been shown to alter the way in which the coating fails. Post-retort scratch testing of the samples produced more tearing whereas piercing is observed when samples were tested for dry adhesion prior to retort (9,10). Further work is required in this area to investigate any chemistry changes to the coating chemistry during the retort and can forming processes.

The literature details several simulants that have been used to test the performance of lacquered metal packaging substrates. The following list outlines several of the simulants used but is not exhaustive:

- 1% NaCl (Brine) (9)
- 1% NaCl, 1% Acetic Acid (Acidified Brine) (9)
- 1% Lactic Acid (Carbohydrate Fermentation) (9)
- 0.25% NaCl, 0.25% Citric acid (Acidified Brine) (9)
- 3% Acetic Acid (11)
- 10% ethanol (11)
- 50% ethanol (11)
- Isooctane (11)
- Tuna and mussels in pickled sauce (27)

2.11.2 Surface Topography

SEM (Scanning Electron Microscopy) has been used successfully to demonstrate that a rough surface produced during the cold-rolling process maintains its morphology even after chromium has been plated on to the surface. Applying a coating had no effect on the morphology of the surface and the coating appeared continuous with no imperfections (4). Whiteside *et al.* studied the effect of strain on surface topography using SEM. Both TCCT and ECCS substrates were studied and it was identified that as the amount of deformation was increased more cracking on the surface was apparent for TCCT samples which was not present for ECCS samples (118).

2.12 Conclusions

An in-depth review of the literature has enabled the focus of the research to be established. It has been identified that significant research has already been conducted to explore Cr(III) as an alternative for Cr(VI) in the electroplating process. TATA Steel have developed TCCT which is a Cr(III) substrate produced as an alternative to ECCS. ECCS has been used for comparative purposes in order to compare their performances to ensure that TCCT performs at the same level. A large amount of the literature looks at corrosion of Cr(VI) substrates by both atmospheric and food stuff influences, however, limited research of corrosion of Cr(III) exists. More recently, research into chemical and mechanical changes occurring on the substrate surface of Cr(III), compared with Cr(VI), has been conducted. As part of the initial research the study of chemistry changes at the substrate surface post-retort will be considered.

It should be noted that in addition to changing the salts used in the substrate electroplating process there is a requirement to replace the lacquer. The replacement of EP lacquers with BPANI lacquers has introduced another variable into experimentation and work on testing BPANI has been completed. The dry and wet adhesion properties of both lacquers in combination with ECCS and TCCT has been studied. The influence of food simulants such as NaCl solution has shown a significant decrease in lacquer performance of BPANI post-retort. Further research is required to test a wider suite of simulants to ensure that the research represents as many foodstuffs as possible that will be packaged within the food cans.

There is still significant research required to improve the performance of the BPANI/TCCT lacquer substrate combination. Areas for improvement include lacquer adhesion, uneven coating weight and slow deposition rate. Studies have been conducted on unstrained and uniaxially strained samples but studies on biaxial strain of steel cans are very limited.

In this present study the lacquers and substrates will be characterised in their unstrained state to establish the effect that the retort conditions and food stuffs have on their performance. This will be achieved by using techniques such as sterilisation (retort), scratch testing, FTIR-ATR spectroscopy and a filiform corrosion set-up. Once the surface performance under these conditions has been established, uniaxial strain will be induced using a tensile tester. The lacquer/substrate performance post-retort

will be studied using a scratch tester and SEM. The final stage of this research will look at inducing biaxial strain into the substrates using an Erichsen cupping apparatus, this is to simulate the DRD stage of can making. The adhesion of the lacquer to the biaxially strained substrates will be studied both pre- and post-retort using a spring-loaded hardness pen. The impact of biaxial strain on both ECCS and TCCT substrates will be established. The aim is to establish whether hardness pen and scratch test failure forces can be interconverted to make them comparable. The final part of this research will use an adaptation of the Preece test and Keyence imaging to identify any defects that are present in the CrOx layer after straining. The overall aim of these chapters of research will be to robustly test the TCCT/BPANI combination and determine its suitability for replacing the commercially available ECCS and EP lacquer.

Chapter 3

Materials and Methodology

3 Materials and Methodology

This chapter outlines the materials, methods and instrumentation used throughout the research chapters. It gives a detailed overview of each experimental method including sample preparation and sterilisation which remain consistent throughout.

3.1 Materials

3.1.1 Steel Substrates

The TCCT and ECCS substrates used for analysis were provided by TATA Steel, further details of which are provided in *Table 3.1*. All batches of TCCT used were experimental batches produced on the pilot line/ETL14 at TATA Steel, Ijmuiden, NL and were explicitly provided for use in the research. The complete batch numbers indicate the production date of each batch of substrate. The production conditions, such as current, along with the corresponding coating thickness are outlined in each instance where a new batch of TCCT was analysed. The current density is an important factor in electroplating as it affects deposition rate and coating thickness (119). The batches of ECCS used for this research were commercial batches produced on the production line at TATA Steel, Trostre, UK and were used for comparative purposes to analyse alongside developmental batches of TCCT. All samples were stored at room temperature and pressure and average humidity. Samples were inspected for noticeable defects or corrosion before use. Current density is included for samples where the information was available for the batch. This is not researched in detail in this work but is important to consider due to it being a variable parameter in the electroplating process.

Table 3.1 Batch specific information for each substrate of TCCT or ECCS used throughout this research

| <u>Substrate</u> | <u>Batch Number</u> | <u>CrOx Weight / mg m⁻²</u> | <u>Current / A dm⁻²</u> | <u>Production Year and Location</u> |
|-------------------------|----------------------------|---|---|--|
| TCCT | 70 | 13.2 | 16 | 2019 TATA, Ijmuiden, NL |
| TCCT | 66 | 9.5 | 18 | 2019 TATA, Ijmuiden, NL |
| TCCT | 74 | 4.2 | 14 | 2019 TATA, Ijmuiden, NL |
| TCCT | 56 | 9.4 | | 2019 TATA, Ijmuiden, NL |
| TCCT | 64 | 12.5 | 20 | 2019 TATA, Ijmuiden, NL |
| TCCT | 04 | 3.5 | 2 | 2019 TATA, Ijmuiden, NL |
| TCCT | TH460 Coil – 277365(AN) | 11.3 | | 2021 TATA, Ijmuiden NL Laon Trials |
| ECCS | 54.20.09.01 (1) | 16.9 | | 2021, TATA, Trostre, UK |
| ECCS | 54.20.12.04 (3) | 11.4 | | 2021, TATA, Trostre, UK |
| ECCS | | 9 | | 2019 TATA, Ijmuiden, NL |

3.1.2 Organic Lacquers

The EP (METLAC, 816222) lacquer is the epoxy-phenolic coating used in industry for lacquering food packaging cans that are currently in circulation. The polyester lacquer, BPANI (METLAC, 816714), used is experimental and has been produced to meet the legislative pressures imposed by France to remove BPA containing lacquers

from food packaging materials. Both of these lacquer types are well established within can making research and have been analysed extensively (12,110,120).

3.1.3 Simulant Solutions

Simulant solutions were used to simulate the impact of the food content being retorted; these are detailed in *Table 3.2*. These provide a more repeatable and controlled scientific means of examining the impact of individual food constituents.

Table 3.2 Food simulants use for this research, their composition and chemical information

| Chemical | Supplier | Purity | Use | Simulation |
|---|---------------|----------------------------|---|--|
| Sodium Chloride, NaCl | APC Pure | ≥99.9% BP, ACS, PhEur, FCC | 0.25-1% NaCl w/v solution in deionised water | Brine (peas/beans) |
| | | | 0.25% w/v solution with 0.25% w/v citric acid in deionised water | Salsify |
| Citric Acid, C ₆ H ₈ O ₇ | Sigma Aldrich | 99% | 0.25% w/v solution with 0.25% w/v NaCl in deionised water | Salsify |
| L-Cysteine hydrochloride, anhydrous | Sigma Aldrich | ≥98% | 0.5 g/L solution in deionised water with 3.5 g/L KH ₂ PO ₄ and 7.22 g/L | Preservative in high protein foods – amino acid (Peas) |

| | | | | |
|---|---------------|---------------------------|--|------------------------------|
| | | | $\text{Na}_2\text{HPO}_4 \cdot 2\text{H}_2\text{O}$ | |
| Sodium Phosphate dibasic dihydrate, $\text{Na}_2\text{HPO}_4 \cdot 2\text{H}_2\text{O}$ | Sigma Aldrich | $\geq 99.0\%$ BioUltra | Used as a buffer at 7.22 g/L in 0.5 g/L cysteine hydrochloride solution with 3.5 g/L KH_2PO_4 deionised water | Emulsifier (Peas) |
| Potassium dihydrogen phosphate, KH_2PO_4 | Alfa Aesar | 99.0% min | Used as a buffer at 3.56 g/L in water with 0.5 g/L cysteine hydrochloride and 7.22 g/L $\text{Na}_2\text{HPO}_4 \cdot 2\text{H}_2\text{O}$ | Emulsifier/stabiliser (Peas) |

3.2 Methodology

The procedures and conditions outlined throughout this section are well-established and have been taken from previous research (12,110,120). They have been determined as a result of round robin testing with TATA Steel and Eviosys (formerly Crown Packaging). Any additions to the industrial methodology came from extensive trialling of the most appropriate, reproducible techniques for a laboratory environment that are representative of real world can manufacturing and food sterilisation processes (12,110).

3.2.1 Substrate lacquering and curing

The sample preparation, retort and scratch testing were completed at SPECIFIC PMRC, Baglan.

Apparatus that is comparable to those used in industry was used to produce lacquered substrates utilising a reproducible method. The process for lacquering the substrates is kept consistent throughout this research regardless of the lacquer/substrate combination used.

An A4 sheet of substrate (TCCT/ECCS) was clamped into place in an K202 RK – K Control Coater with a 400 x 450mm bed as shown in *Figure 3.1*. A setting bar was pushed into place and adjusted to calibrate the machine to the correct pressure for the substrate. A meter bar with an 80 μm diameter wire was clamped into the coater, this deposits a wet film 12 μm thick which is approximately 8-10 μm (121). A schematic showing the bar and how the coating was applied to the substrate is shown in *Figure 3.2*. A layer of lacquer (~3 ml) was applied to the substrate. The coater was set to speed four and the dial turned to forward. The coater was stopped approximately 2 cm from the edge of the substrate once coated. The coated substrate was placed into the 3 m drying oven shown in *Figure 3.3* (THIEME KPX) at 215°C and was dried at a speed of 0.2 m/min amounting to a total cure time of 15 minutes which is in line with the manufacturers recommended practice.



Figure 3.1 An RK-K Control bar coater used for lacquering steel

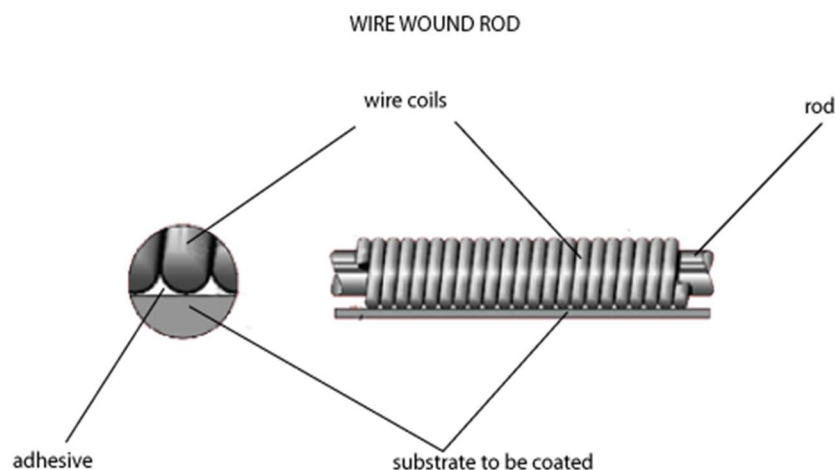


Figure 3.2 Labelled schematic of the bar/substrate/lacquer interaction that occurs during use of the Meyer bar coater (122)



Figure 3.3 THIEME KPX drying oven used for curing the BPANI and EP lacquers

3.2.2 Sample Preparation

Once cured, the sheets of coated substrate were cut into 120 x 40 mm samples as shown in *Figure 3.4*. All sample were uniquely labelled with the substrate batch number, lacquer name and then the sample number. A fast-drying two-part epoxy sealant (Loctite Double Bubble) was applied to the edges of all samples, which were then air dried for 15 minutes producing the samples in *Figure 3.4*. The edges of the samples were sealed in order to prevent water ingress which would cause the coating to peel.



Figure 3.4 a) A 120 x 40mm EP lacquered sample of TCCT b) Sample with epoxy coated edges

3.2.3 Retort

In order to simulate the food sterilisation process used in industry the samples were retorted using the CertoClav Multicontrol 2 autoclave shown in *Figure 3.5*. The same conditions that are used by Crown Packaging, 121°C for 1 hour 30 minutes, were utilised. The conditions within the vessel were studied and analysed using a TMI Orion data logger and Qlever2 software to ensure they remained consistent with the outlined conditions (110), these are plotted in *Figure 3.6*.

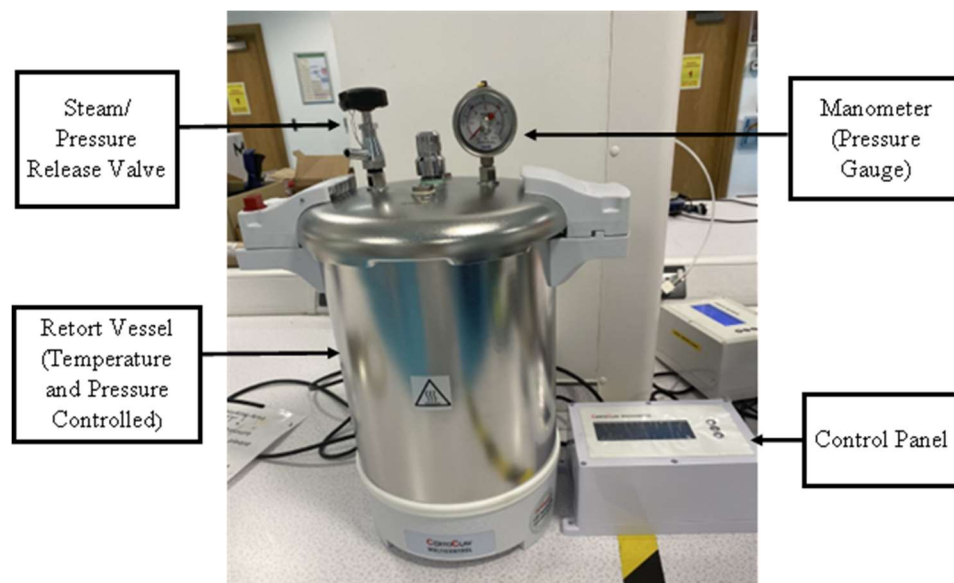


Figure 3.5 Labelled image of the CertoClav Multicontrol 2 autoclave used for retort processes

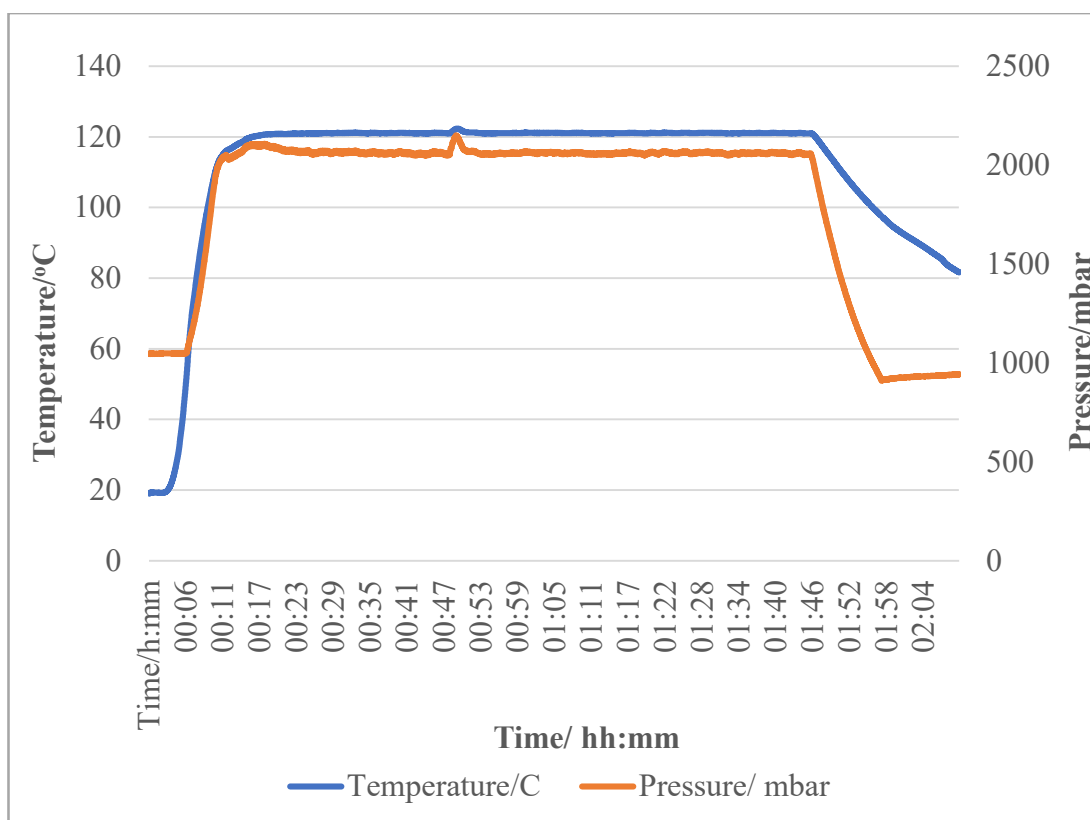


Figure 3.6 Temperature and pressure data for the validation of the Certoclav MultiControl 2 retort apparatus used for this research

Four kilner jars were filled to 80% capacity, each with a different simulant solution. The simulant solutions were selected to replicate some of the chemistry of common foodstuffs that are subjected to the sterilisation process, see *Table 3.2*. It should be noted that other chemical species may be present in the foodstuff that are not accounted for in the food simulant, however, the main active species that cause material degradation are accounted for and enabled initial laboratory trials to be completed. Four samples were placed inside each jar with care being taken to ensure the samples were in minimal contact with each other. A lid with a rubber seal was labelled with the simulant used and the jar sealed with the lid. Deionised water, with a pH of ~7, was added to the base of the autoclave past the minimum fill line. The four filled jars were placed in the base of the autoclave as per *Figure 3.7* and *Figure 3.8* and the lid sealed shut. The autoclave was set to retort the solutions at a pressure of around 1.2 bar at 121°C, held for 90 minutes. Once completed the apparatus and samples were left to cool before the lid was removed.



Figure 3.7 Sample loading and inside of the retort apparatus

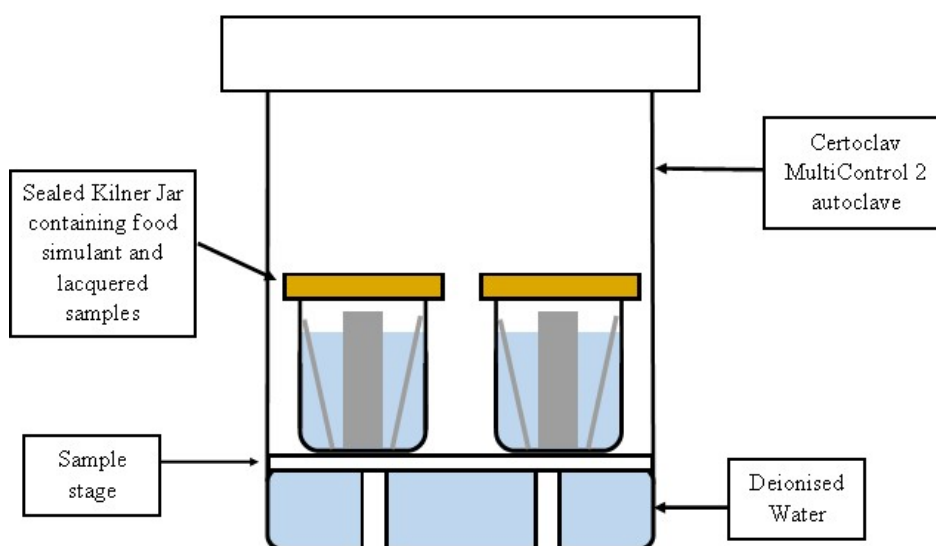


Figure 3.8 Labelled schematic of the inside of the retort vessel

3.2.4 Scratch Testing

Once the samples were cooled sufficiently adhesion testing was completed using the Sheen BS3359 Automatic Scratch Tester, with a 1mm tungsten carbide tip, pictured in *Figure 3.9* (76). To operate the instrument the sample was clamped in place and a weight added to the machine. The machine was turned on and the metal needle moved automatically along the surface of the sample when set to 'scratch'. When the weight was sufficient to remove the lacquer and expose the metal surface, then the metal needle and the steel substrate made direct contact. This direct contact enabled an

electrical circuit to be completed and a voltage spike was observed on the reader. An overview of how this occurs is shown in *Figure 3.10*.

Any spike in voltage was classed as a failure of the coating. To establish the exact value the weights were decreased accordingly until a ‘failure weight’ was established. This is the minimum weight required to remove the lacquer. In instances where no voltage spike was observed the weight was gradually increased until the ‘failure weight’ was established. The failure weights were converted to failure forces using *Equation 2.1*. The error in the failure force values was calculated using *Equation 3.1*.

$$\text{Std. Error} = \frac{\text{Stdev.P}}{\text{Sqrt}(\text{number of values})} \quad (3.1)$$

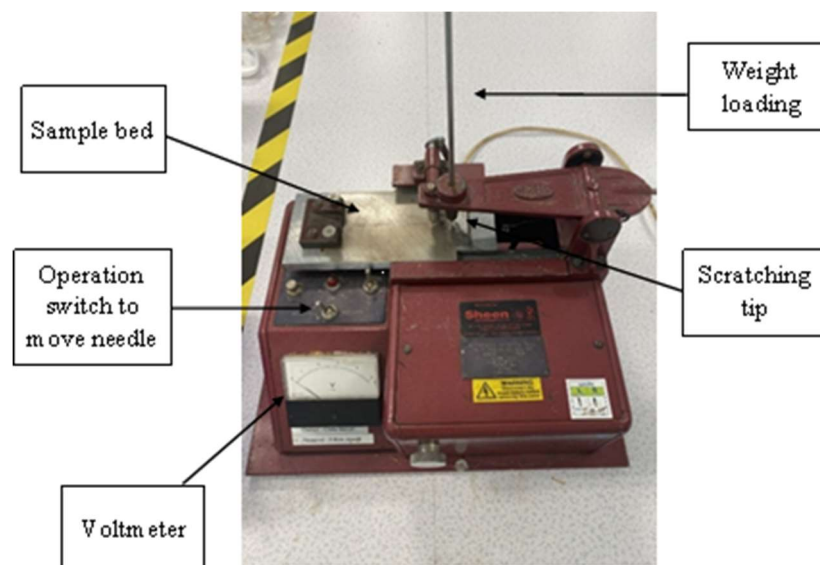


Figure 3.9 Labelled image of the sheen automatic scratch tester BS3359 used to establish failure forces of the samples post-retort

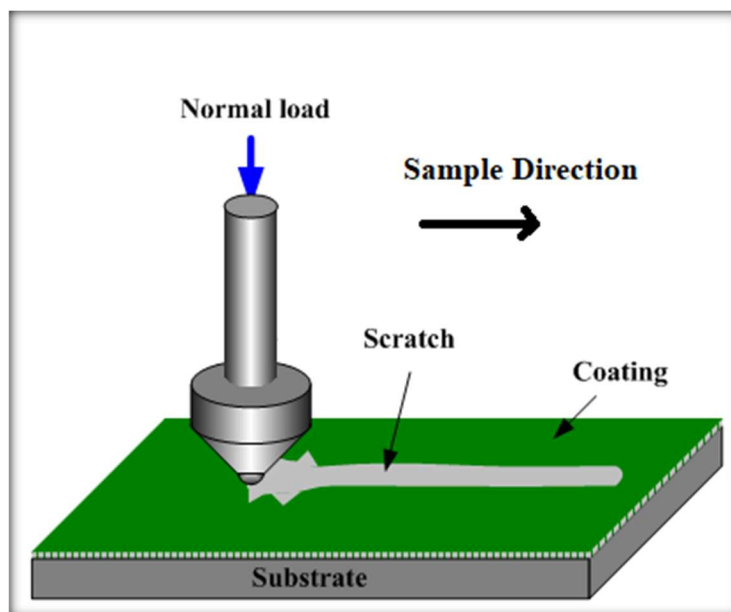


Figure 3.10 Schematic showing how the scratch test is performed (123)

It should also be noted that the post-retort adhesion values presented in this piece of work were measured directly after completion of the retort process to demonstrate the stage in the lifecycle where the can performance is most compromised. Post-retort adhesion has been shown by several researchers such as Allman *et al.* to improve over time and return to near its pre-retort state. (10) Therefore dry adhesion measurements provide a valuable insight into the long-term performance capabilities of food packaging materials.

3.3 FTIR-ATR Spectroscopy

FTIR-ATR spectroscopy is a well established and widely used method for organic sample analysis (44,124–127).

The degradation of polyester coatings in salt solution were studied using FTIR-ATR spectroscopy. The BPANI coated TCCT samples were prepared and retorted as described in *Sections 3.2.1, 3.2.2 and 3.2.3.*

The simulants used were:

- Deionised water
- 0.5 and 1.0 % w/v NaCl Solutions

For the purpose of this work, FTIR-ATR spectroscopy was selected as it allows a broad range of samples to be analysed and unlike conventional IR spectroscopy, it is non-destructive and no sample preparation is required. This is particularly important for this piece of work where the lacquer cannot be removed from the substrate surface. The use of a UATR accessory means that the IR light travelling through the crystal is totally internally reflected at the crystal-sample interface as per *Figure 3.11*. This occurs at least once before the sample reaches the FTIR detector. During total internal reflection some of the IR light enters the sample and can be absorbed, known as the evanescent wave. The depth of penetration of the evanescent wave is determined by the difference in refractive index between the ATR crystal and the sample. As a result several materials are utilised as ATR sensors to account for the variation in refractive indexes of materials. The FTIR detector measures the reflected IR beam and produces an FTIR spectra (128).

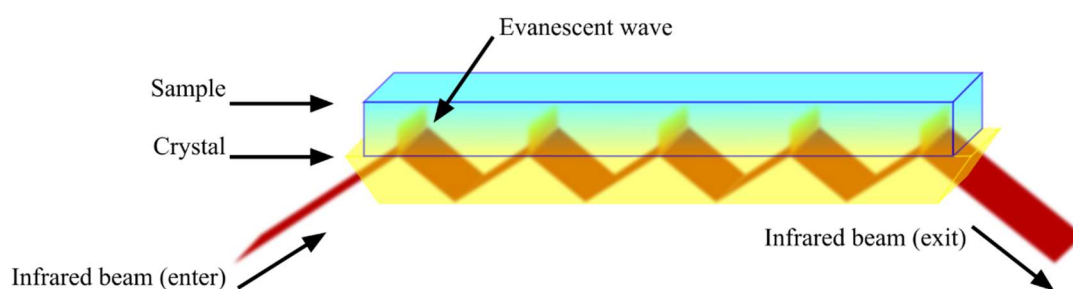


Figure 3.11 Labelled schematic showing total internal reflectance of an IR beam within an ATR crystal (129)

The BPANI coated TCCT samples were analysed in duplicate using a Perkin Elmer Spectrum 100 FTIR Spectrometer with a UATR accessory which is pictured *Figure 3.12*. The sample was placed coating side down covering the crystal and pressure was applied using the sample pressure control. The pressure was increased gradually until an optimal intensity for the spectrum was achieved. The sampling depth of the UATR accessory was a few microns. The same pressure was used for each sample to ensure consistency. A requisition time of 30 seconds was sufficient to reduce the signal to noise ratio to a level where it did not impinge on peak identification. A scan range of range of 4000 to 450 cm^{-1} was selected as it encompassed all of the absorption frequencies for different bond vibration types. This was crucial to be able to study any chemical reactions that may occur during the retort process and result in formation of new chemical bonds and breaking of others. A resolution of 4 cm^{-1} used to give

smooth and clear, well-defined peaks within the spectra which would enable a specific peak to be attributed to a particular bond vibration (130) . The spectra were processed using Perkin Elmer Spectrum IR software version 10.6.2.1159.

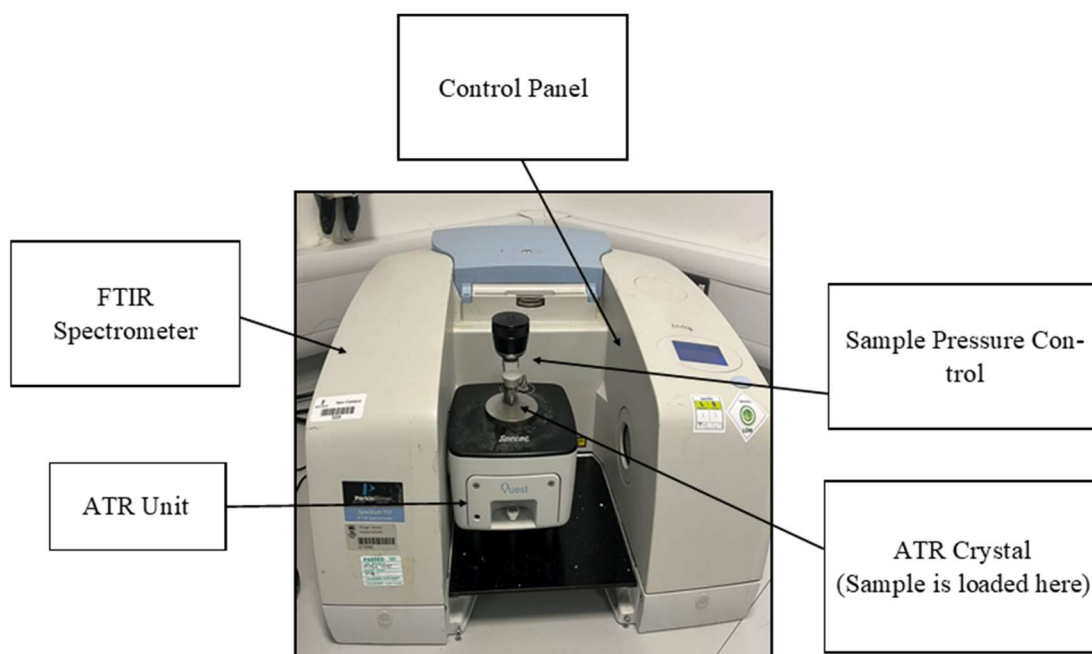


Figure 3.12 Perkin Elmer FTIR Spectrometer used for sample analysis

3.4 Filiform Corrosion Study

The aim of the FFC study was to gain further information about the corrosion resistance of the novel Cr(III) substrate and the BPANI lacquer. The intention was to assess their performance against the commercially available ECCS/EP which is established and known to provide adequate corrosion resistance properties. This was used as a benchmark to which TCCT/BPANI could be compared. PVB coated samples of ECCS and TCCT were used as a control to ensure FFC had been initiated correctly.

3.4.1 FFC Materials

The PVB and sodium sulfate solution used in the FFC study was prepared freshly at the beginning of the study, their constituents are detailed in *Table 3.3*.

Table 3.3 Chemicals used to produce materials for the FFC studies

| Chemical | Supplier | Purity | Use |
|---|-----------------|------------------------------|--|
| Sodium Sulfate Decahydrate, $\text{Na}_2\text{SO}_4 \cdot 10\text{H}_2\text{O}$ | Sigma Aldrich | 97%, reagent grade | Saturated solution with deionised water |
| Iron (II) Chloride, FeCl_2 | Sigma Aldrich | 98% | 2.5×10^{-3} M and 0.01M solutions made with deionised water |
| Poly(vinyl butyral-co-vinyl alcohol-co-vinyl acetate) | Sigma Aldrich | Average M_w 70,000-100,000 | For making PVB - 15.5% w/v in ethanol |
| Ethanol absolute | VWR Chemicals | $\geq 99.8\%$ ACS, Ph Eur | For making PVB - 15.5% w/v in ethanol |

3.4.2 FFC method

The TCCT samples used in this section of research were produced on the pilot line at TATA Steel, Ijmuiden. ECCS samples were provided by TATA Steel, Ijmuiden.

Sheets of both ECCS and TCCT were lacquered and cured with EP and BPANI lacquers using the same process outlined in *Section 3.2.1*. Steel samples were cut into 5x5 cm coupons. Two separate 10mm linear defects were scribed into the surface using a surgical blade, in order to expose the iron beneath. The experimental concentrations, volumes and conditions were adapted from previous research (22,131–133). FFC was initiated by pipetting 2 μ l of 2.5x10⁻³ M FeCl₂ solution into each defect. The samples were elevated inside a transparent plastic container containing saturated Na₂SO₄.10H₂O to maintain the relative humidity levels required for FFC initiation. The experimental set-up is shown in *Figure 3.13*. The temperature was held at 20°C (22). A Lascar EasyLog temperature and humidity EL-USB-2 data logger was kept in the container for the duration of the experiment to ensure the temperature and humidity were consistent.

A camera was set up in a Photosimile light box and the samples were removed from the container at regular intervals, photographed to capture images of the FFC propagation and then replaced into the container. A total of two samples (one coupon) were used for each lacquer/substrate combination.

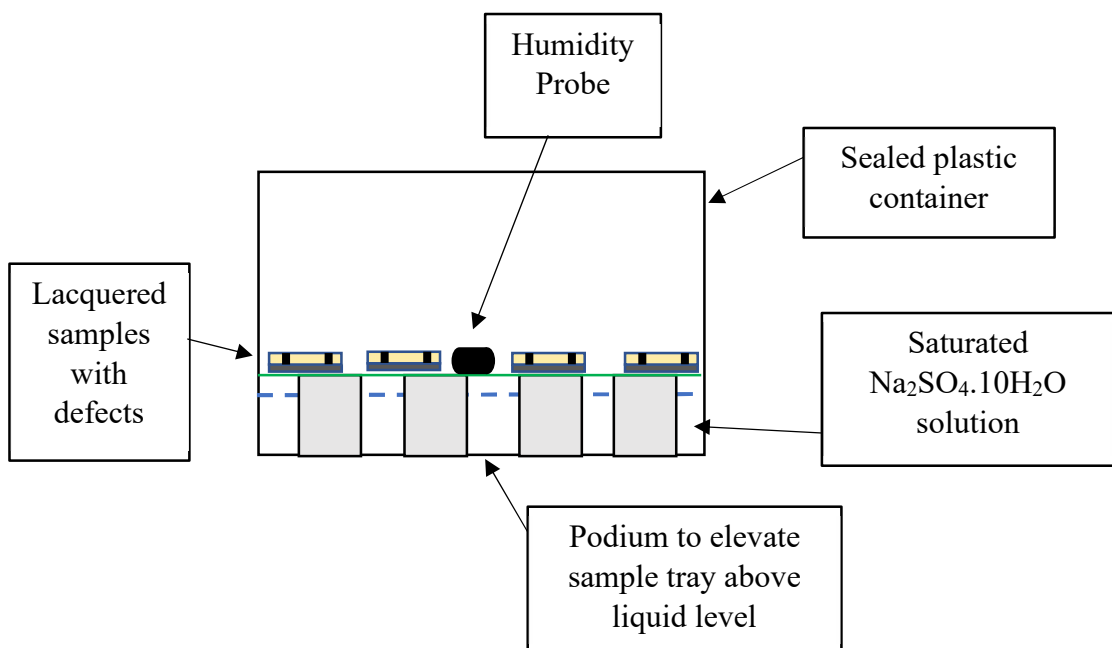


Figure 3.13 Diagram showing the set-up of a FFC experimental study

The above method was repeated using 2 μ l of 0.01M FeCl₂ solution and with the addition of 15.5% w/v PVB coated samples as a control to ensure FFC was initiated correctly. The PVB coating was conducted using a glass rod at room temperature and the samples were dried at room temperature for 24 hours. The thickness was controlled through the use of electrical tape on the edges of the sample to obtain a dry film thickness of \sim 30 μ m.

3.4.3 FFC Area Analysis

FFC images were analysed using ImageJ Software, Version 1.53e. The images were uploaded to the software and the defect area was cropped to select the analysis area. This was selected as 260x390 pixels which is equivalent to 10x15 mm. The colour threshold of the images was adjusted until only the corroded area was highlighted as per *Figure 3.14*. The area that was grey in colour was considered substrate and anything that was not grey was considered to be FFC. Several parameters including area were measured using the software, all output values were in pixels. These were converted to mm based on a conversion factor of 676 which was predetermined by using a ruler from the original images as a scale. Each pixel therefore represents 38.5 μ m. Area measurements are \pm 1 pixel equivalent to \pm 38.5 μ m

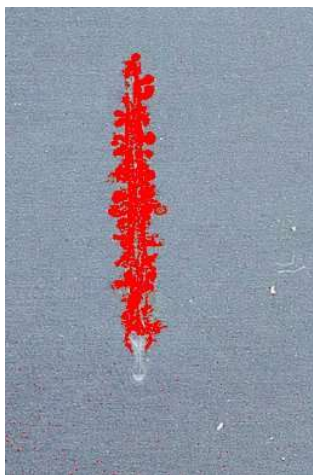


Figure 3.14 Example image showing the selection of the corroded sample area for numerical analysis using ImageJ

3.5 Uniaxial Strain

3.5.1 Dog Bone Samples

All dog bones samples were cut by TATA Steel, Trostre using samples from TATA Steel with various CrOx weights. The sample dimensions are outlined on the image shown in *Figure 3.15* (134).

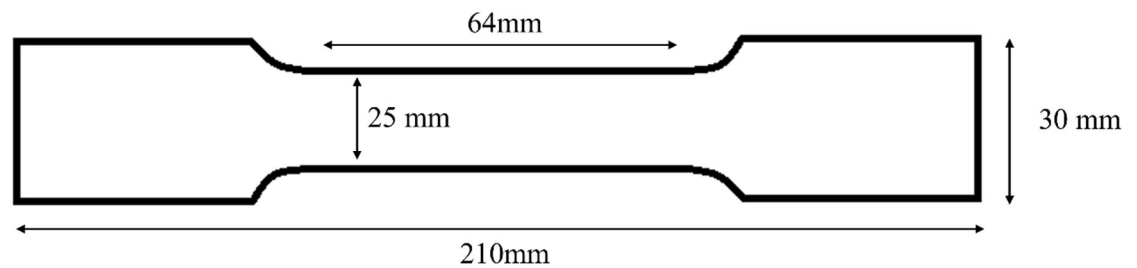


Figure 3.15 A dog bone sample with dimensions outlined

3.5.2 Hounsfield Tensile Tester

A Hounsfield Tensile Tester instrument shown in *Figure 3.16* was calibrated with the parameters in *Table 3.4*. Industrial can making speeds can exceed 5000 mm s^{-1} which is not in the same range as what can be achieved with a laboratory scale instrument. The speed selected for this experiment was selected to be safe for the operator whilst also considering that the straining speed would still not reflect a true can making apparatus even if the instrument was operated at maximum speed. It has been demonstrated that an increase in strain rate correlates with an increase in elongation percentage, however, this relationship is non-linear (135). It is important to consider this when selecting the extension values as at higher strain rates these maximum extension values may correlate to higher strain values.

Table 3.4 Instrument Calibration Parameters for Sample Straining

| Parameter | Numerical Value |
|--------------------|-------------------------|
| Speed | 3 mm min^{-1} |
| Record Repeat Time | 1 second |
| Maximum Load | 25 kN |
| Maximum Extensions | 0.64/3.2/6.4/9.6 mm |

The samples were loaded into the clamps and the clamps were tightened. They were extended up to a maximum extension which was predefined to be either 1, 5, 10, or 15% of the gauge length of 64 mm. These were selected to cover a wide range of strain values up to the maximum of 20% seen within a food can (136). The actual extension of the samples was measured after sample deformation and the true strain values were calculated.

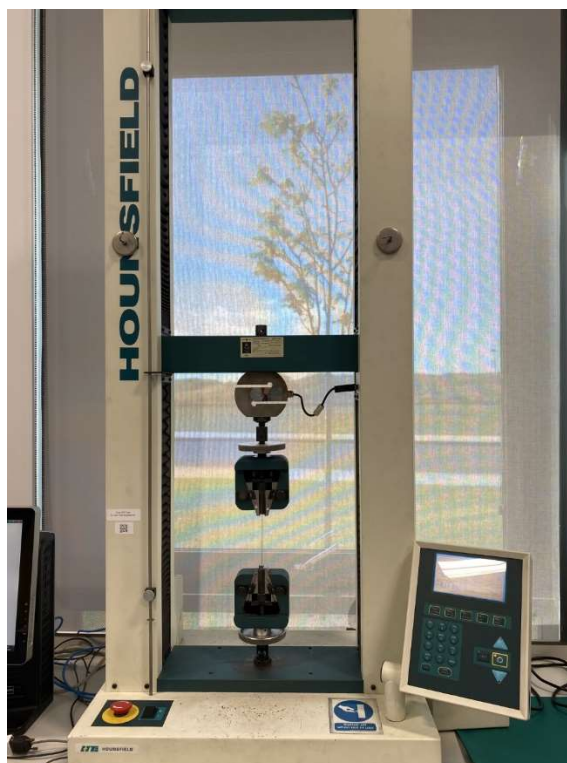


Figure 3.16 The Hounsfield tensile tester used for straining the TCCT/ECCS samples, maximum load of 25 kN

After the samples had been strained, they were lacquered using the same process as described in *Section 3.2.1*. The ends of the samples were cut off such that the total sample length was 120mm in order for the samples to fit in the retort jar and scratch tester. The samples were then sealed, retorted and scratch tested using the same procedure as described in *Sections 3.2.2, 3.2.3 and 3.2.4*. The simulant solutions selected were DI water and 1% NaCl as these represent both extremes of food

simulants and their influence on lacquer adhesion. Dry adhesion of each strain value was also measured for comparison purposes.

3.5.3 SEM

Surface images were taken of unlacquered samples of low, medium and high CrOx weight TCCT and ECCS which were strained at 0, 5 and 15%. In the SEM images the straining direction of each sample is denoted by SD and the rolling direction is denoted by RD. The samples were imaged using either a TM4000 Plus Hitachi SEM or a FEI Quanta 600 FEG-SEM. The working distance (WD) for all images were between 8 and 12 mm. The accelerating voltages (HV) were 15 or 20 kV.

3.6 Surface Metal Identification

Quantification of free iron and chromium on a surface gives an indication of the uniformity of a CrOx coating. An adaptation of the Preece Test (137) has been applied successfully by Dodd to quantify copper deposits on a chromium coated steel surface (120). Since iron and chromium are more electronegative than copper in the electrochemical series they can displace Cu^{2+} ions from Copper Sulfate solution. The displacement reaction results in a precipitate of copper being deposited on the surface at sites where free iron or chromium are present i.e. where the coating is non-uniform and the metal below the CrOx layer is exposed. This is significant as this will impact product performance when the coated substrate is used in packaging steel. Since the copper on the surface is deposited only on sites where free iron or chromium are present then the amount of surface covered with copper should correlate with the amount of iron/chromium present i.e. a higher percentage of copper means more exposed chromium/iron. It is of importance to consider that copper nodules are known to form in a mushroom shape so the actual numerical value for copper area on the sample surface is not a true reflection of the exact value (120). Despite this it enables accurate comparison between different samples and conclusions can be drawn on the uniformity of the surface.

Unlacquered samples at low, medium and high CrOx weights were prepared by uniaxially straining them at 5 and 15% using the method outlined in *Section 3.5.1 and 3.5.2* and biaxially straining at dome heights of 1-5mm (7-20%) using the method

outlined in *Section 6.2*. Unlacquered, unstrained samples were also used for comparative purposes.

Table 3.5 Chemical constituents used to produce the Copper Sulfate solution

| | | | |
|----------------------------------|------------------|--------|--|
| Copper (II) Sulfate Pentahydrate | Sigma Aldrich | 98+% | 8g w/v in 500ml deionised water with 2 ml H ₂ SO ₄ |
| H ₂ SO ₄ | Sigma Aldrich | 95-98% | 27 g/L w/v in deionised water |

A copper (II) sulfate solution was prepared from 8g CuSO₄.5H₂O and 2ml H₂SO₄ in 500ml of deionised water as per *Table 3.5*. The samples were dipped in the copper (II) sulfate solution for 60 seconds then removed and rinsed with deionised water before being drip dried prior to analysis. The samples were imaged using a Keyence VHX-7100 optical microscope and 3D depth profiling to produce in-focus images. All images were taken at 1000x magnification and have a scale bar of 50µm. The images were analysed using ImageJ software by filtering the pixels by colour as per *Figure 3.17*, in order to differentiate between the copper and the CrOx surface. The number of pixels that were a different colour to the surface were measured and this was used to calculate the percentage of copper on the surface.

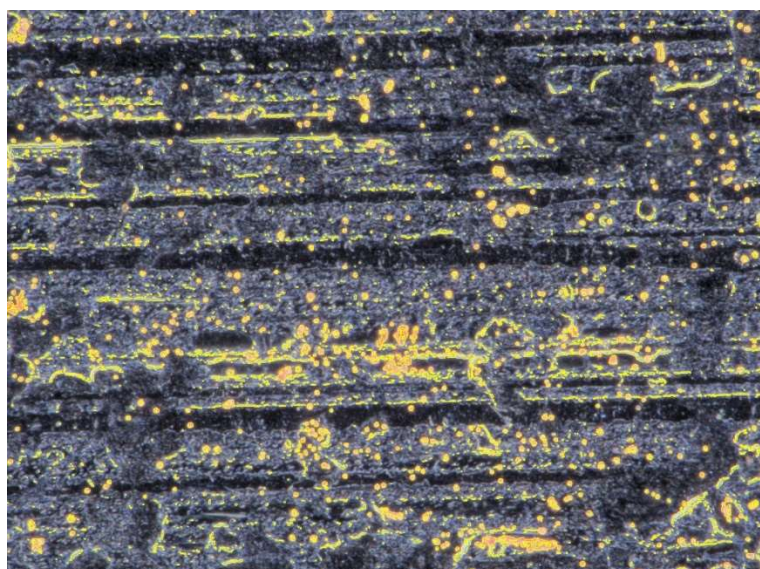


Figure 3.17 Filtered image of a TCCT sample showing how the surface copper was measured in Image J

3.7 Conclusion

This chapter has given an in-depth overview of materials and methodology that will aid the reader in understanding how the research has been conducted. These materials and methods have been utilised throughout to simulate can lacquering and the food sterilisation process used in industrial settings. Further methods such as FTIR-ATR spectroscopy and FFC are also outlined as these are well-established and have been adapted for this work.

Chapter Four

The Influence of Food Simulant Concentration and CrOx Weight on Lacquer and Substrate Performance Pre- and Post-Retort

4 The Influence of Food Simulant Concentration and CrOx Weight on Lacquer and Substrate Performance Pre- and Post-Retort

4.1 Introduction

The legislative pressure which has led to the development of a novel can making substrate, in conjunction with the drive to make the protective lacquer BPA free has resulted in new materials being developed. There is limited research into the performance of these materials and their suitability for commercial use (8,10,18).

The influence of the food stuff, the lacquer type and the CrOx coating weight are some key factors in determining the adhesion of a lacquer to a substrate post-retort. The conditions required for sterilisation mean that both the substrate and lacquer are subjected to high temperatures, pressure, and moisture during the retort process. These can all impact the adhesion and other materials properties meaning it is important to extensively study the substrates and lacquers to gain an insight into their suitability for long term food storage. Other factors such as current and bath chemistry used during electroplating may also influence the final substrate, however, these are not explored in this section.

There were several aims of this section of the research. The initial intention was to understand the performance of commercially available and developmental lacquers and substrates during the food sterilisation process using different food simulants. The purpose was to establish which food simulants impacted the adhesion and performance the greatest and select the most influential food type for further analysis. A variation in CrOx coating weight for the developmental and commercial substrates was provided and used to distinguish between the influence of the substrate coating weight and the influence of the simulant solution. The same studies were also run on a newer developmental batch of TCCT which has been produced after process improvement and supplied to the customer for internal packaging tests. In order to compare the different lacquers and substrates, dry and post-retort adhesion were studied for each sample type and the ECCS substrate and EP lacquer were included for comparison purposes.

To ensure consistency across all samples and to ensure the samples match those of substrates that would be manufactured at TATA Steel the following conditions were used:

- Consistent and even lacquers within the range of 7-12 μm – pre-defined by the customer
- Reproducible adhesion values within ± 1 N of each other – this is to remain consistent with previous work conducted using the same methodology and substrates
- CrOx weight variation in samples in the range of 4-25 mg m^{-2} which vary due to the difficulty in controlling the electroplating process parameters – limited information was supplied by TATA Steel regarding the processing parameters
- Comparison of all results to ECCS/EP as this is commercially available and therefore its adhesion is acceptable – useful tool for comparative analysis and deciding whether the performance of developmental material is suitable for the intended application

All measurements were carried out in accordance with the methodology outlined in *Section 3.2*. Based on previous research multiple simulants were selected to provide a broader understanding of the effects of different food simulants on the can substrate and organic lacquer. It was essential to use varied CrOx weights substrates as it has been demonstrated by previous research that there is a correlation between CrOx weight and lacquer adhesion (8,120).

Water uptake has been observed in organic can coatings and has been proven to reduce the adhesion of the lacquer to the substrate and compromise the integrity of the packaging material (126). The aim was to study the level of water uptake in polyester coatings using FTIR-ATR spectroscopy and establish the influence that both food type and CrOx coating weight have on the amount of water absorbed by the coating. The presence of water in a coating can increase corrosion, lead to swelling and cracking/peeling of the lacquer and reduce the overall lifespan of the lacquer (138).

Corrosion of un-lacquered substrates is known to occur within a humid environment containing a corrosion initiating species, similar to that within a food can. Can making substrates are lacquered in order to prevent this corrosion from occurring however any defects in the lacquer such as those caused by denting would expose the substrate beneath and leave it susceptible to corrosion (22,43,131). FFC is one particular corrosion type that commonly occurs within a food can and as such was selected for study in this piece of work.

All of these studies were conducted with the aim of establishing how different conditions within the can making and food sterilisation processes affect the lacquer and substrate. It was the intention of the researcher to comparatively study both the developmental and commercial lacquers and substrates to establish if the TCCT/BPANI combination is a suitable replacement for ECCS/EP to meet legislation. Several important internal can conditions were considered such as food simulant type, humidity, moisture and corrosion protection.

4.2 Materials and Methodology

The materials and methods used in this section are outlined in *Chapter 3*. For initial food studies solutions used are detailed in *Table 3.2* Food simulants use for this research, their composition and chemical information. For salt studies deionised water and salt solutions between 0.25% and 1.0% w/v NaCl were used.

4.3 Multi-simulant testing

Dry adhesion and multi-simulant testing was conducted for both EP and BPANI coated TCCT and ECCS substrates, the results of which are shown in *Figure 4.1*, *Figure 4.2* and *Figure 4.3* and discussed further in *Sections 4.3.1* to *4.3.4*.

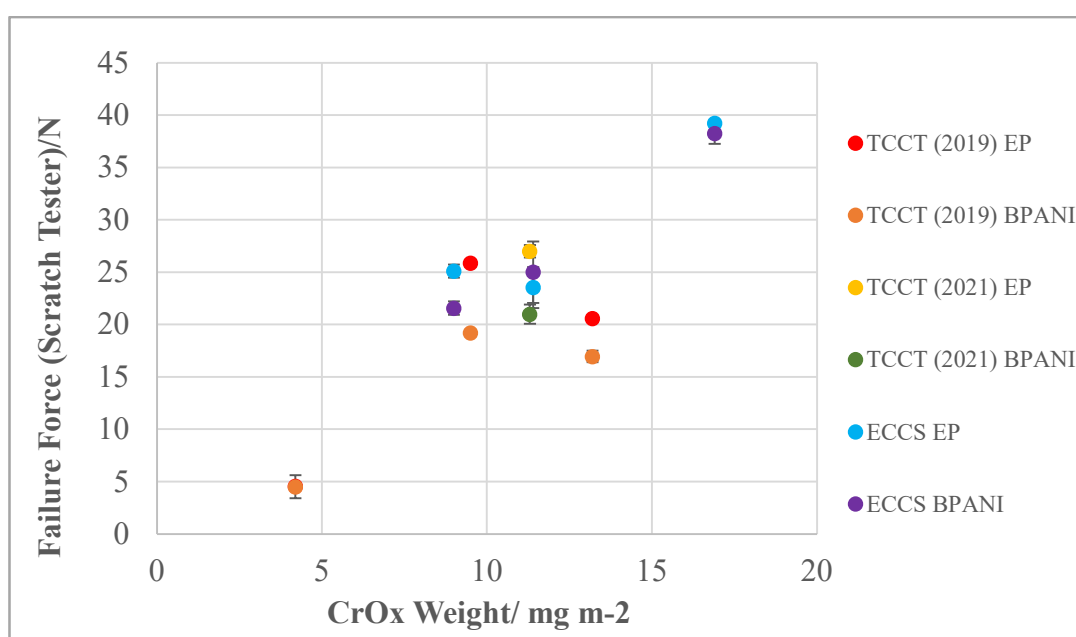


Figure 4.1 Dry adhesion of BPANI and EP lacquers to ECCS and TCCT substrates

4.3.1 Dry Adhesion

Dry adhesion results as shown in *Figure 4.1* can provide a useful insight into the performance of each lacquer before any chemical or physical changes occur during the food sterilisation process. These changes could be due to the influence of the food simulant, heat or humidity. It can also be used as a standard value to which all other adhesion results can be compared for that particular lacquer/substrate combination as the performance is optimal (73). Dry adhesion measurements are a useful quality control tool as they can give an indication of incorrect lacquer curing or lacquer contamination (10). In this instance, the general trend in data shows an increase in failure force as the CrOx weight on ECCS is increased. The relationship between CrOx

weight and failure force for TCCT substrates is non-linear suggesting there are other substrate factors affecting the performance not just the quantity of CrOx present. It should be noted that despite the true failure force values being lower for BPANI than EP, the failure force of the BPANI lacquer is still at a similar level and therefore any reduction in performance seen post-retort may be as a result of the food simulant or retort conditions altering the lacquer properties. These findings are in line with the findings in literature (10,120).

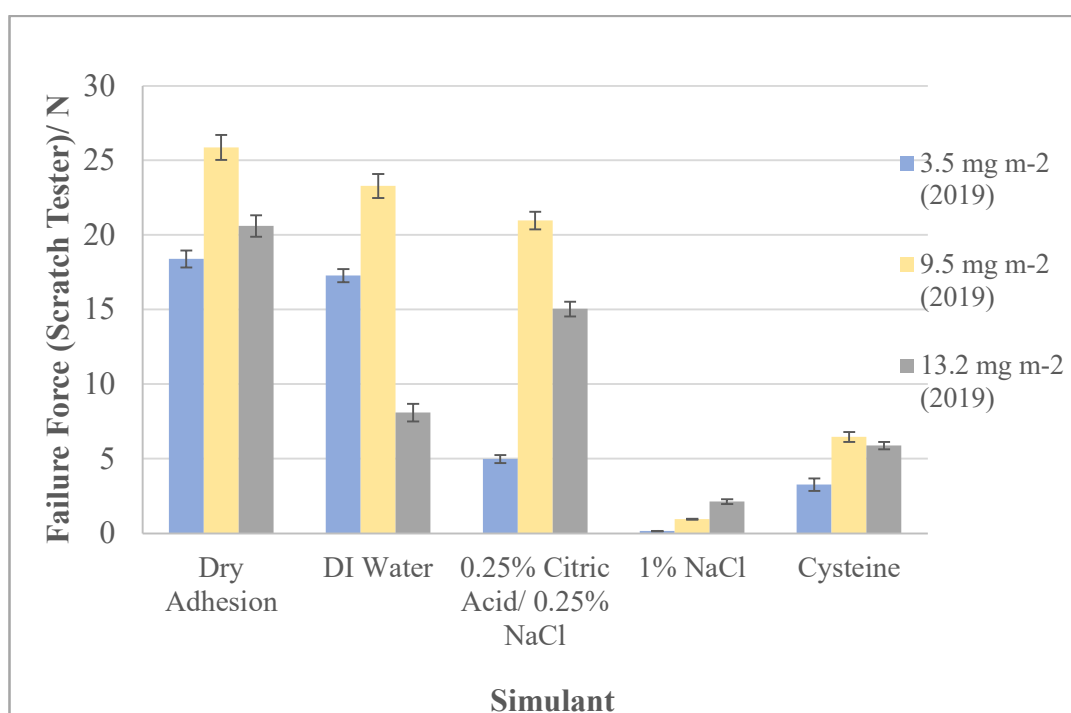


Figure 4.2 Failure force of EP coated TCCT after retort in various food simulants

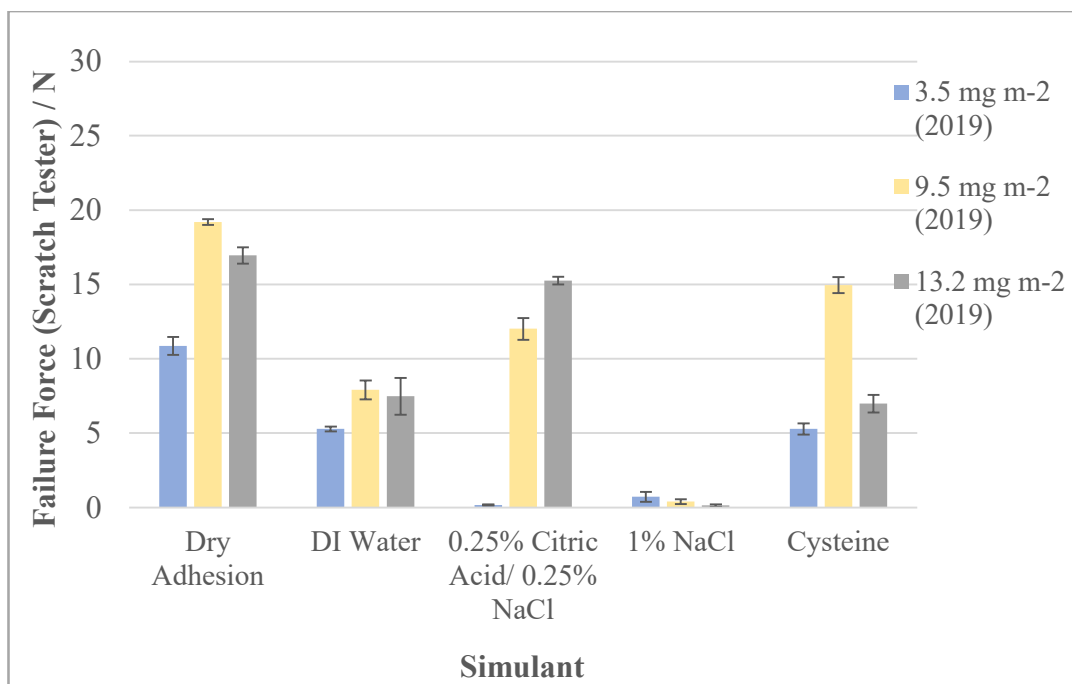


Figure 4.3 Failure force of BPANI coated TCCT after retort in various food simulants

4.3.2 DI Water

Retorting samples in DI water gives an accurate representation of the influence of the sterilisation conditions on the post-retort adhesion performance independent of the influence of a food simulant. The presence of water alone causes a small reduction in the adhesion from dry adhesion values suggesting there is a small chemical/physical change in the lacquer/substrate interface. The failure force of the EP lacquer in *Figure 4.2* compared with the BPANI lacquer in *Figure 4.3* suggests that the water has a much greater influence over the polyester lacquer than the epoxy phenolic lacquer. It suggests that the polyester lacquer is subject to water ingress through the coating which reduces the adhesion between the lacquer and substrate and accounts for the reduction in failure force that is observed. The presence of water and heat can disrupt the lacquer/substrate bonding of BPANI, in addition to the water presence softening the lacquer. The combination of both of these effects can account for the drop in measured failure force. This is studied in more detail in *Section 4.5*.

4.3.3 Citric Acid, Cysteine and NaCl

The results in *Figure 4.2* and *Figure 4.3* demonstrate that the failure forces of the EP lacquer are generally higher than the BPANI lacquer, this inference stands for all food simulants with the exception of cysteine. The performance of both EP and BPANI coated TCCT in NaCl is very poor and little difference is seen in the failure forces

between the two lacquers in *Figure 4.2* and *Figure 4.3*. The increase in failure force of the citric acid/NaCl (pH ~3) combination compared with the NaCl alone shows that citric acid improves the adhesion where salt is present. The increase in adhesion is so significant that the performance of the samples post-retort in citric acid/NaCl is comparable to that of DI water. This improvement in adhesion is supported by Allman et al's research which showed that a citric acid pre-treatment prior to retort in NaCl increased the adhesion to much greater levels than a sample that had not been pre-treated (139). This suggests that the citric acid is passivating the surface by oxidising the metal and reducing the corrosive effect of NaCl during the retort process. This correlates with the improved adhesion seen as more sites for bonding are available on the substrate surface due to the chromium oxide layer. An increase in lacquer/substrate bonding means the lacquer provides a more uniform surface coverage with less defects through which corrosive species can penetrate and initiate corrosion (12). Previous work using fruit acids as inhibitors has shown them to be effective in reducing corrosion of steel (140,141). This suggests that free iron is exposed on the surface which enables this inhibition with fruit acid to work effectively. Conversely there is also the question of how the performance of the citric acid/NaCl would be altered if the free iron was not present on the surface.

The presence of salt has a catastrophic impact on lacquer adhesion suggesting that corrosion plays a significant and detrimental role on adhesion. It is of value to investigate how salt concentration impacts lacquer adhesion as it may help to identify mechanisms and provide recommendations for operational limits.

4.3.4 CrOx Weight

The failure forces for both EP and BPANI lacquers in *Figure 4.2* and *Figure 4.3* demonstrate a lack of correlation between CrOx weight and failure force. This suggests that the primary mechanism may simply be to do with the condition of the surface and whether any defects are present as opposed to the thickness of the chromium oxide layer. It is likely that the deposition current and the line speed used when electroplating which influence the uniformity of the CrOx layer will have a greater impact on the final performance of the substrate. It is also possible that if the CrOx layer was too thick then it could cause it to be brittle and as such less formable and more prone to cracking during the can forming process (120). This was not

investigated in this research; however, it is of significance for future research to aid in optimising chromium electroplating processes for can making.

4.4 Varying Concentration of Salt Solution and CrOx Weight

The significant negative effect that salt has on lacquer adhesion has prompted a more in-depth study of how increasing the concentration of salt simulant solution affects lacquer adhesion, the results of which are shown in *Figure 4.4* and *Figure 4.5*.

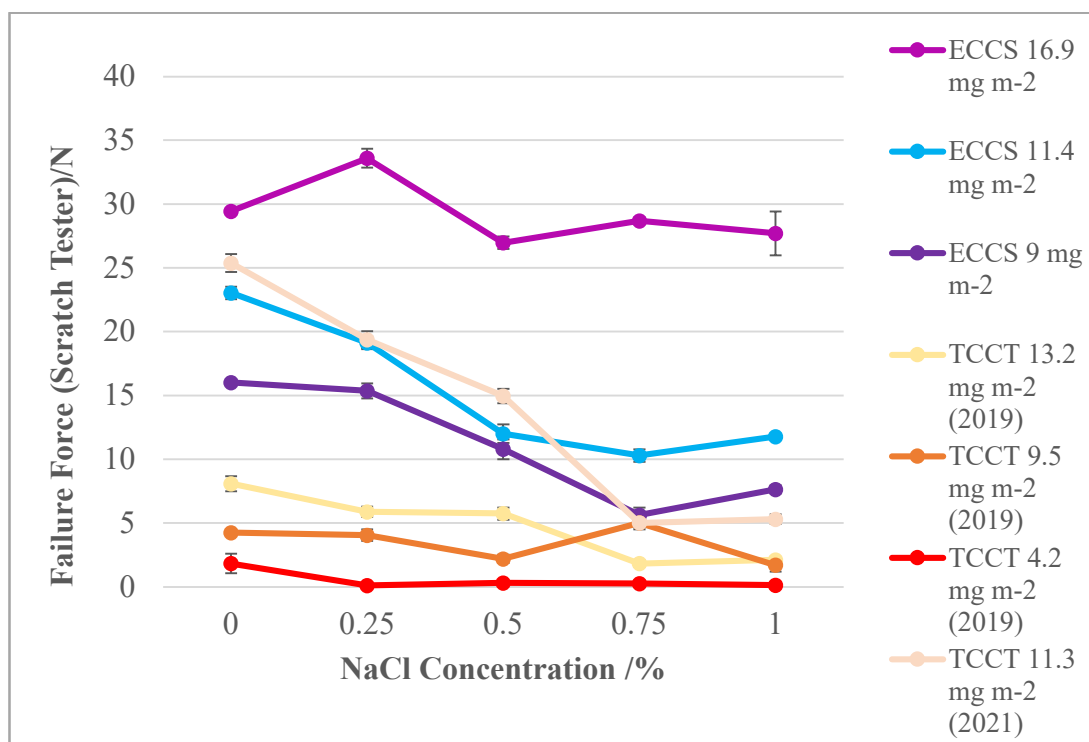


Figure 4.4 Failure forces for EP lacquer on different CrOx weight TCCT and ECCS substrates in varying concentrations of salt solution

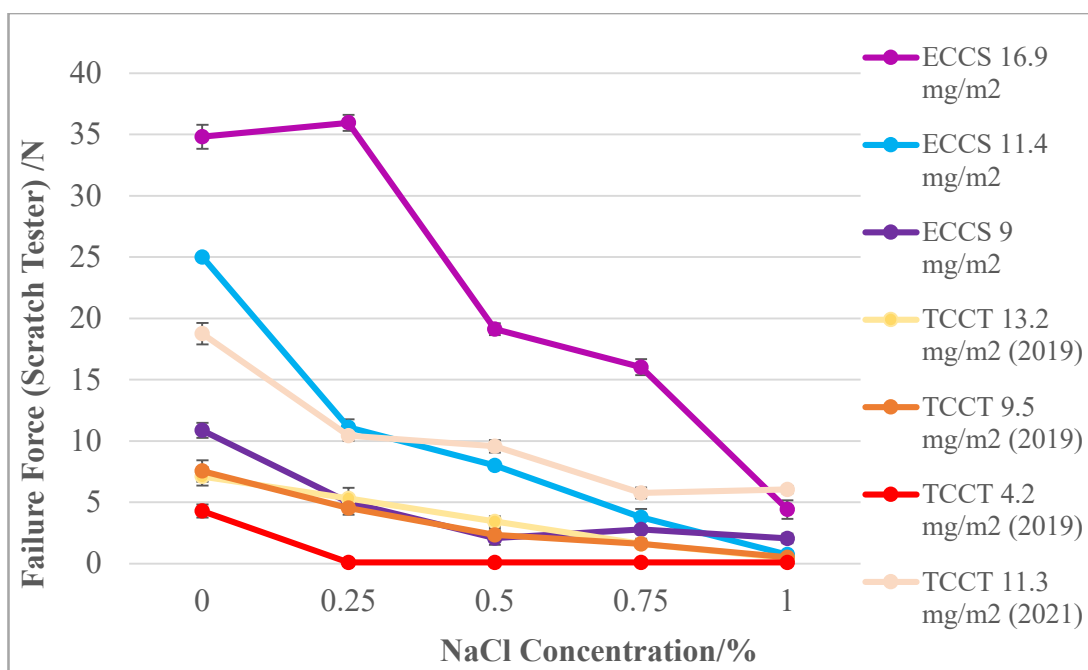


Figure 4.5 Failure forces for BPANI lacquer on different CrOx weight TCCT and ECCS substrates in varying concentrations of salt solution

4.4.1 DI Water/Salt

The adhesion of all substrate/lacquer combinations post-retort in DI water (0% NaCl) as shown in figures *Figure 4.4* and *Figure 4.5* are at an adequate level as the material performances are comparable to the dry adhesion results in *Figure 4.1*. When the samples are scratch tested after retorting in DI water the coating is pierced and exhibits the same behaviour as with dry adhesion. In instances where salt is added to the simulant solution it changes the failure mechanism as the coating peels when scratched tested (10). The introduction of salt into the simulant solution leads to changes in the adhesion mechanisms of EP and BPANI lacquers and as a result, changes in failure force are recorded. TCCT coated in EP lacquer does show a decrease in failure force as salt concentration increases up to 1%, however, this is less significant than for the BPANI lacquer, suggesting salt has a greater chemical influence on polyester than epoxy phenolic lacquers. At low NaCl concentration the CrOx weight is key to determining the adhesion level with higher CrOx weight substrates exhibiting higher adhesions than lower CrOx weight substrates. This is shown in the difference of failure force between the blue and purple lines in *Figure 4.4* and *Figure 4.5*. At higher NaCl concentrations all BPANI coated samples fail regardless of the coating weight or

substrate material. In conjunction with a reduction in failure force, delamination of the BPANI lacquer is also observed for some samples that have been retorted in high salt concentrations. The coatings exhibit visible peeling post-retort, prior to any adhesion testing being performed on the samples. It is well understood that an acid or base can act as a catalyst for ester hydrolysis in the presence of excess water (142–144). In order to confirm whether the delamination or reduction in adhesion are as a result of ester hydrolysis an FTIR-ATR spectroscopy study was conducted in order to study changes in chemical bonding and establish if hydrolysis was occurring.

4.4.2 CrOx Coating Weight

It has been demonstrated previously that CrOx coating weight has an impact on lacquer adhesion to a substrate (73). The results in *Figure 4.4* show the change in EP lacquer adhesion with increasing salt concentration across several CrOx weight substrates. Since EP/ECCS is a commercially available product the performance of EP/ECCS is acceptable for all CrOx weights with a general decrease in adhesion from higher to lower CrOx weights. This downward trend in overall adhesion is also observed for EP/TCCT but is less profound which most likely results from the overall lower performance, so any percentage changes are more difficult to observe on a 1N scale. From *Figure 4.5* it can be noted that a similar trend with CrOx weight and adhesion performance can be seen for BPANI coated samples. Despite this, the overall adhesion is generally lower, and the increasing salt concentration has a more profound effect on the adhesion of BPANI than it does with EP. At lower salt concentrations a decrease in CrOx weight correlates with a decrease in failure force with ECCS substrates outperforming 2019 TCCT substrates. At very low CrOx levels on 2019 TCCT, the CrOx weight has a significant impact on adhesion regardless of the lacquer used, this is exhibited by the red lines in both *Figure 4.4* and *Figure 4.5*. At lower CrOx weight there is more active surface exposed as the CrOx coating is thinner and therefore less homogenous due to the non-uniform nature of the blackplate. The roughness, which has been studied on these substrates previously, is not compensated for when using thinner CrOx coatings meaning that there are less lacquer substrate bonding sites accounting for the general reduction in adhesion observed (120). At higher CrOx weights there is a sufficient amount of chromium oxide to cover the steel surface so the impact of the CrOx weight on adhesion is much less. It is apparent that

the performance of 2019 TCCT substrates is not matched with ECCS substrates of similar CrOx weights. Based on the findings from this NaCl simulant study, the suitability of TCCT to replace ECCS would be dependent on: the final CrOx weight for each batch of TCCT; the surface uniformity, and its performance under the conditions to which the substrate must withstand.

Conversely, the performance of the 2021 TCCT substrate is at a similar level to that of the ECCS substrate at the same CrOx weight of 11 mg m⁻². This suggests that changes in the production process have been made to improve the homogeneity of the CrOx surface and reduce the amount of active surface that is exposed. Any improvements made to the production process have been significant in achieving the desired performance level of the developmental TCCT substrate making it a suitable replacement for ECCS providing the CrOx levels are high enough to meet customer requirements. The changes in these processes are reflected in the increase in failure force seen for the 2021 TCCT samples in both *Figure 4.4* and *Figure 4.5*. Further work is required to understand how the different generations of TCCT substrates vary and what changes have been made to the surface to improve the performance of the material.

4.4.3 Additional factors influencing adhesion

Other factors that may influence adhesion should also be considered when determining the suitability of a particular substrate and lacquer for use in can making

While food simulants are useful at replicating the impact on a substrate and lacquer during the food sterilisation process, they often present an extreme case of can degradation exacerbated by its contents. To achieve a truer reflection of the processes occurring within a food can this research could be repeated using the actual foodstuffs. Actual foodstuffs have a much more complex combination of chemicals some of which may counteract the effects of each other and reduce the impact this has on the lacquer adhesion and other material properties

Corrosion was observed during this section of research on the unlacquered parts of samples that were retorted in high salt concentration solutions. Since corrosion was not observed on the lacquered side it suggests that the lacquer is providing a good level

of corrosion protection for the underlying substrate. This raises a question about if corrosion would occur internally in the can if it were dented.

The current used in the electrodeposition process could have a significant influence on adhesion due to the high current used to compensate for using a higher line speed, resulting in hydrogen evolution (21). Defects such as pinholes may occur due to insufficient time for the hydrogen evolved to dissipate away from the metal surface (57). As a result of the presence of microdefects such as pinholes, this can cause failure at much lower values than would be observed on a defect free sample of the same substrate (145).

The study of the impact of salt concentration showed that even small quantities of salt can cause a significant reduction in adhesion, particularly at low CrOx levels and when a BPANI substrate is used. This suggests that some of the salt solution must be penetrating the lacquer and disrupting the lacquer-substrate bonding. To study this further FTIR-ATR spectroscopy will be used to study the chemistry at the interface.

4.5 Spectroscopic Analysis of the Influence of Salt Concentration on the Level of Water Uptake in BPANI Lacquers

Water uptake was visible in BPANI coated TCCT samples that had been retorted in high salt concentrations, examples of which can be seen in *Figure 4.10*. As a result, a further study was conducted using FTIR-ATR spectroscopy to compare the level of water uptake in different CrOx coating weights samples that were retorted in different salt concentrations. It should be noted that the sampling depth of the ATR crystal is a few microns and as such would not reach the CrOx/lacquer interface but will give a good representation of water uptake of the lacquer. Water uptake was not observed when EP lacquer was used, and it is surmised that the porosity of the BPANI lacquer enables transportation of water ions through the lacquer to CrOx surface at a much greater rate than with EP lacquer (68).

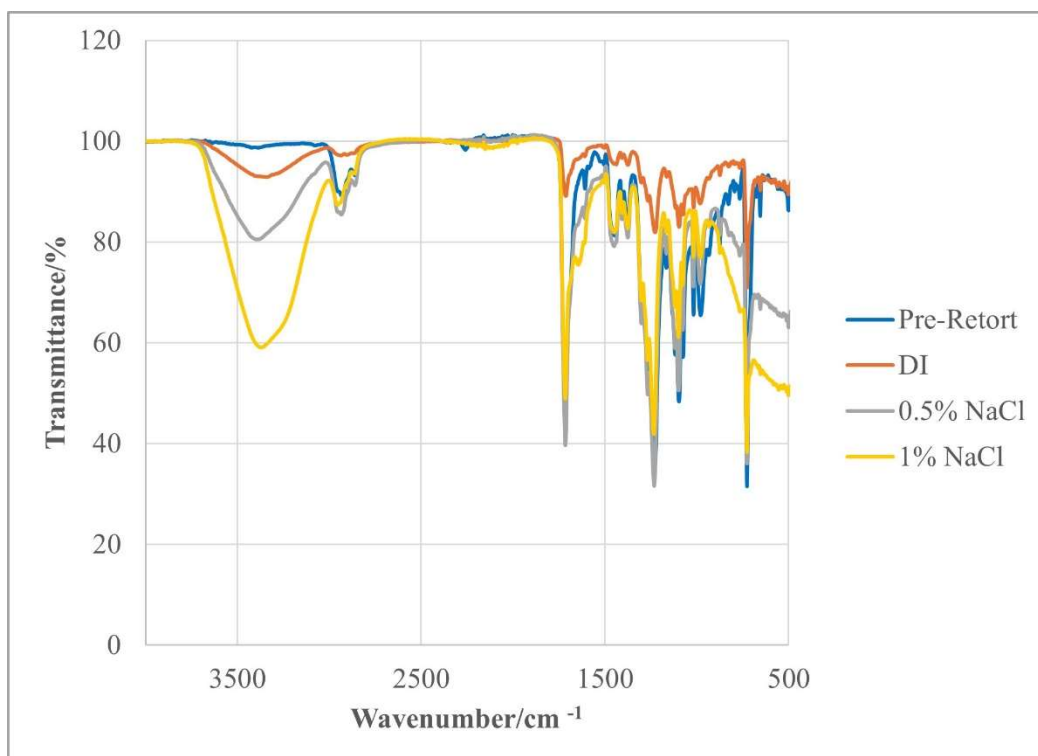


*Figure 4.6 FTIR spectrum for samples of 4.2 mg m⁻² CrOx weight (Batch 74) TCCT
Pre- and post-retort*

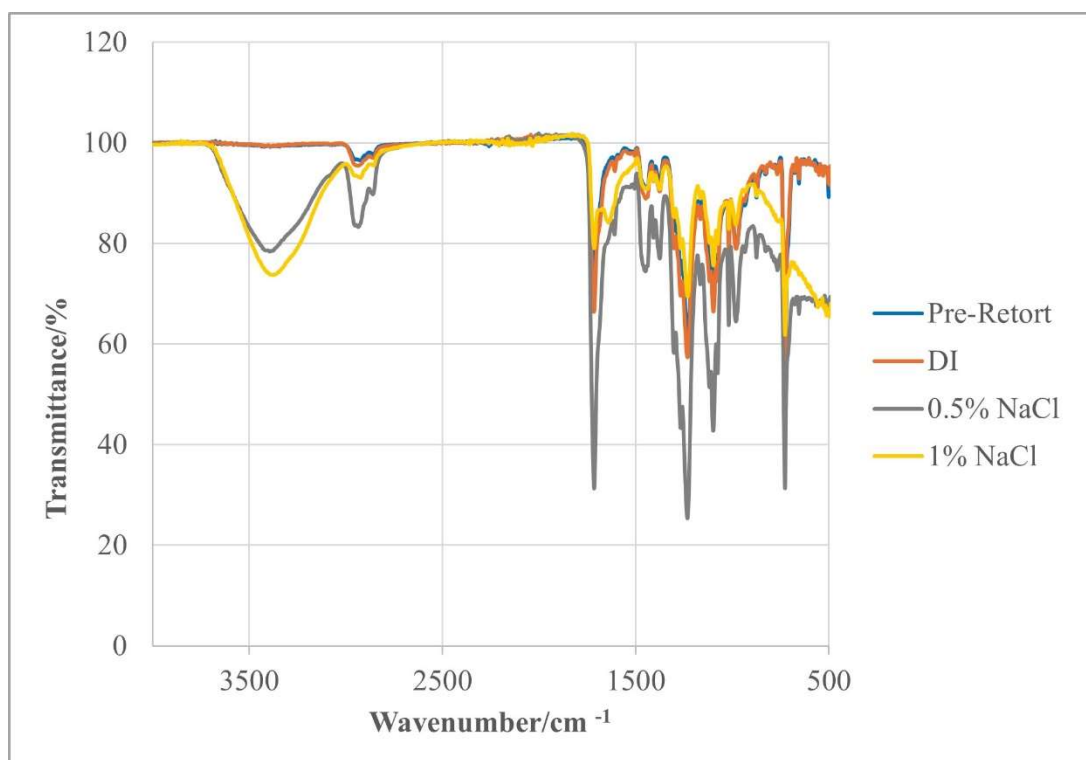


*Figure 4.7 FTIR spectrum for samples of 9.4 mg m⁻² CrOx weight (Batch 56) TCCT
Pre- and post-retort*

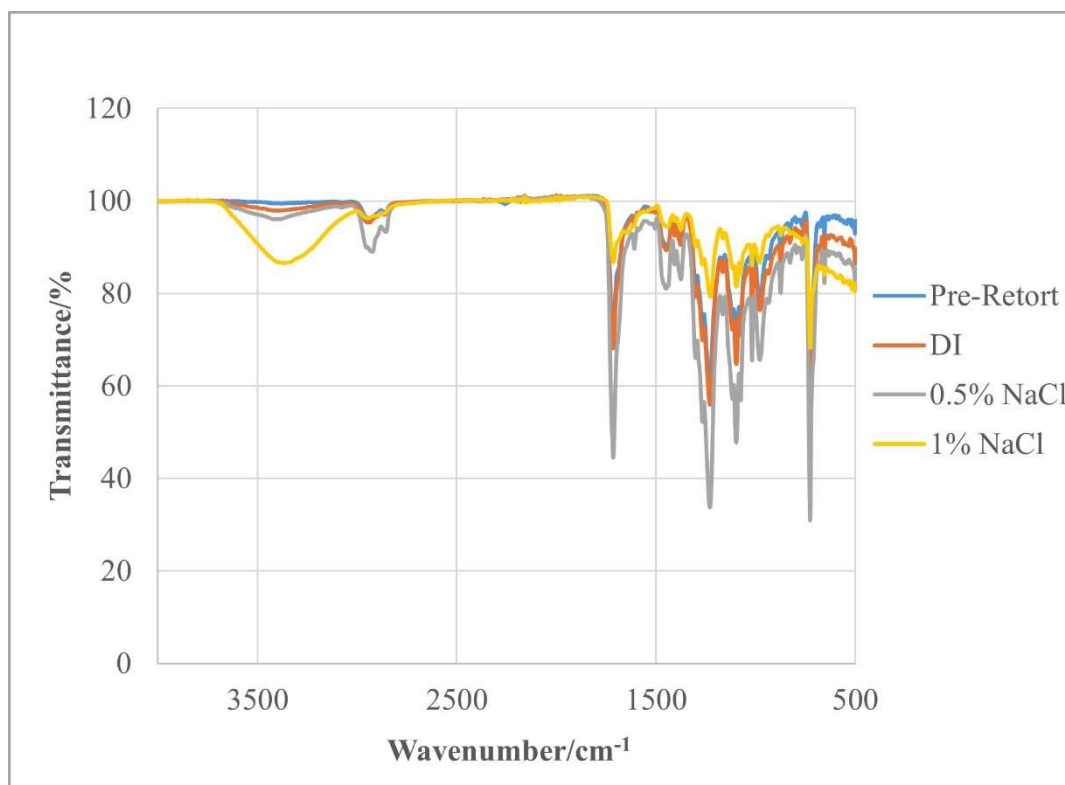


*Figure 4.8 FTIR spectrum for samples of 12.5 mgm⁻² CrOx weight (Batch 64) TCCT
Pre- and post-retort*

4.5.1 Simulant Influence

The spectrum in *Figure 4.6* shows that with increasing salt concentration there is more water present in the coating, this is shown by the increasing transmittance of the broad O-H stretching peak at $\sim 3400\text{ cm}^{-1}$ and the H-O-H bending peak at $\sim 1600\text{ cm}^{-1}$ (146,147). This is also observed for the higher CrOx weight coatings shown in *Figure 4.7* and *Figure 4.8*, however, it is much less prominent, and a significant change is only seen for 0.5 and 1% NaCl solutions. It should be noted that due to the presence of the carbonyl stretching peak at 1700 cm^{-1} the smaller H-O-H bending peak is masked and is therefore not accurately quantifiable as it cannot be distinguished.

The remaining functional peaks, such as the carbonyl stretching peak at 1700 cm^{-1} and the peak at 2900 cm^{-1} , which are characteristic of a methyl or ethyl ester group, are still present (148). If ester hydrolysis of the polyester lacquer had been initiated by the retort conditions and the presence of water and/or NaCl, the peak at 2900 cm^{-1} would not be present (149). It is clear that this is not the case so it can be surmised that a chemical reaction has not occurred. The spectral peaks present suggest that the salt

solution does not initiate a chemical reaction of the polyester coating but rather a physical change enabling water uptake. This is more significant at lower CrOx weights than higher CrOx weights (68).

Water uptake by BPANI has been quantified previously by Allman et al. (12) who demonstrated that adhesion decreased with increasing retort time, and this correlated with an increase in mass of the BPANI lacquer. Conversely, there was no significant water uptake observed with the EP lacquer. It has been proposed that if water absorption is occurring then this process should be reversible providing corrosion has not occurred and placing the sample in a dry environment enables the adhesion to return to near its original level (10). The significance of this is the performance of the product may be determined solely on this wet adhesion and is not indicative of its long-term performance capabilities. Conversely if a measurement is not taken soon enough post-retort, then it may not be a true reflection of wet adhesion and the sample may lose water and its adhesion will improve prior to analysis.

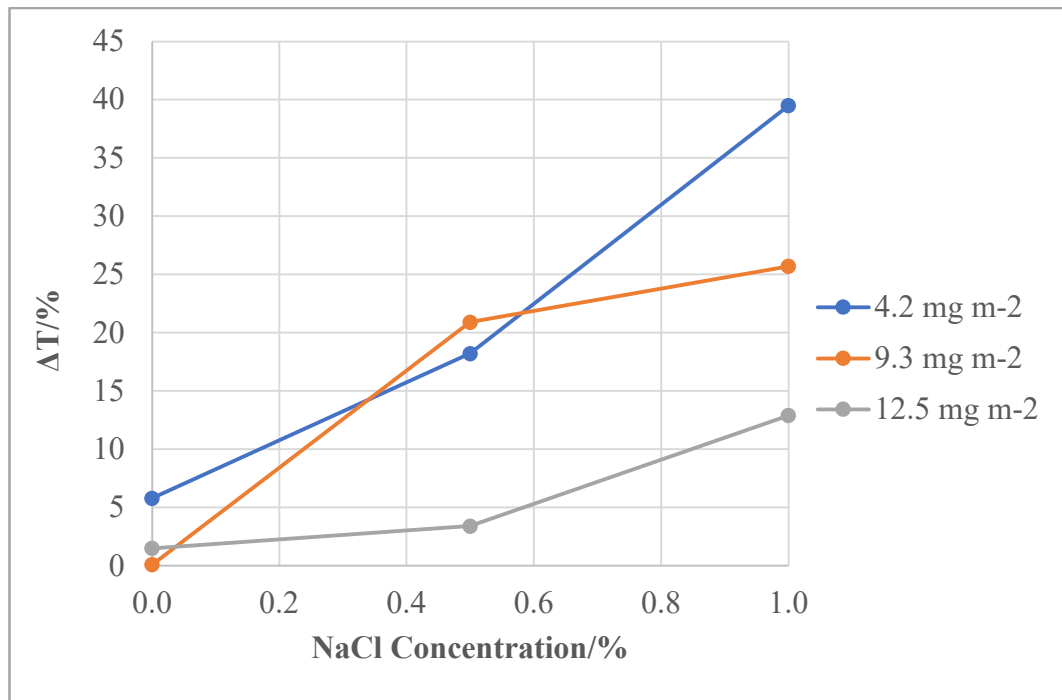


Figure 4.9 Change in Transmittance of O-H Bending Peaks at 3600cm⁻¹ with CrOx Weight and Salt Concentration for TCCT Substrates

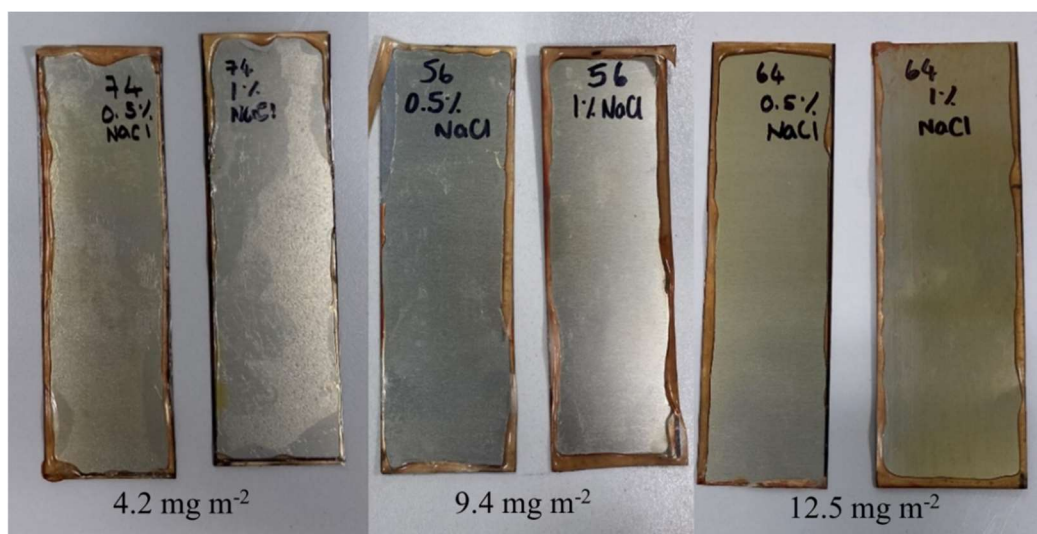


Figure 4.10 Images comparing the visible differences in the coatings on 120 x 40mm samples post-retort on different CrOx weight batches of TCCT.

4.5.2 CrOx Weight

The graph in *Figure 4.9* shows how the transmittance of low, medium, and high CrOx weight samples changes between the pre-retort sample and samples retorted in increasing salt concentrations. At 4.2 mg m^{-2} of CrOx on TCCT, the difference in transmittance between a dry sample and a sample retorted in 1% NaCl is 40%. Whereas for a 9.3 mg m^{-2} sample it is lower at 25% and significantly less at 13% for the 12.5 mg m^{-2} sample. From this data it can be deduced that the CrOx coating weight on TCCT is what influences the amount of water uptake rather than the salt concentration directly. When the CrOx coating is thinner (e.g. 4.2 mg m^{-2}) the influence of the salt solution that is present is much more profound on the substrate which then causes delamination of the coating, enabling water ingress. It is proposed that in the presence of NaCl, delamination of the lacquer occurs due to a cathodic disbondment mechanism. Due to the presence of sodium ions in solution, water/oxygen is reduced at the cathodic site on the metal surface and hydroxide ions are produced. This increases the local pH and promotes lacquer hydrolysis which weakens the lacquer/substrate bond leading to disbondment. Sodium ions increase the

ionic conductivity of the electrolyte and as such enhance corrosion processes which further reduce the bonding between the lacquer and substrate (150).

For the low CrOx weight batch at 4.2 mg m^{-2} the water under the coating in 0.5 and 1% NaCl solution is visible to the eye which can be seen in *Figure 4.10*. Some water ingress is seen for the 9.4 and 12.5 mg m^{-2} CrOx weight batches at 1% NaCl but it is much less significant than what is observed for the lower CrOx weight batch.

It is widely understood that the diffusion of water through the coating determines the time taken for delamination to occur. The process by which this water diffuses through the coating is determined by the coating thickness and the solution surrounding the samples (68). There are two routes by which reactive species can diffuse through a coating leading to cathodic disbondment and subsequently de-adhesion of the lacquer, these are through the intact coating and at the site of disbondment. It is proposed that if the lacquer is uniform then diffusion would occur through the coating. Once delamination of the lacquer has occurred then diffusion can also occur through the site of disbondment. This would speed up the process of delamination. The presence of water and cations (Na^+) within a food can will initiate this mechanism and provide the optimal environment for delamination to occur. The presence of chromate can improve lacquer adhesion and reduce the delamination rate. This can account for the improvement in lacquer adhesion that is observed with an increase in CrOx coating weight. This is demonstrated in *Figure 4.11*.

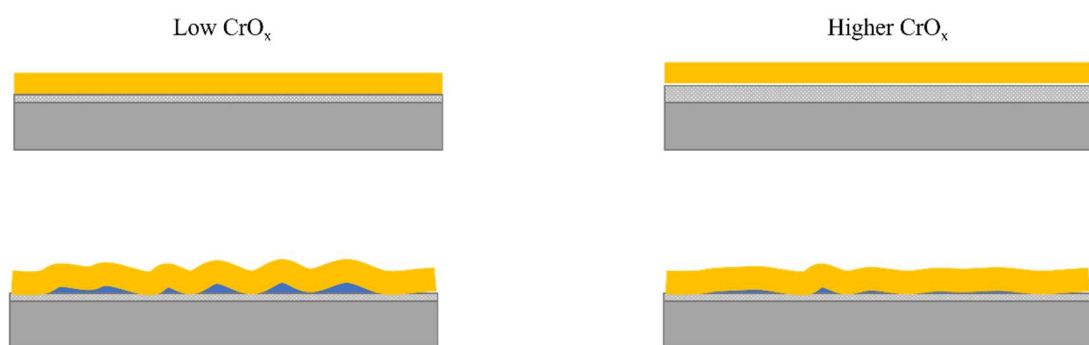


Figure 4.11 Lacquer Delamination for Low and High CrOx Weight Substrates

For lower CrOx weight substrates lacquer bonding would be poorer due the presence of exposed metal due the layer of Cr layer being insufficient to cover the metal surface beneath. If there are parts of the surface with no Cr present then no CrOx would be

present and as such no bonds would be formed between the lacquer and substrate in these areas resulting in a reduction in the chemical interaction between the lacquer and substrate. Due to a reduction in the number of bonds ions can penetrate through the coating and disbondment can occur more easily, enabling an increase in liquid transport. The result of which is an increase in corrosion which can reduce bonding even further. Once disbondment has occurred the cations can diffuse not only through the coating but also through the site of disbondment. While this process can occur on higher CrOx weight substrates it is much less significant due to the increased sites for lacquer adhesion and a reduction in the amount of corrosion present. The result of which is a dominance of cation diffusion through the coating rather than under the coating as there are less sites at which lacquer disbondment has occurred. This is much less detrimental to the lacquer adhesion than diffusion at the disbonded interface.

4.5.3 Other effects

Coating defects that are produced during deformation can increase the amount of water uptake during sterilisation as the water ions can reach the polymer/metal interface. In addition to this where the defects are deep enough to expose the iron beneath the chromium metal surface, anodic activity can occur initiating corrosion with the substrate (73). In order to validate the corrosion and the protective ability of the lacquer a filiform corrosion study was conducted; this is detailed in *Section 4.6* that follows.

In addition to the condition of the surface to which the lacquer is bonded the external factors must be considered when studying water uptake. It has been demonstrated previously that an increase in retort time correlated with an increase in water uptake for older iterations of TCCT (12). It is therefore of value to study this effect on newer iterations to see if the impact is as significant or if process improvements have led to changes in the surface and improvements in adhesion quality.

4.6 FFC Study

Corrosion was observed on unlacquered parts of some samples from previous sections. (4.3 and 4.4) Whilst the lacquered side of the samples did not exhibit any visible substrate corrosion, there is question around whether a dent or scratch in the lacquer that could be caused during transport would expose the substrate to corrosion. It was

determined that a FFC study was an accurate way to investigate this effect without the influence of any other experimental factors such as heat.

4.6.1 Initiation of FFC using 2.5×10^{-3} FeCl₂

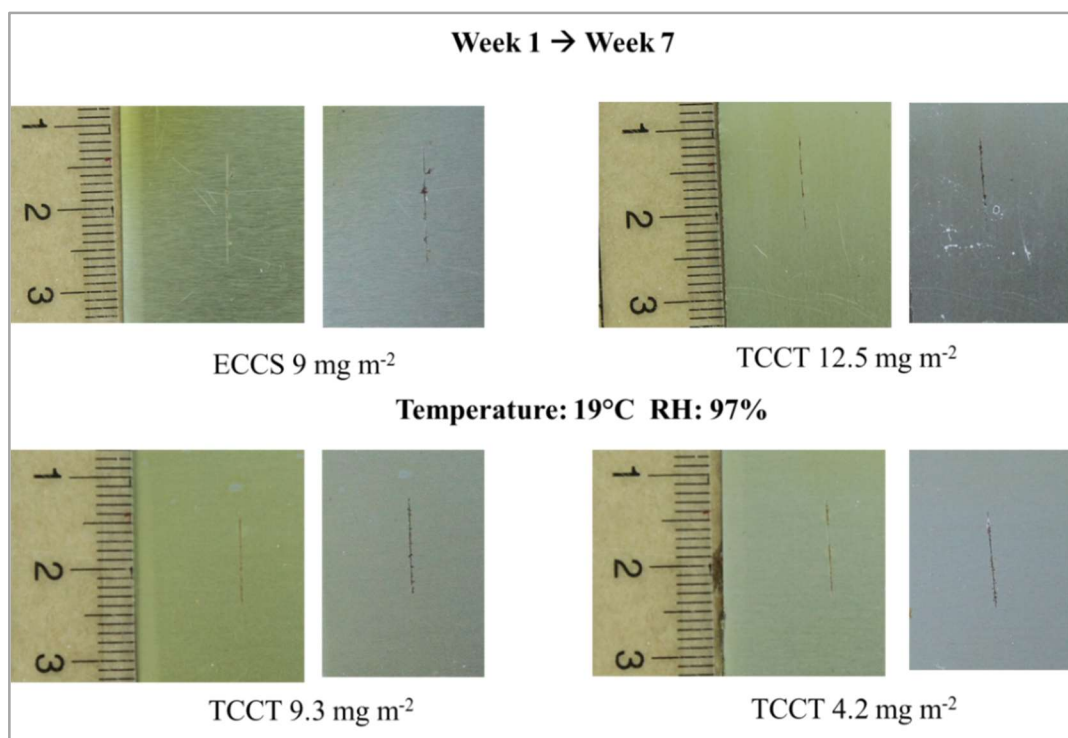


Figure 4.12 FFC images of EP coated samples over a 7-week period

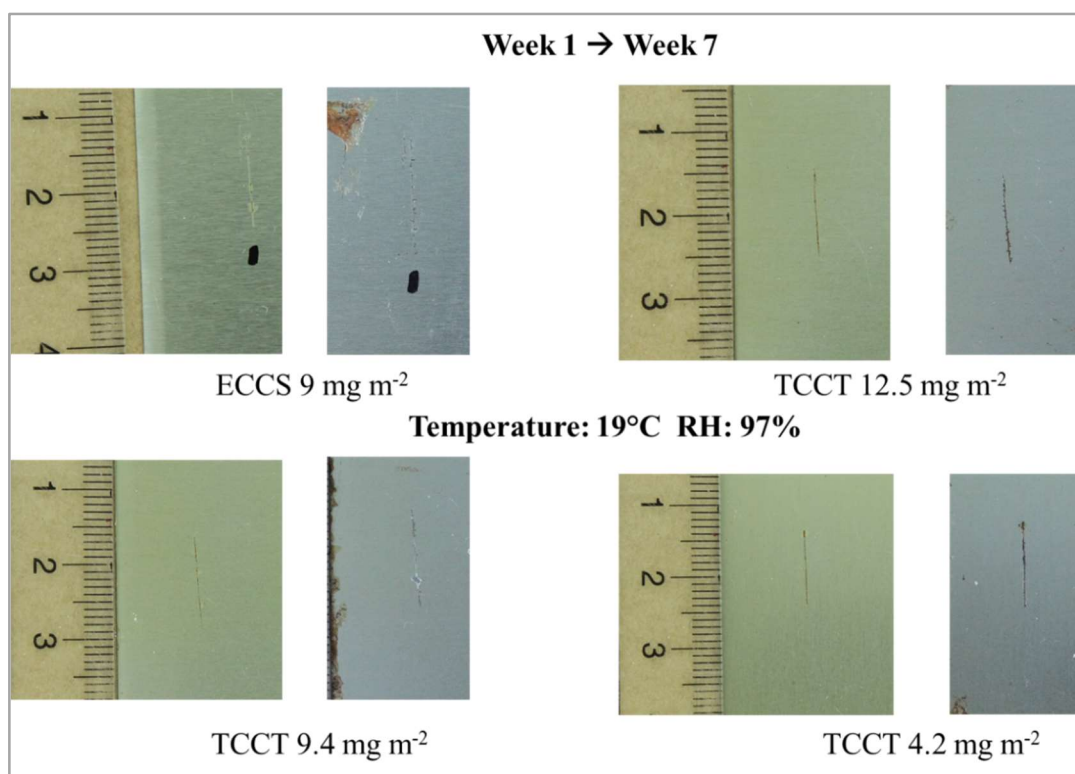


Figure 4.13 FFC images of BPANI coated samples over a 7-week period

The images in *Figure 4.12* and *Figure 4.13* show some corrosion has occurred in the defect over a 7-week period but no worm-like features that are typical of filiform. This is true for both EP and BPANI. The filiform corrosion that has occurred at the unlacquered edges of the sample shows that the environment in the container was humid enough to initiate corrosion suggesting that the lacquers are good at protecting the surface and preventing corrosion. In order to confirm that the lack of corrosion seen was due to the quality of the lacquers rather than failure to initiate the corrosion, a further FFC experiment was set up with an increasing concentration of FeCl_2 and a PVB control. PVB-substrate bonding is known to be weaker than that of epoxy-based coatings and as such FFC can be initiated more easily. Therefore PVB is a useful control to ensure the environment within the container is optimal for FFC initiation (151).

4.6.2 Initiation of FFC using 0.01M FeCl₂

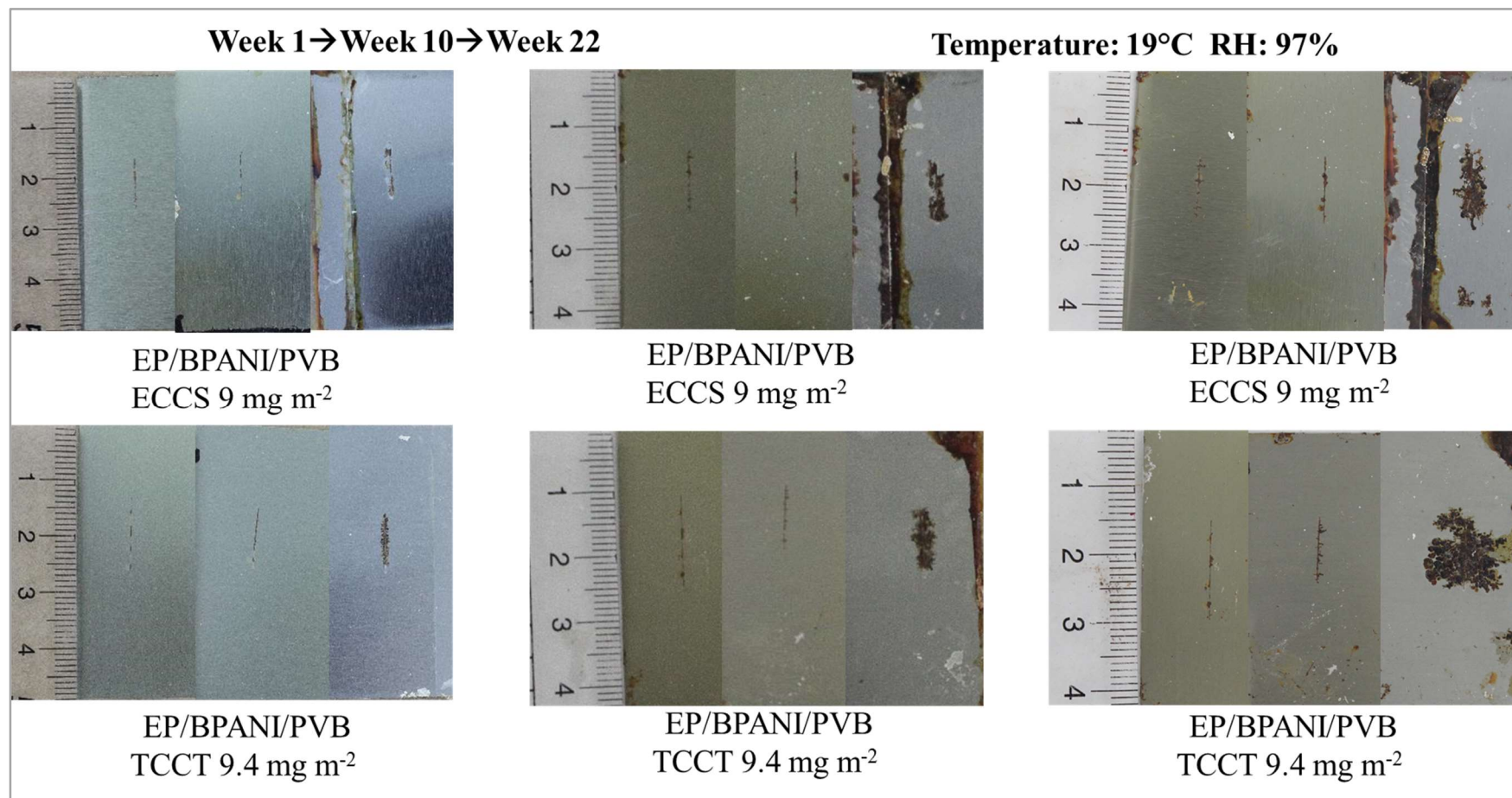


Figure 4.14 FFC images of corrosion of samples with 0.01M FeCl₂ over a 10-week and 21-week period

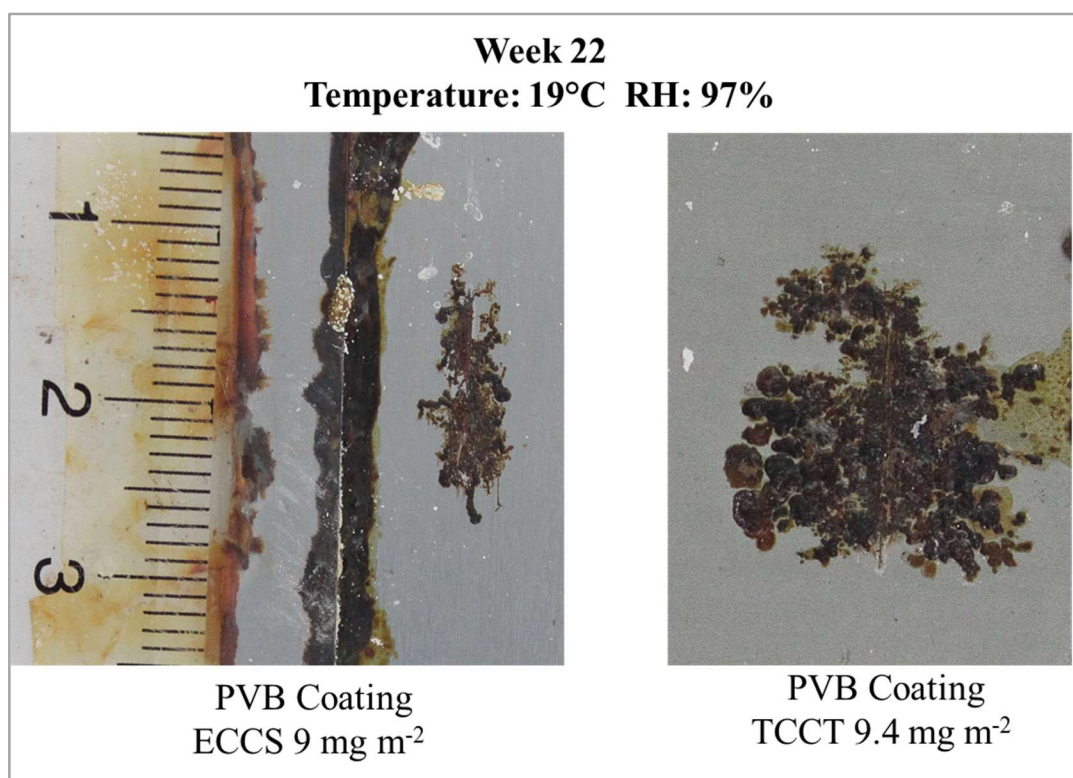


Figure 4.15 Close-up images of PVB coated ECCS and TCCT after 22 weeks of FFC corrosion experiment

The week one images in *Figure 4.14* show clear initiation of FFC for the PVB samples that are not observed for EP and BPANI. Over time the FFC filaments formed on the PVB increase in length confirming that the mechanism is occurring. The EP and BPANI coated samples exhibit limited corrosion, which is contained within the defect, suggesting the lacquers are effective at inhibiting corrosion of the underlying substrate. For PVB samples from weeks 10 to 22, significant growth of the existing filaments are observed along with the appearance of new filaments. Due to the nature of the growth of the filaments the corrosion spreads over a larger area giving the appearance that the filaments have grown over each other which it is known does not occur. The close-up images of week 22 PVB coated samples in *Figure 4.15* show areas where the filament has either changed direction or stopped growing altogether which is typical of filiform corrosion (106). The amount of FFC seen on the TCCT sample covers a larger area than that of ECCS, both of which have the same weight of CrOx applied to the surface. This suggests that ECCS substrates have better corrosion resistance properties than TCCT. This confirms previous findings that Cr(VI) pre-treatments are more effective than Cr(III) at preventing substrate corrosion (22). An

increase in the weight per unit area of chromium also has been shown to increase the inhibiting ability of the coating (106). The findings also show that EP and BPANI lacquers are both equally effective at preventing corrosion of the underlying substrate under the conditions used in this study. This is significant in the canning industry as the lacquer must withstand the environment within the food can without compromising the integrity of the material which would reduce the shelf-life of the food product. It also highlights that in terms of corrosion resistance BPANI is a suitable alternative to EP for can lacquering.

4.7 Numerical analysis of FFC area

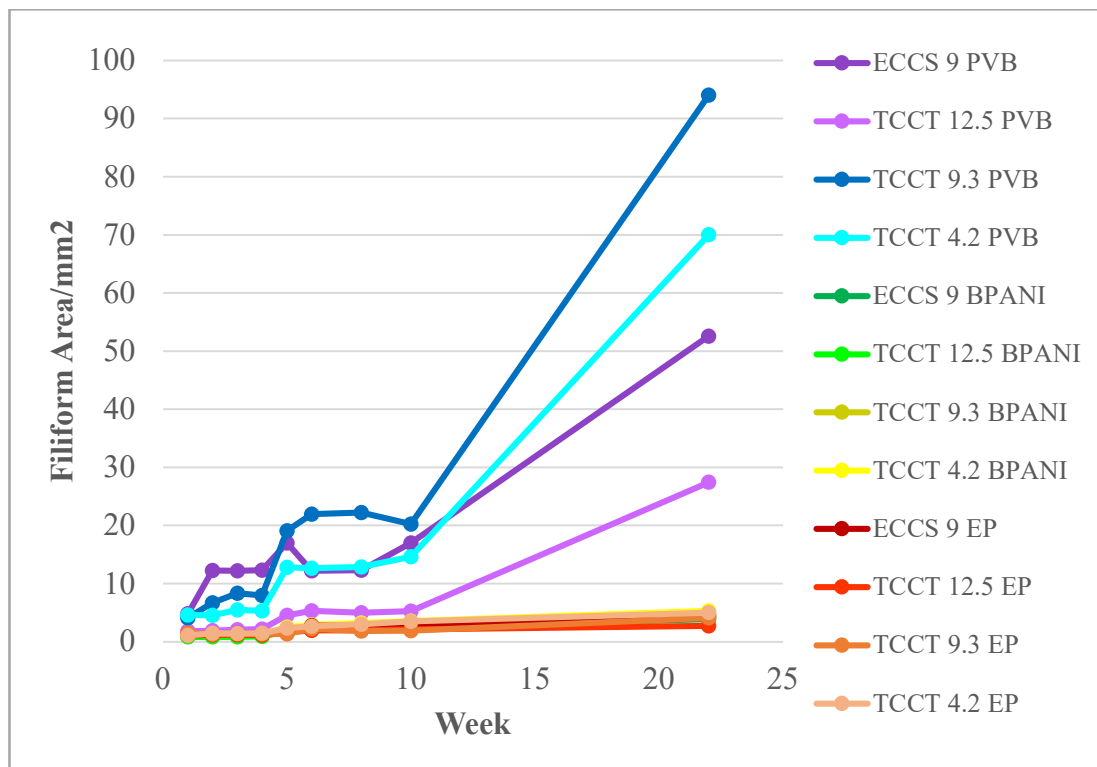


Figure 4.16 The change in FFC area over time for various EP/BPANI/PVB coated ECCS and TCCT substrate

4.7.1 PVB

An ImageJ analysis of FFC samples was performed to establish whether there was a quantifiable trend in the corroded area, the results of which have been plotted as an area versus time graph show in *Figure 4.16*. The filiform area for PVB (purple and blue lines) shows a much greater corrosion area than for EP and BPANI lacquers showing that there is significant corrosion occurring. It should be noted that this would

be expected as PVB is only mechanically bonded to the substrate so provides minimal corrosion protection for the surface when chemical species are present (151). The diffusion coefficient of PVB is in the order of 10^{-5} mm²/s which is 10x greater than that of BPANI lacquers and 100x more than EP lacquers (69,70,152). The significance of this is that in addition to the difference in bonding strength to the surface the PVB is also more prone to diffusion through the coating which would enable corrosive species to penetrate through it and account for the significantly more corrosion that is observed on PVB coated substrates. The data indicates that there is a steady increase in the amount of corrosion over time with a significant increase from week 10 to 22 for PVB. There is no discernible correlation between CrOx weight on the substrate surface and the corrosion area suggesting that CrOx weight is not the factor determining the amount of corrosion in this instance. It is likely since a correlation between FFC area and CrOx weight is not observed then the results may be as a consequence of the homogeneity of the substrate surface. Work by Dodd (120) using atomic force microscopy and white light interferometry confirms that there is a lack of correlation between surface roughness and CrOx weight suggesting that what is proposed is the likely scenario.

Previous work has demonstrated that the chromium layer on TCCT substrates is less homogenous in nature than the corresponding ECCS substrate meaning there are more defects in the surface and thus a higher level of free iron/chromium is exposed (120). It has been demonstrated that free iron or chromium on the surface of can making substrates can initiate FFC so it can be surmised that if there are more defects on the surface then there may be a higher level of corrosion (73). The significance of this means the amount of corrosion may not correlate with the thickness of the CrOx layer when thinner layers are deposited. It is more likely in the range of CrOx weights being used for this work that any microdefects in the surface below would have a greater influence on the amount of corrosion as the CrOx layer is not sufficient to cover these defects. These defects would be increased by using higher currents and faster line speeds as the hydrogen evolution reaction is occurring at the substrate surface. The high line speed and high current used do not give sufficient time for any hydrogen gas that has evolved to dissipate away from the surface. Since PVB is not bonded to the substrate surface it does not afford the substrate any further lacquer protection unlike with EP and BPANI and as such the amount of corrosion is determined by the

homogeneity of the CrOx layer and how evenly the iron and chromium surface below are protected.

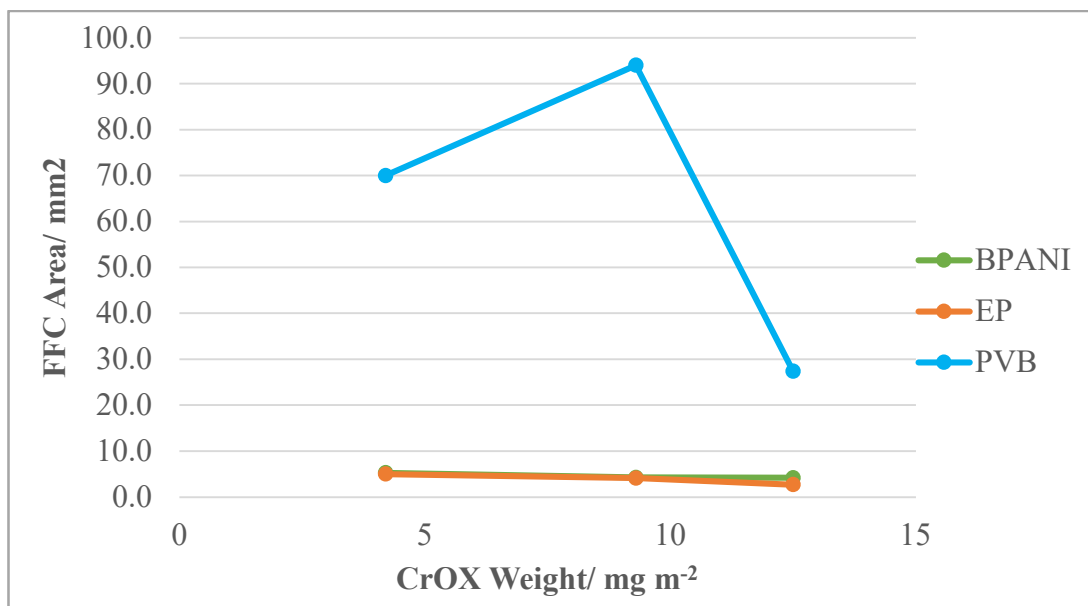


Figure 4.17 The total corroded area of TCCT for each CrOx weight/coating combination after 22 weeks

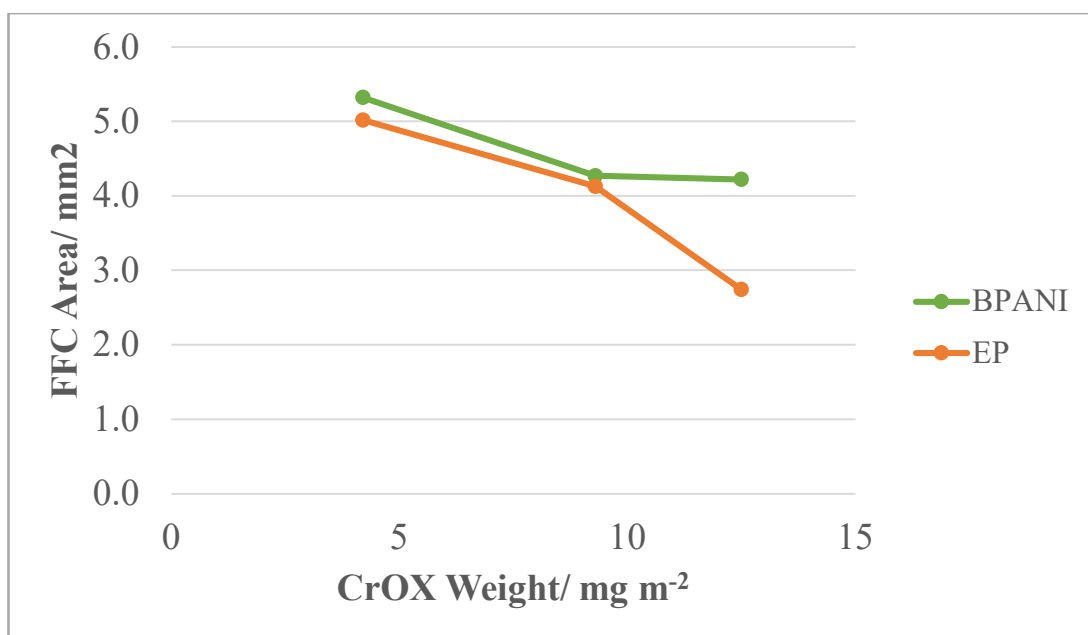


Figure 4.18 The total corroded area of each TCCT substrate lacquered with EP and BPANI after 22 weeks

4.7.2 EP and BPANI

The graphs shown in both *Figure 4.17* and *Figure 4.18* demonstrate that there is a significantly lower amount of FFC on EP and BPANI coated substrates compared with PVB coated substrates. This suggests that the lacquer is acting to prevent propagation of filaments across the substrate and provides corrosion protection properties. The use of an organic lacquer to provide another layer of corrosion protection to the underlying substrate has been documented previously by Wint et. al (22).

It is surmised in this instance that the main factor influencing the amount of corrosion within the defect is the thickness of the CrOx layer that has been deposited onto the substrate. As the CrOx weight is increased the amount of FFC appears to decrease. As such better protection is afforded to the underlying substrate as there is a reduction in the amount of the substrate that is exposed. For BPANI coated TCCT the reduction in the corroded area was approximately 1 mm² (~20%) and for EP coated TCCT it was 2.5 mm² (~50%) for EP. Since more CrOx is present it can be surmised that there are more lacquer bonding sites. Research both within this thesis (e.g. Sections 4.3.1 and 4.4.2) and by others (11,12,120) has shown that EP provides better substrate protection than BPANI and this explains the greater reduction in corrosion area of EP coated TCCT as CrOx weight is increased.

4.7.3 Cathodic delamination by Sodium Cations

It should be noted that in a food can with defects in the lacquer the presence of a group(I) metal chloride will not only initiate FFC corrosion but also cathodic delamination. It is well accepted that cathodic delamination will happen radially from a defect and upon it slowing down FFC corrosion will be initiated at the site where delamination has occurred (104,133). For the purpose of this piece of work, only the mechanism of FFC was studied for simplicity of substrate analysis. Future work could include a cathodic delamination study of the lacquers and substrates used for this work.

4.8 Conclusion

The aim of this section was to characterise the substrate surface and study how different parameters in the can making and food sterilisation process influence the substrate and lacquer. This research has highlighted the impact that the inner food can conditions have on both the substrate and the lacquer. Initial studies with a range of food simulants showed NaCl to have the greatest detrimental effect on the lacquer and substrate with the greatest reductions in failure force seen. In general, an increase in CrOx weight on the substrate resulted in an increase in initial/dry adhesive failure force. However, the uniformity of the surface condition must be considered particularly with earlier generations of TCCT before process improvements were made.

Further studies with varied concentrations of NaCl confirmed that at low concentrations of NaCl the CrOx weight of the substrate has the greatest influence over the failure force of the lacquer, conversely at high concentrations of NaCl, the salt had a much greater influence on the failure force independent of the CrOx weight/substrate type. It should be noted that the performance of ECCS/EP was consistently better than TCCT/BPANI. Retort of BPANI lacquered substrates in salt showed visible water underneath/within the coating which was examined further using FTIR-ATR spectroscopy. FTIR spectra showed an increased transmittance of the O-H peaks as salt concentration was increased indicative of an increase in water uptake within the lacquer. There were no absence/addition of any structural peaks suggesting a chemical reaction was not occurring between the polyester lacquer, BPANI, and the salt simulant solution. It was concluded that the BPANI lacquer is has a less dense crosslinked structures than its EP counterpart and enables mechanical transport of water ions through the lacquer to the interface between the CrOx layer and the lacquer.

Substrate corrosion was seen throughout retort studies on unlacquered areas of substrate. For this reason, it was necessary to conduct a FFC study to establish if the EP and BPANI lacquers can provide sufficient corrosion protection to the underlying substrate. Initial studies showed that the lacquers prevented FFC at low concentrations of FeCl₂ solution, when the solution concentration was increased some corrosion was observed on EP and BPANI which was contained within the defect. PVB coated samples showed significant FFC corrosion covering large surface areas from 30-90%.

Higher CrOx weight substrates had smaller areas of FFC supporting the theory that substrate performance and lacquer adhesion is improved at increasing CrOx weights.

Chapter Five

The Impact of Uniaxial Strain on Chromium Coated Steel Substrates Used in Can Making

5 The Impact of Uniaxial Strain on Chromium Coated Steel Substrates Used in Can Making

5.1 Introduction

In the previous chapter the influence of the foodstuff and CrOx weight on the substrate performance was studied. Whilst this gives a clear simulation of the effects of retort conditions, food stuff and CrOx weight on the performance of the substrate it does not account for mechanical changes that can forming induces in the metal. Post-manufacture the coated steel is usually deformed to achieve the necessary shape which can damage the coating and reduce its protective performance. The analysis of can making materials under strain is crucial in simulating how they will perform during the can shaping process in a large-scale industrial setting. In order to simulate real food cans more accurately, it was deemed necessary to study strained substrates both pre-retort and post-retort after exposure to food simulants in the food sterilisation process.

The influence of strain on lacquer adhesion to chromium coated steel has been studied previously. EP can coating performance under strain has been studied by Allman (12). EP coatings are already approved for use in commercial can coatings indicating that their adhesion performance post straining and retort is acceptable. Therefore, it was deemed unnecessary to repeat these studies for this section of work and the performance of BPANI coated TCCT and ECCS was investigated.

NaCl was selected as one of the food simulants to be studied as the research in *Chapter 4* showed it was the most discriminatory of the food stuffs available. DI water was used as water is in every food can and is the least destructive so gives an accurate picture of the influence of heat and humidity on the can before food chemistry is considered.

It should be noted that the samples were lacquered after they were uniaxially strained to eliminate a non-natural edge from being formed when the samples were cut into a dog bone shape. In a real world can forming process the can body is cylindrical and as such there are no exposed edges during the food sterilisation process.

The following conditions were imposed on all samples throughout this chapter:

- Uniform uniaxial straining with a target extension range of 1-15% of the original length. True strain calculated from measured sample extension. Strain rarely exceeds 20% in can forming (136)
- Consistent and even lacquers within the range of 7-12 μm – pre-defined by the customer and controlled using a 0.15 mm meter bar to ensure accurate and reproducible lacquer thickness.
- Experiments were carried out using established methods that are given in *Chapter 3*.
- Low, middle and high CrOx weights of TCCT were used to deduce whether CrOx weight influences sample performance post-straining
- ECCS with a CrOx weight within the acceptable limit of 7-25 mg m^{-2} for the customer was included as a control

5.2 Uniaxially Strained Substrates

5.2.1 Adhesion of Lacquers to Strained Samples Post-Retort

To improve the methods used to study can making substrates it was deemed necessary to study them when subjected to strain with the intention of trying to emulate the can making process more closely. The adhesion of BPANI lacquer to uniaxially strained ECCS and TCCT substrates after retort in DI water and 1% NaCl was studied. The results from this study can be seen in *Figure 5.1* and *Figure 5.2*.

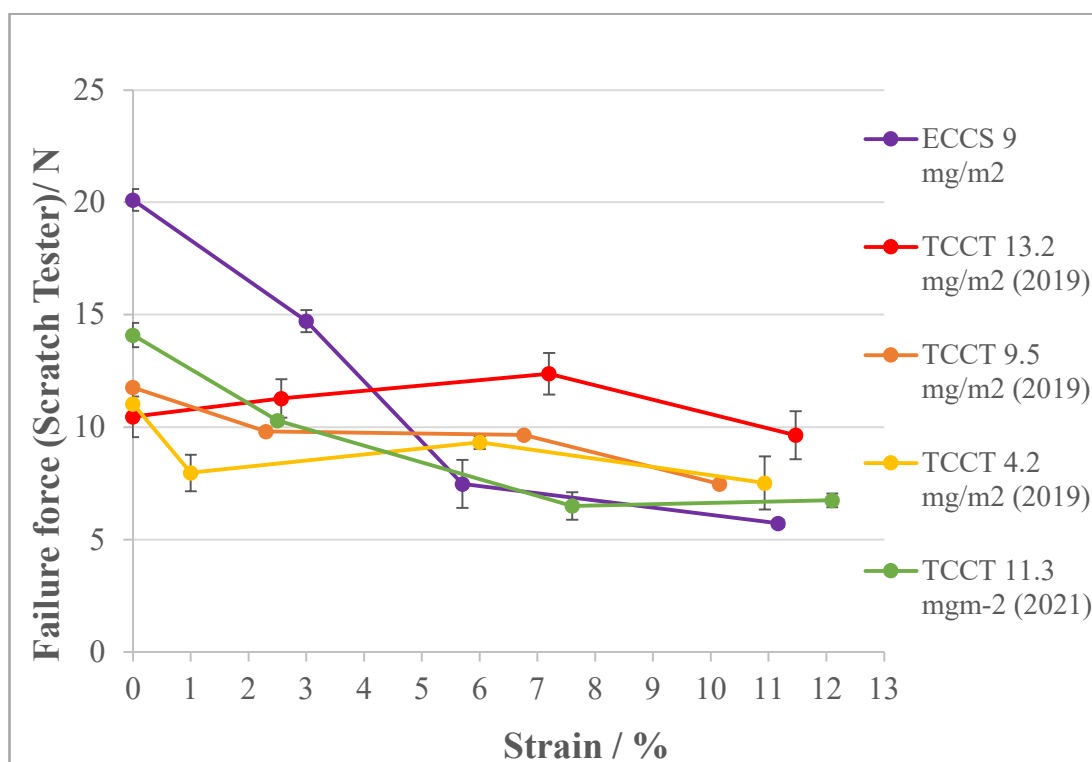


Figure 5.1 The influence of strain on BPANI lacquer adhesion post-retort in water

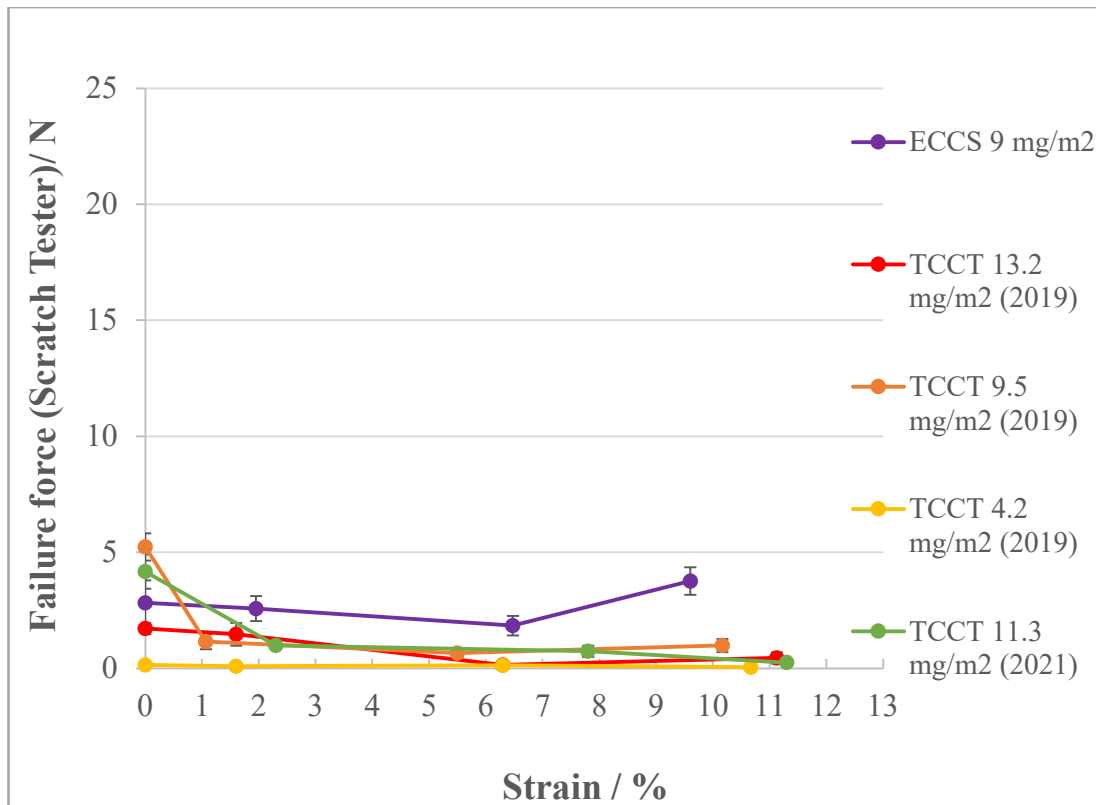


Figure 5.2 The influence of strain on BPANI lacquer adhesion post-retort in 1% NaCl

5.2.2 TCCT

The results in Figure 5.1 show that strain has a minimal influence on the adhesion of BPANI to 2019 TCCT substrates post-retort in water. This correlation stands for all CrOx weights measured. The reverse is true for ECCS as increasing the strain results in a 15 N decrease in overall adhesion. The failure force of BPANI on ECCS is around 8N higher than TCCT at 0% strain, however, as the strain is gradually increased the lines converge to similar failure forces. The results suggest that the strain has more of an influence over the adhesion/bonding between the lacquer and the chrome oxide surface of ECCS substrates than TCCT 2019 substrates. This could be because of the TCCT surface already being non-uniform so the steel below is exposed in the unstrained sample meaning it has the effect of less adhesion sites and therefore a lower failure force overall. This would mean that even when strain is induced little change is seen in the CrOx surface because there is existing poor lacquer adhesion so minimal changes are seen in failure force. It should be noted that the trend in failure force and adhesion performance of the TCCT 2021 substrate more closely reflects that of ECCS.

This suggests that process improvements have been made to make the CrOx layer more uniform and would account for the improvement in performance that is observed.

5.2.3 ECCS

A more significant decrease in the failure force seen in *Figure 5.1* for ECCS could be due to the uniformity of the surface on an unstrained sample. It is proposed that if the ECCS sample surface is more uniform and less steel is exposed there would be better lacquer adhesion and thus a higher failure force. The brittleness of the CrOx layer means that as the sample is strained more steel is exposed and overall lacquer adhesion is reduced accounting for the reduction in failure force (118,136). The effect of strain on the surface of uncoated ECCS has been demonstrated by Zhang *et al* (136) who found that inducing strain produced more defects in the CrOx layer and exposed more of the steel surface underneath. They found that an increase in strain correlated with a decrease in corrosion resistance. Adding an organic layer for protection improved the corrosion resistance and performance of the substrate. Exposed iron can be present on the substrate after deformation and if new lacquer-substrate bonds are not formed then the surface is more exposed which facilitates ion diffusion. Ion diffusion can then facilitate sample corrosion in the presence of activating species such as salt (73). To establish whether this is the case, an SEM study of the chromium coated steel substrates was conducted on both strained and un-strained samples.

5.2.4 The effect of a NaCl simulant on adhesion

Figure 5.2 shows how strain influences lacquer adhesion to both TCCT and ECCS after retorting in 1% NaCl solution. The results show that the strain has a minimal effect on the failure force, however, all values are under 5N even when no strain is induced. This suggests that the NaCl solution is so detrimental to the BPANI lacquer and adhesion that it significantly reduces the failure force so any differences in force as a result of induced strain are smaller, and thus more difficult to measure given the apparatus. It can be surmised that the simulant solution is the primary influence over the adhesion as opposed to the strain.

5.3 SEM analysis of unlacquered TCCT and ECCS Samples at 0,5 and 15% Strain

In all of the images in this section, straining direction is denoted as SD (blue) and rolling direction is denoted as RD (red). The straining direction in relation to rolling direction changes due to the way dog bone samples were cut from the substrate sheets. As such the samples were strained along the axis in which the dog bone was cut.

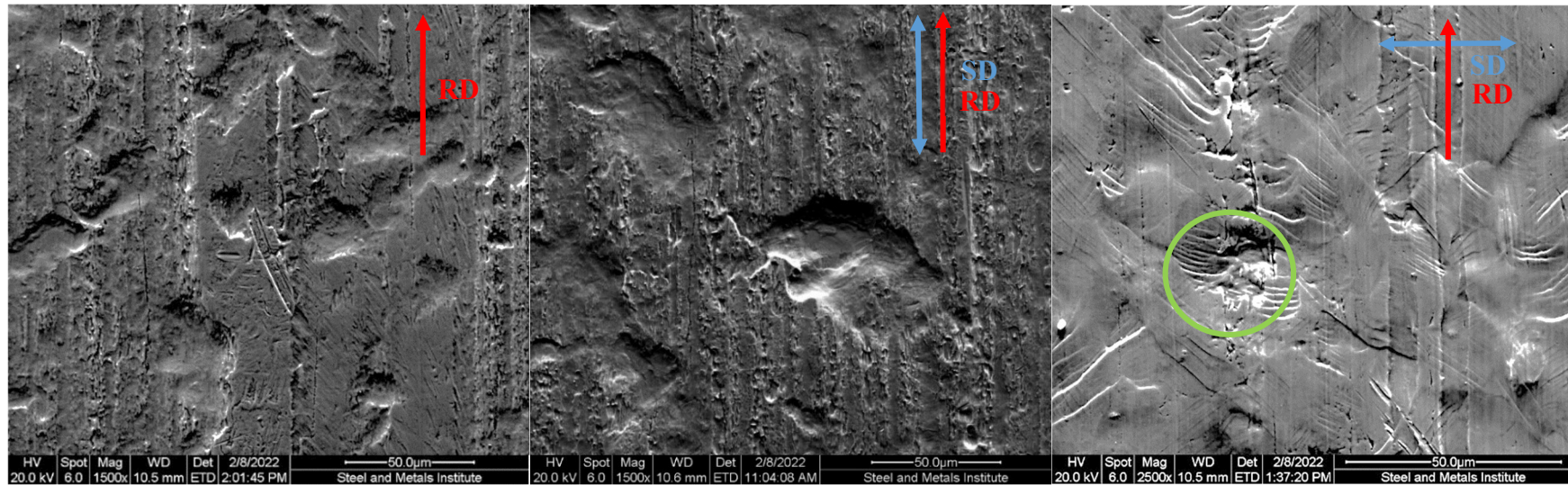


Figure 5.3 SEM images of ECCS 9 mg m⁻² CrOx weight surfaces from left to right: no strain, 5% strain, 15% strain. The green circle indicates Lüder bands

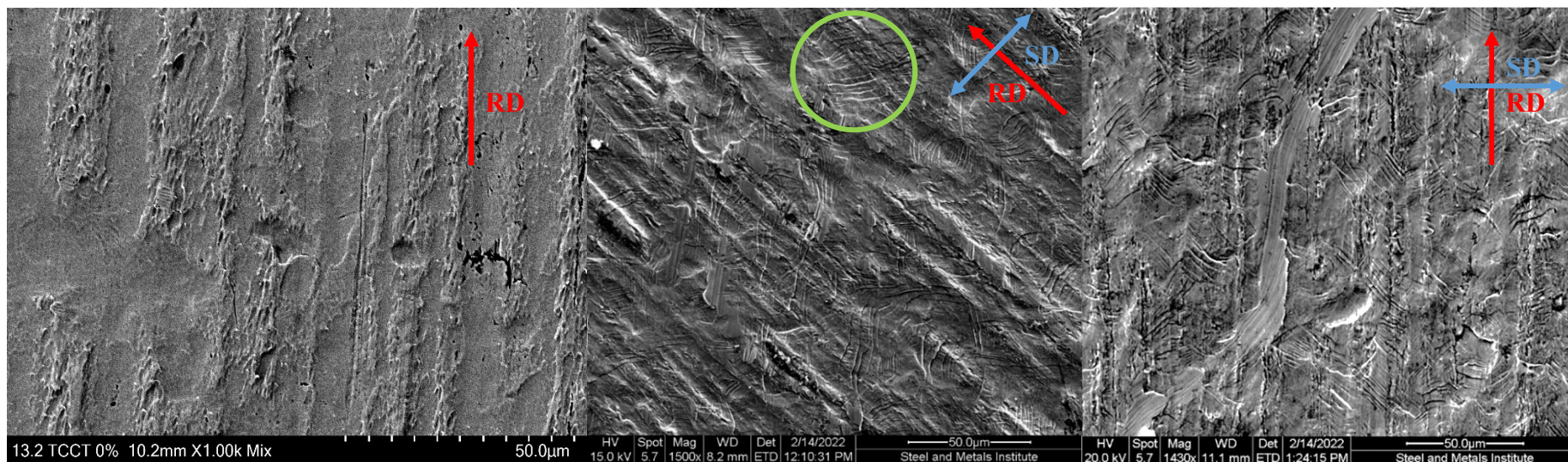


Figure 5.4 SEM images of TCCT 2019 $13.2 \text{ mg m}^{-2} \text{ CrOx}$ weight surfaces from left to right: no strain, 5% strain, 15% strain. The green circle indicates Lüder bands

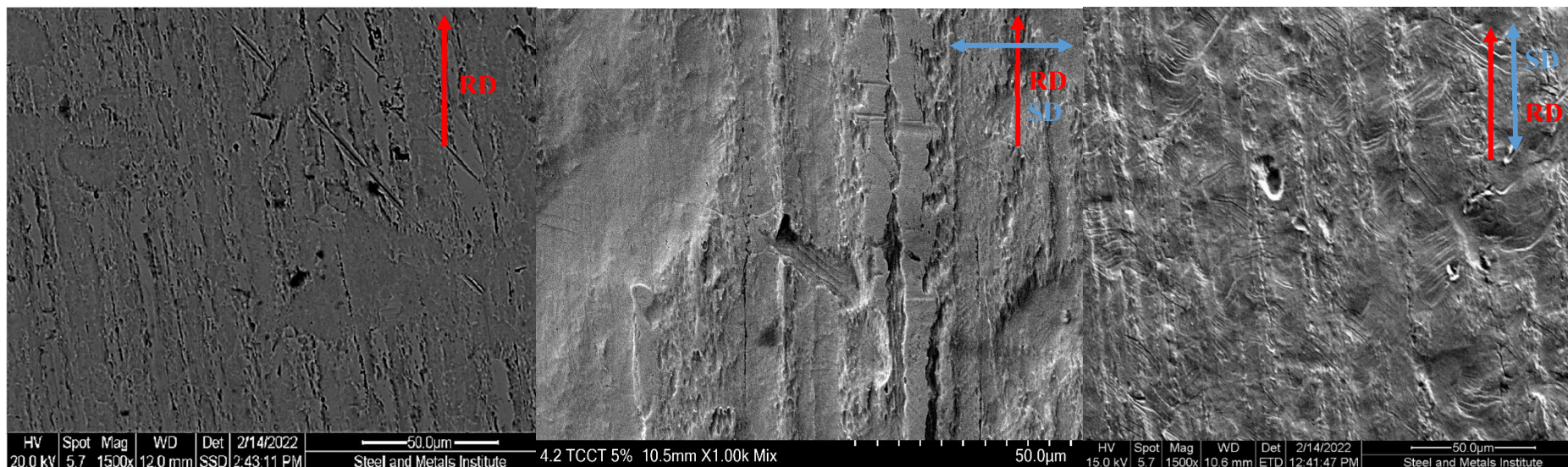


Figure 5.5 SEM images of TCCT 2019 4.2 mg m⁻² CrOx weight surfaces from left to right: no strain, 5% strain, 15% strain

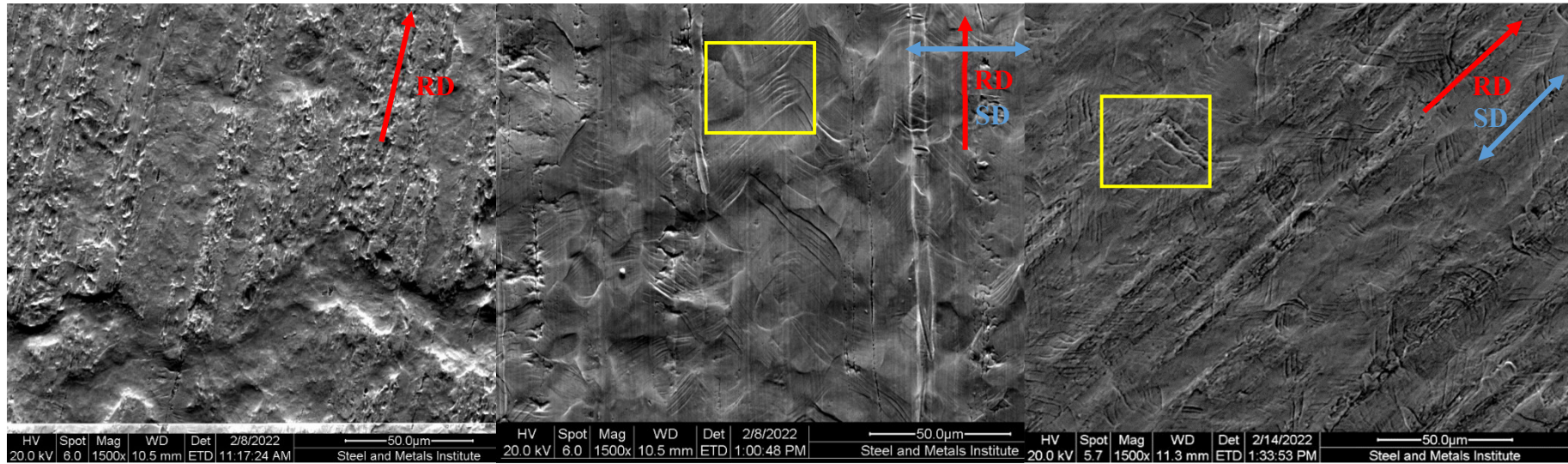


Figure 5.6 SEM images of TCCT 2019 9.5 mg m⁻² CrOx weight surfaces from left to right: no strain, 5% strain, 15% strain. The yellow squares indicate the apparent change in depth of the Lüder bands as strain is increased.

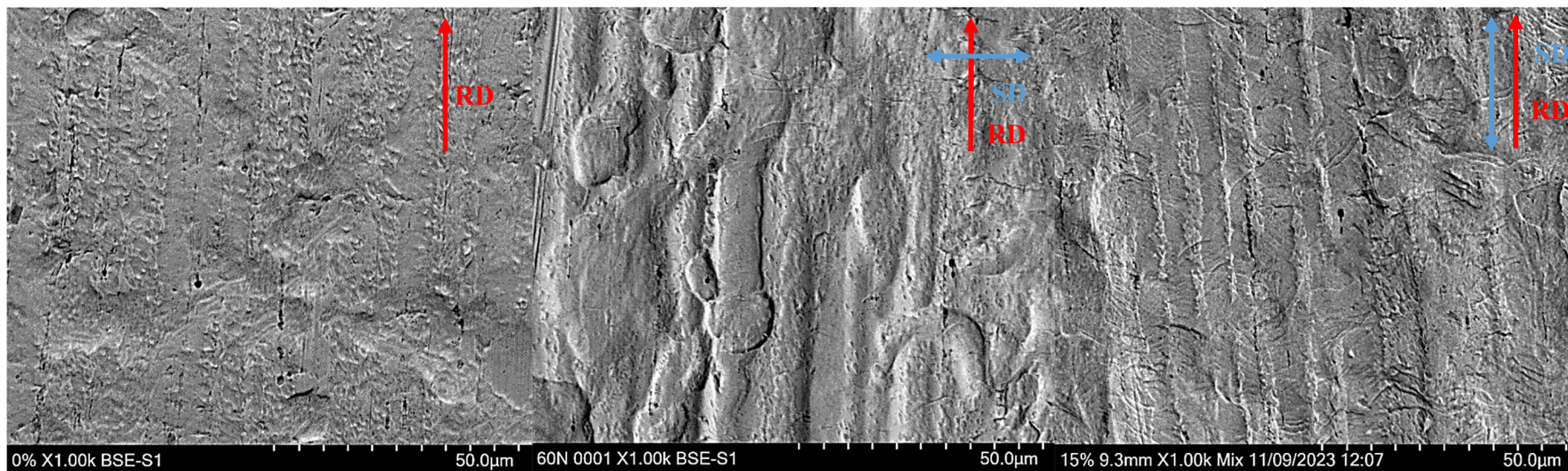


Figure 5.7 SEM images of TCCT 2021 11.3 mg m⁻² CrOx weight surfaces from left to right: no strain, 5% strain, 15% strain

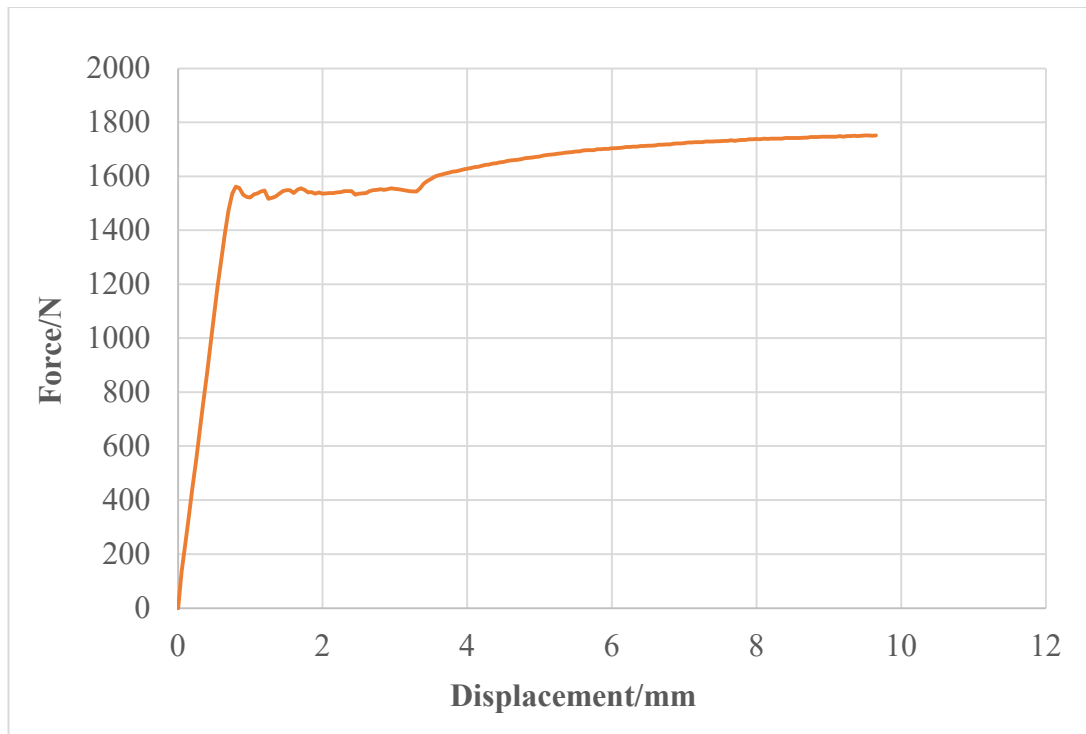


Figure 5.8 Force-Displacement graph for 15% nominal strain of TCCT 2021 substrate

The influence of strain on lacquer adhesion to both ECCS and TCCT was demonstrated earlier in this chapter. The difference in Cr(III) and Cr(VI) surfaces over the strain range of 0-15% which accounts for this change in adhesion was studied using SEM, the results of which are shown in *Figure 5.3*, *Figure 5.4*, *Figure 5.5*, *Figure 5.6* and *Figure 5.7*. The rolling direction, denoted by RD, on the substrates is visible in all of the SEM images and is the main factor influencing the surface topography for unstrained samples. In addition to the changes in bulk material properties and overall performance, changes in the material can also be visualised on a microscopic scale. Lüder band (highlighted by the green circles in *Figure 5.3* and *Figure 5.4*) formation during straining results in plastic, irreversible deformation of a metal (153). The presence of the Lüder bands supports the trend seen in the tensile graph in *Figure 5.8* where discontinuous yielding is present during tensile testing of the sample. Discontinuous yielding is commonly observed for low carbon steel which is what the substrate used for can making is. (136,154). Lüder bands form at an approximate angle of 45° to the straining direction which is denoted by SD (155). The amount and depth of the Lüder bands present (see yellow area in *Figure 5.6*) increases when the strain is increased from 5 to 15% indicating that the surface roughness of the substrate is increasing (136,156). It was observed that at 5% strain, no Lüder bands were visible

for the ECCS substrate in *Figure 5.3* suggesting it has a higher yield strength and can resist plastic deformation up to higher strain values than TCCT 2019 substrates. The TCCT 2021 5% strain image shown in *Figure 5.7* has a very small number of Lüder bands compared with TCCT 2019 substrates. They also appear to be shallower in depth, this suggests that TCCT 2021, as with ECCS, has a higher yield strength and allows for elastic deformation up to higher strain values. Lüder band formation has been shown to cause inhomogeneous deformation in metals regardless of the strain rate (157). This is significant as it means that the slower strain rate used for this research compared with industrial can making strain rates, may have less of an impact on the overall sample deformation than would be expected.

Defects, defined as being 1-5 μm in diameter, are visible in unstrained samples of TCCT such as those in *Figure 5.5*. It has been proposed that the defects result from the chromium metal deposition and the CrOx layer that is subsequently deposited is not sufficient to cover these defects (120). This can account for the initial lower adhesion results in *Figure 5.1* as there are less lacquer bonding sites on the substrate surface. Since the surface of ECCS is more homogenous with less defects, the initial failure forces are much higher. This is also the case for TCCT 2021 substrates which were produced after process improvements to the production methods had been made. Induction of strain in both ECCS and TCCT substrates showed defect formation on the surface and a reduction in lacquer adhesion. The reduction in failure force for ECCS and TCCT 2021 is much greater than that of TCCT 2019 suggesting there are greater changes in the surface. The apparent amount and depth of Lüder bands of both substrates at high strain suggests the surfaces have a similar amount of defects, this suggests that there is more free iron exposed. The composition of the substrates, despite their This would mean there are less free OH sites for lacquer bonding and accounts for the reduction in failure forces seen and the similar adhesion values exhibited by both ECCS and TCCT in *Figure 5.1*.

To further investigate the amount of free iron present on these surfaces a oxide pin hole identification study was conducted to measure the free metal on the substrate surface as this directly correlates with the amount of defects on the CrOx surface (120). This can be seen in *Chapter 6*. Defects in the surface can also correlate with an increase in corrosion (158). Straining the sample increases the defects which implies that more of the iron below the chromium surface is exposed and thus the amount of corrosion

that occurs during the retort process and over longer periods of time during storage will also increase. The implications of sample corrosion are not only aesthetic they also alter the material properties and can affect the contents within the can.

5.4 Conclusion

This chapter has outlined the findings of uniaxial strain studies and described the effect that uniaxial elongation has on both the surface condition and post-retort performance of ECCS and TCCT substrates. Initial retort studies demonstrated significantly better performance of ECCS and TCCT 2021 substrates at low strain values compared with older generations of TCCT. As strain was increased these values converged to a similar region. The introduction of a 1% NaCl solution into the retort vessel proved to have a significant and dominating effect on the post-retort adhesion of the strained samples. The simulant effect was the primary influencer over the strain rather than the substrate type in this instance.

Straining samples of ECCS and TCCT caused the formation of Lüder bands which were observed using SEM. It appears visually, that the number of Lüder bands and their depth increased as strain was increased, however, this was not quantified in this piece of work. There were more defects on the surface of TCCT substrates than ECCS which can account for the poorer adhesion values seen in *Section 5.2.1*. Upon straining the number of defects on ECCS substrate surfaces appears to increase more than on TCCT substrates, suggesting a reduction in uniformity of the surface and also the TCCT surface being less uniform initially in its unstrained state. The nature and number of defects on the surfaces of ECCS and TCCT is studied further in *Chapter 6*.

Chapter Six

Method Development and Analysis of Biaxially Strained Can Making Substrates

6 Method Development and Analysis of Biaxially Strained Can Making Substrates

6.1 Introduction

The can making process involves several stages which introduce strain into the metal substrate. Initial strain studies conducted using a tensile tester and automated scratch tester in *Chapter 5* provide a useful insight into the influence of uniaxial strain on substrate and lacquer performance during the can forming and sterilisation process. However, these are not representative of the drawing stage of DRD can making. The main aim of this section of work is to develop a reproducible method that is capable of simulating the can shaping process more closely while also providing accurate, reproducible results of lacquer adhesion.

Various methods exist for sample straining on a laboratory scale but not all are representative of the can forming process. Sample deformation with an Erichsen Cupping apparatus can simulate the ‘drawing’ stage of the DRD can making process as it emulates the reduction in bonding between the substrate surface and the protective lacquer when a sample is strained. It has been demonstrated that the can shaping process also roughens the steel substrate and thins the organic lacquer. This can have the effect of changing the path of migration of ions through the coating (73). Erichsen cupping tests are used as a QC tool in industry to evaluate whether, or not, a material is suitable for the application based on whether, or not, it can withstand being strained to a specified IE (Erichsen Index) value. Whilst useful as a QC tool it does not given any insight into coating properties, however it does provide a consistent, reproducible way of preparing samples that can then be directly compared with each other (145). Research by Cheong found that coated substrates had higher failure strains compared with their free-film counterparts. This is attributed to the high stiffness of the substrate preventing high levels of deformation around any pinholes or defects and as such failure will occur at a higher strain value than that of the free film. This makes it difficult to model coating failure using the Erichsen cupping apparatus alone (145).

In addition to establishing a method by which the strain can be induced, a method for measuring lacquer adhesion will also be developed. Several standardised and widely used methods exist for testing coating adhesion including automated scratch testing (76) and tape testing (82), however, these are not applicable to testing the adhesion of

lacquers on non-planar samples. A hardness pen (spring-loaded stylus pen) can be used to measure the failure force of a coating on a non-planar sample. The working range of which is 0.5 to 20 N so is within the scope of the failure forces observed in this piece of work (80). It is also important to consider that the failure force values measured by scratch testing may not be interchangeable with those measured by hardness pen.

The SEM images in *Chapter 5* highlighted an increase in surface defects after straining. Based on the metallic structure of ECCS and TCCT these defects were attributed to the presence of free iron or chromium. An oxide pin hole identification method has been adapted successfully to study surface condition and to quantify any free metal present (120). While this method does not give a true quantitative amount of copper that has been deposited, due to the mushroom shape formed by the nodules, it is a useful analytical tool for comparing sample types and their surfaces. This section of work will adapt this method to enable comparison between different substrate types and CrOx weights.

Past studies using the scratch methodology to produce an adhesion figure of merit have been carried out on flat substrates (12,110,120). It has proven to be useful means by which the strength of the bond at lacquer/substrate interface can be characterised by a single number. The nature of the measurement requires gravity (the applied force) and the surface being measured to be perpendicular. As the literature has highlighted (*Section 2.9.2*) methods for controlled biaxially strain which maintain a flat specimen are difficult to produce for a larger scale substrate. Biaxial strain can be readily induced by deforming the substrate in a plane perpendicular to the sheet, but this results in a non-flat substrate making the measurement of adhesion using the standard scratch methodology impossible. Subsequently, a novel method had to be developed which could allow a single figure of merit of adhesion on non-planar substrates. Several possible methodologies were reviewed, and where possible attempted. Each was considered with reference to the requirements of being quick, safe, appropriate for thin (125 micron) substrates, able to deal with lacquered materials, low cost and able to provide a single metric of adhesion. This section describes the methodology developed which required a controlled known biaxial strain, coupled with non-planar adhesion measurement

6.2 Method Development

Biaxial deformation was imparted into the substrate using an Erichsen 202 EM cupping apparatus as per *Figure 6.1*. This allowed for a repeatable deformation of the substrate.



Figure 6.1 Erichsen cupping apparatus used for biaxially straining samples

The depth of the domed penetration into the substrate can be controlled with an accuracy of ± 0.1 mm. The depth of the penetration, known as the Erichsen Cupping Index (IE), induces the deformation as per *Figure 6.2*. There is no ready means by which the localised deformation (strain) can be correlated to depth of penetration using the apparatus alone. A method had to be developed to measure each strain value that correlates to each IE. Considerations were taken to ensure that strain measurements were made at the peak of the dome each time to ensure consistency across all sample types. Erichsen dome mapping in literature has demonstrated that strain distribution across a dome is not uniform (92,159). As such selecting the same area for analysis on

each sample is crucial for accuracy and consistency and ensures the method is robust and widely applicable (92,159).

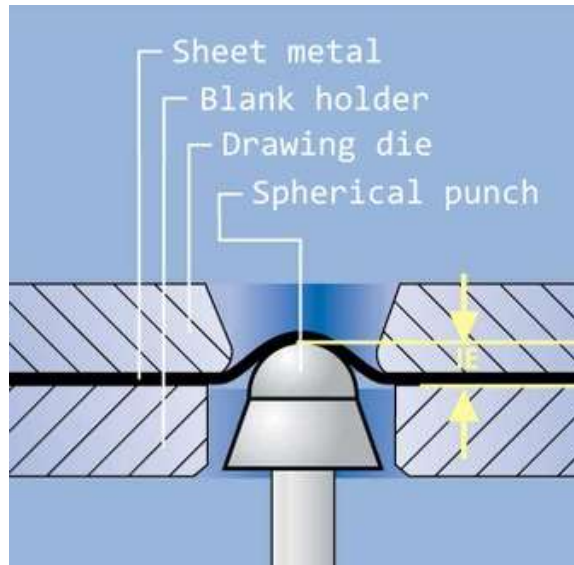


Figure 6.2 Schematic of the Erichsen Cupping Apparatus Operation (160)

The Erichsen cupping apparatus was selected as it enables biaxial strain to be induced into to a sample on a laboratory scale. In turn enabling analysis of a variety of strained substrate/lacquer systems and their post-retort performance when ‘cooked’ in different food simulants. There are limitations to the method as it is only representative of the DRD stage of can forming and does not produce a real can shape so does not encompass all of the strain within a real food can. The dome height (IE) range of 1-5mm was selected as it was observed that some samples showed mechanical failure at dome heights of 6mm and above which made them unsuitable for experimental analysis.

6.2.1 Reference Scale

Sheets of TCCT and ECCS were lacquered with BPANI or EP then cured as outlined in *Section 3.2.1*. The sheets were loaded onto a Laserscript LS3060 LSCT laser printer bed. The laser was removed and a Wago ultra-fine inedible marker was affixed into the mount such to provide a repeatable X-Y mechanism. The software was set to draw four 70 x 70 mm grids with a constant spacing of ~2 mm between each line. The grid was drawn only on the surface and as such should have no effect on the

lacquer/substrate interface. The sheets were cut into samples 100 x 100 mm in size as per *Figure 6.3*.

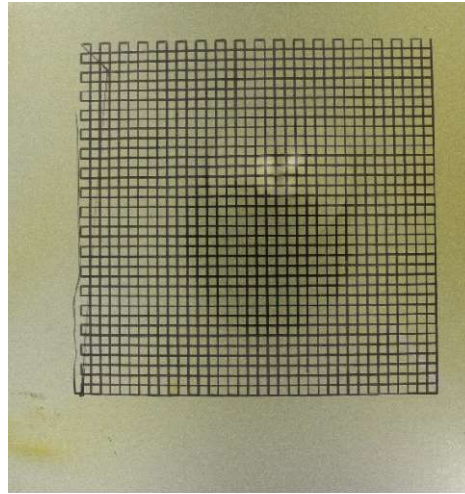


Figure 6.3 An example of the strained samples used with a reference grid

A reference image of an unstrained sample was taken with a Canon EOS 500D digital camera in a Photosimile light box with a ruler for scale. ImageJ software was used to take reference measurements as per *Figure 6.4*. All measurements were taken from the start of one line to the start of the next in order to eliminate any variations in line thickness. The reference ruler 1mm width was measured four times and averaged giving a conversion factor of 23.7 pixels to 1mm and 1 pixel to 42 μm . The error in the measurements was calculated using *Equation 6.1*.

$$\text{Error} = 2 \times \frac{\text{Field of View (mm)}}{\text{Number of Pixels}} = 2 \times \frac{14.6}{3456} = \pm 8.4 \mu\text{m} \quad (6.1)$$

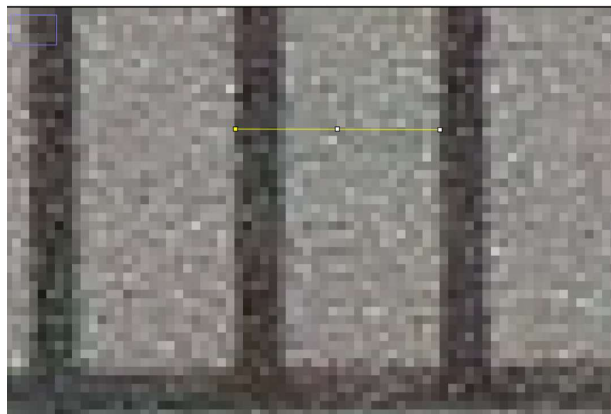


Figure 6.4 ImageJ measurements taken to calculate conversion factors

6.2.2 Strain/Dome Height Calibration

The samples were deformed using an Erichsen 202 EM cupping apparatus (pictured in Figure 6.1) to BS EN ISO 20482:2013 using Erichsen cupping index (IE) values from 1 – 5 mm at 1 mm intervals (161). The samples were not deformed past 5 mm as test samples of the same material showed breakage at 6 mm. The deformation was conducted at room temperature at a rate of 12 mm min⁻¹ (162). The deformed samples were photographed using the same set-up as the reference sample. The images were processed using ImageJ to establish a strain value corresponding to each dome height. The width and height of four cells on the reference sample were measured and averaged to give an unstrained cell length. To calculate the strained cell length, the width and height of one cell at the top of each dome was measured and averaged from four samples (8 measurements). The strain percentage was calculated using *Equation 6.2*.

$$\text{Strain \%} = \frac{\text{Strained cell length} - \text{reference cell length}}{\text{reference cell length}} \times 100 \quad (6.2)$$

The calibration curve in *Figure 6.5* was produced using the method outlined. The strain values were measured consistently at the peak of the dome each time to ensure as much reproducibility as possible when selecting the area for analysis. Whilst it is recognised from DIC that this is not always the area of highest strain, it is deemed the simplest part of the sample to identify when presented with a different sample each time thus reducing measurement error (92). *Figure 6.5* represents strain values from approximately 7-20%. This strain range is representative as it covers the ‘real world’ strain values as the average strain in a can is typically below 20% (136). This calibration curve is useful to enable rapid sample analysis without the need to measure strain of each individual sample and is valid for quick analysis of post-retort samples to ensure they meet pre-determined QC standards. As a calibrated instrument is used to produce the domed samples it eliminates any human error and should have high accuracy when producing samples. This means that each time a dome height is selected the strain percentage should remain the same for the substrates used within this research.

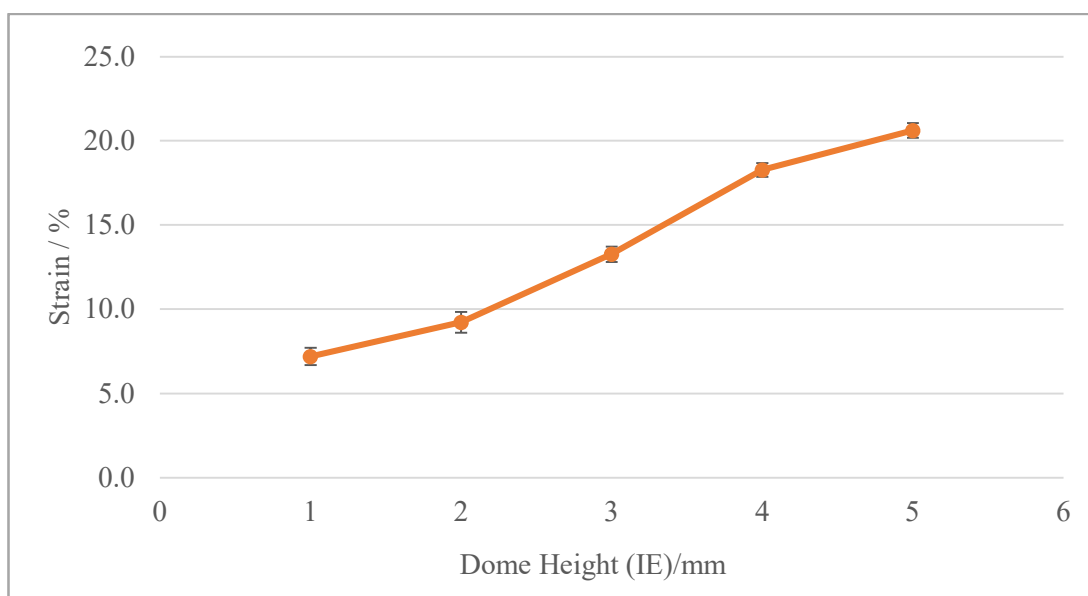


Figure 6.5 Calibration curve representing strain values that correspond to Erichsen dome heights

6.2.3 Biaxial Strain Analysis

Lacquered samples were strained at dome heights of 1-5mm, four samples were analysed for each lacquer/substrate combination at each dome height. In order to fit within the kilner jars for the sterilisation process the samples were cut to 100 x 40 mm, encompassing the whole dome. The edges of the cut sample were sealed using epoxy resin prior to retorting in both DI water and 1% NaCl solution using the same procedure and conditions as *Sections 3.2.2 and 3.2.3*.

The adhesion of the lacquers post-retort was measured using a TQC Sheen Hardness Pen according to BS EN ISO 22557 (80,81). This enabled adhesion to be measured across the whole dome as it can be moved over the non-planar surface. The pen is loaded with a spring of an appropriate failure force range and a stylus of a chosen diameter. The setup of the instrument is depicted in *Figure 6.6*. In this instance a 0-10 N (± 0.5 N precision) spring was used unless the failure force was significantly low and required more precision in which case a 0-3 N spring with a precision of ± 0.1 N was selected. The tip of the selected stylus was 1 mm in diameter.

Establishing lacquer failure force using a hardness pen is similar to that of an automated scratch tester. The pen is set to a specific force and manually scratched over the surface until the coating is removed. As the pen is moved across the surface the tip pushes back into the pen compressing the spring, this can only happen to a certain force which is set by adjusting the locking screw. This ensures consistency across the testing regime. To determine the failure force of the EP and BPANI lacquers used here the force was adjusted until the lowest force required to remove the coating and expose the underlying substrate was ascertained. This was recorded as the failure force of the coating/substrate. An average of four samples was taken for each lacquer/substrate combination at each dome height.

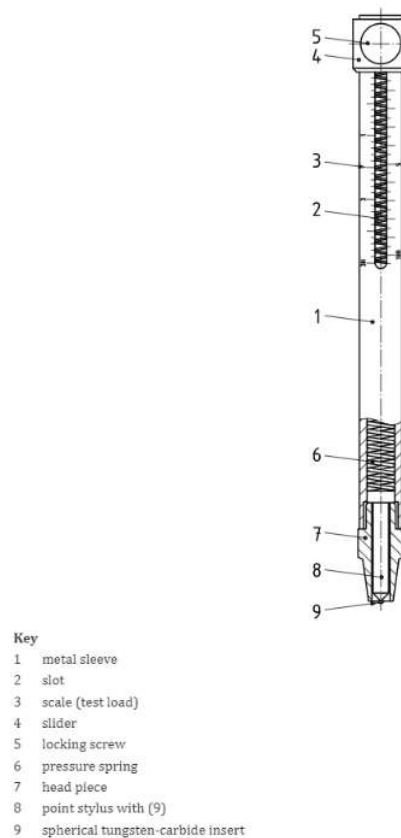


Figure 6.6 Spring-loaded hardness pen with components labelled (80)

6.3 A Systematic Study Comparing Failure Forces Values Obtained from Scratch Testing and a Spring-Loaded Hardness Pen

A systematic study was conducted to compare the failure force values obtained by scratch testing and hardness pen to see if there was a correlation between them enabling them to be interconverted to the same measurement units using an equation. The failure forces for uniaxially and biaxially strained samples were converted to the same measurement unit and plotted to establish if the numerical values of uniaxial and biaxial strain are equivalent. The decision to use an automated scratch tester for the remainder of this research rather than a hardness pen was to remain consistent with a well-established methodology and for ease of direct comparisons between generational batches of TCCT. It enabled improvements in processes to be observed and proper characterisation to be achieved (12,110,120). Automated scratch testing also allows for higher precision down to $\pm 0.1\text{N}$ for all measurements compared with the spring-loaded hardness pen which can only offer this level of precision between 0 and 3 N otherwise it is $\pm 0.5\text{N}$ in the range of 0-10N or $\pm 1.5\text{N}$ in the range of 0-30N.

6.3.1 Converting Hardness Pen Failure Force to Scratch Test Failure Force

A large selection of substrates coated with EP or BPANI lacquers were selected to ensure a wide sample set. Four samples of each lacquer/substrate combination were used and the failure force was measured using both a hardness pen and a scratch tester.

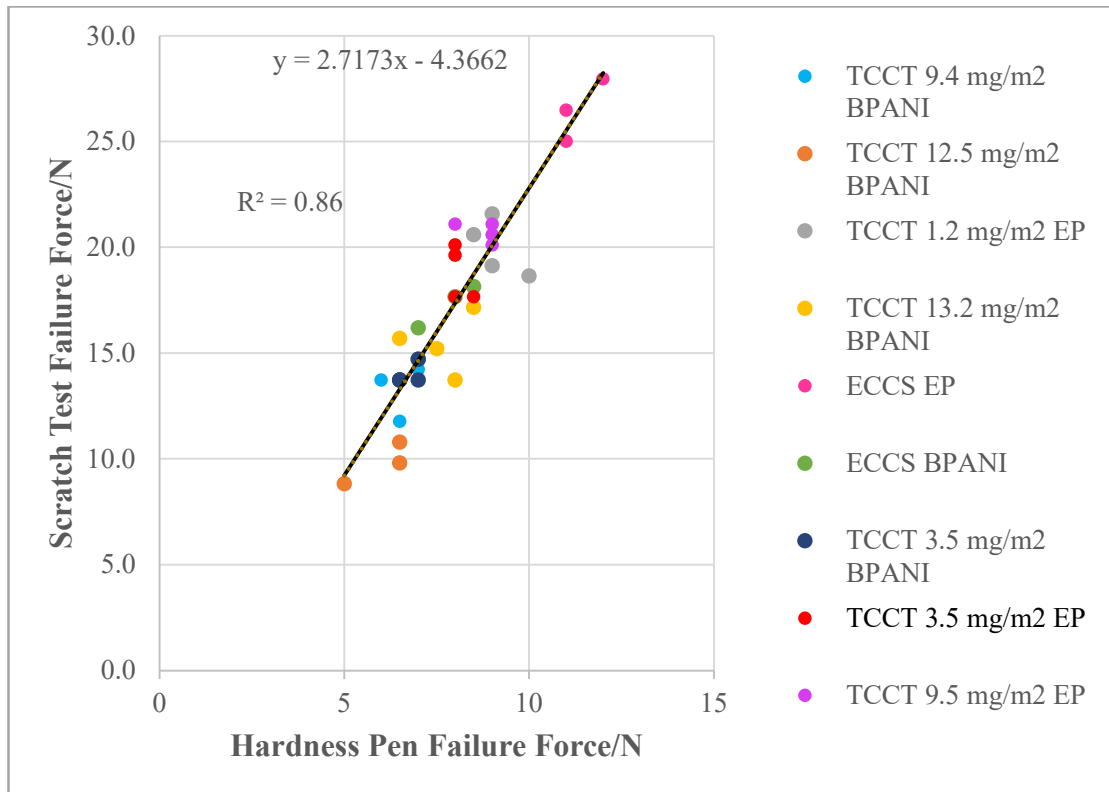


Figure 6.7 A scatter plot of failure forces for scratch testing versus hardness pen

The data in Figure 6.7 was plotted as a scatter graph with a line of best fit in order to conclude whether there is a correlation in the data set and enable any values to be converted using the graph. The line of the graph does not go through the 0,0 point as the precision of the hardness pen does not enable accurate measurements to be made in this range. In addition to this, the samples selected do not exhibit failure forces this low so there is no data to plot in this region. It is clear from the graph that there is a discernible correlation between hardness pen and scratch test failure forces and the line equation of the graph. Equation 6.3 can be used to convert between values in order to give an approximate value and enable two different data sets to be compared. The R^2 value of the graph is 0.86 which suggests the data is a good fit to the trendline and as such the conversion between both types of failure force should be accurate for comparison purposes. While this method is not highly precise, it is reproducible and

can give an approximate range of failure force enabling a comparison to be made between undeformed, uniaxially deformed and biaxially deformed substrates.

$$\text{Scratch Test Failure Force} = (2.71 * \text{Hardness Pen Failure Force}) - 4.36 \quad (6.3)$$

6.3.2 Comparing Uniaxial versus Biaxial Failure Forces

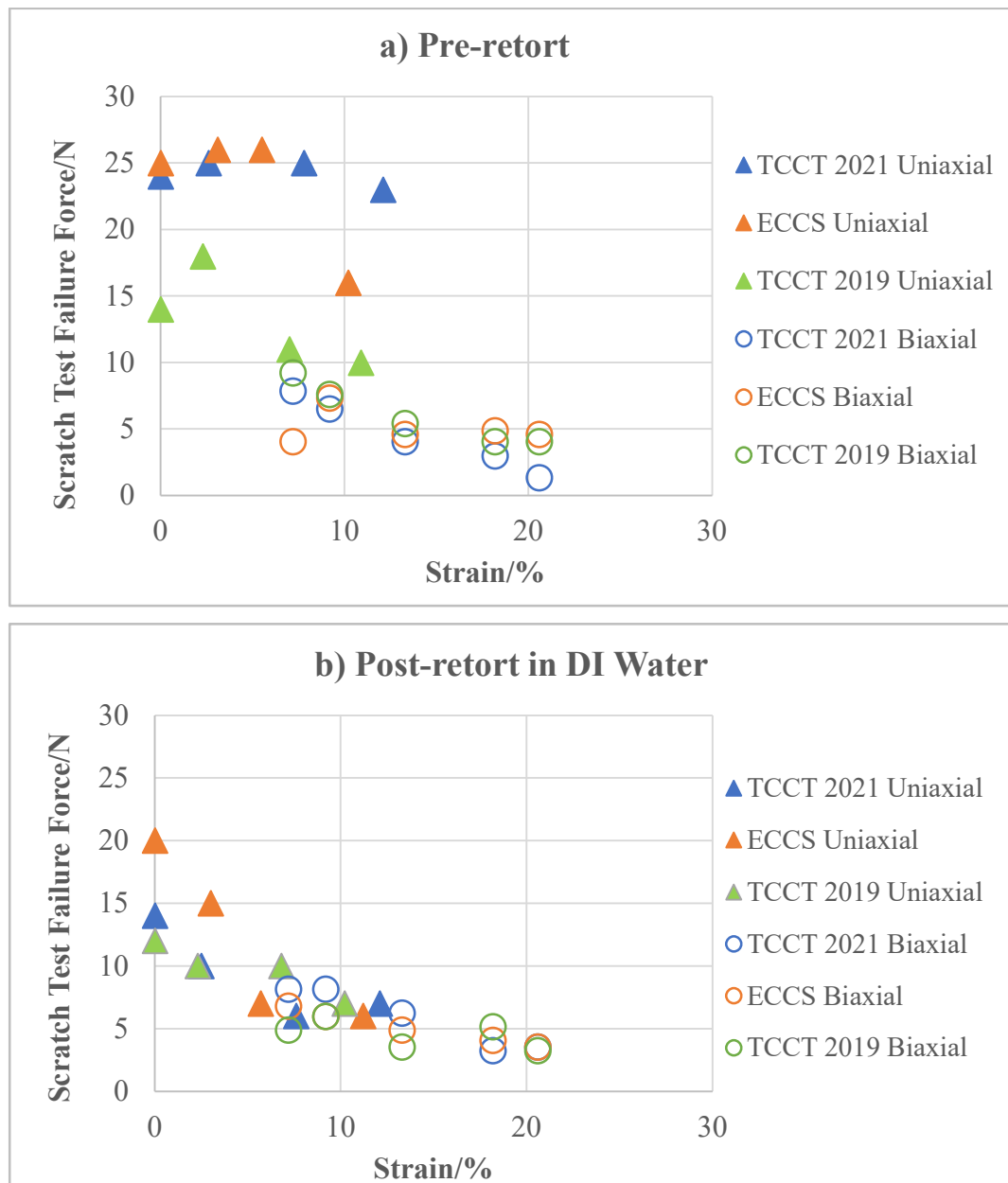


Figure 6.8 Uniaxial and biaxial failure forces for BPANI Coated ECCS and TCCT substrates a) pre-retort and b) post-retort in DI Water plotted against percentage strain

Uniaxial and biaxial failure forces were plotted against strain percentage in order to establish if the numerical strain value of a uniaxial sample is equivalent to that of a biaxial sample, the results of which are shown in *Figure 6.8*. In order to make the comparison as accurate as possible the TCCT and ECCS samples used all had CrOx coating weights in the same range of 9-11 mg m⁻². It can be seen from *Figure 6.8* that there is no correlation between the measured failure forces of uniaxially and biaxially strained samples at the same strain values which means that there is likely to be fundamental difference in the substrate between uniaxial and biaxial strain. This was observed by Whiteside *et al.* (118) where cracks in the surface CrOx were observed under strain. Uniaxial sample types exhibited higher failure forces, up to 20N greater in the case of pre-retort BPANI coated TCCT samples in *Figure 6.8a*, than their biaxially strained counterparts.

DIC (Digital Image Correlation) has been used in literature to strain map both uniaxially and biaxially deformed samples. DIC has demonstrated that the point of highest strain in uniaxially deformed samples is localised in a band at the centre of a sample (91). The area of highest strain in biaxially deformed samples was in a ring around the edges of the sample where the most thinning occurred (92). Since biaxial strain was not confined to a single point on the dome there is much greater strain within the dome shape than the conventional dog bone shaped uniaxial tensile sample. This implies that a uniaxially strained sample is not strained significantly enough compared to a biaxial sample at the same numerical value of strain. This is supported by the lower failure forces in *Figure 6.8* for biaxially strained samples compared with uniaxially strain samples. The significance of this is that in order to run laboratory strain experiments to assess material performance a biaxial strained sample must be used in order to get the best representation of a real food can as the strain is not uniaxial (136). These behaviours also may relate back to the CrOx layer thickness and its formability. Thicker layers of CrOx may be able to withstand uniaxial deformation but not biaxial.

Post-retort samples in *Figure 6.8b* demonstrated overall higher failure forces for uniaxially strained samples than their biaxially strained counterparts. In comparison with the pre-retort samples, post-retort values were lower and were converging to similar failure forces as strain was increased. This suggests that while the retort process is detrimental to both uniaxially and biaxially strained samples it has more of

an influence on the uniaxially strained samples. It is hypothesised that any strain which leads to the cracking of the CrOx layer results in exposure of the Cr or Fe metal, this could be verified in future work using techniques such as XPS or EIS and are discussed further in section 6.6.1. Under dry conditions, the impact of the small surface cracks is minimal, but once exposed to retort conditions, corrosion mechanisms dominate the failure. It is proposed that even a small amount of CrOx cracking results in some degree of localised corrosion leading to a reduction in adhesion.

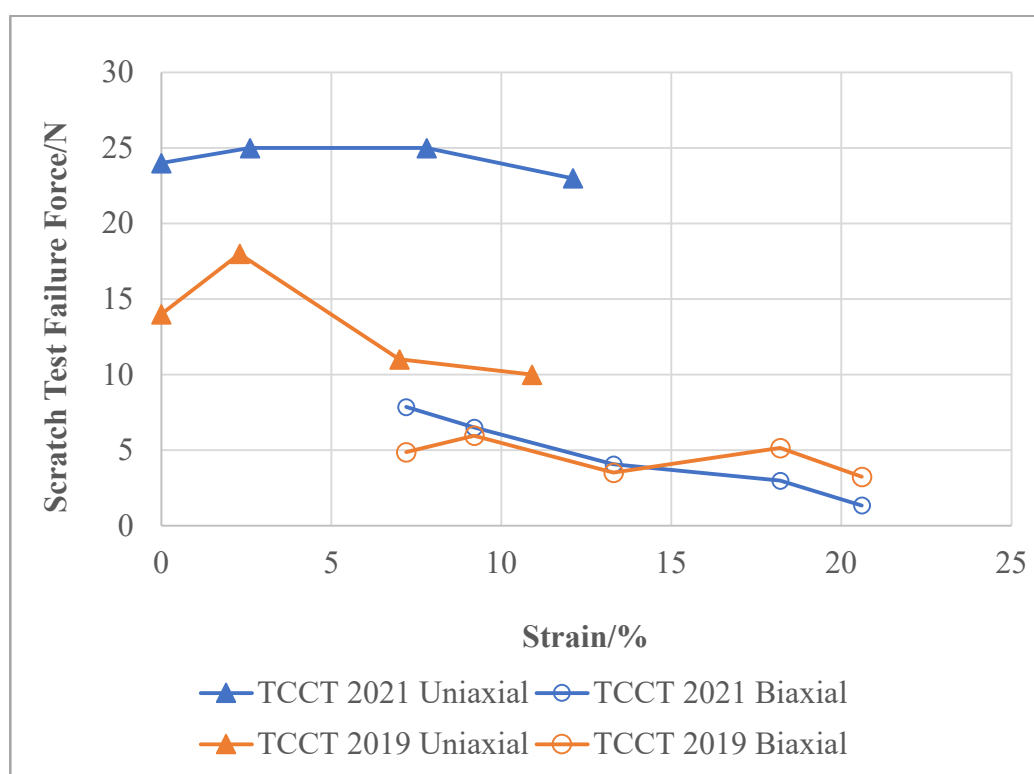


Figure 6.9 Comparing uniaxial and biaxial failure force results for BPANI coated TCCT Samples Pre-Retort

Figure 6.9 demonstrates a direct comparison between BPANI coated TCCT substrates, one of which was uniaxially strained and the other biaxially strained. It is evident from the graph that even when converted to the same measurement units that the failure forces for uniaxially and biaxially strained samples are different. For example, at 10% strain there is approximately 18N difference between the biaxially and uniaxially strained samples of TCCT 2021. Where the strain values for each graph overlap in the range of ~7-13% this difference of 18N between the strain values remains consistent. Despite the difference being consistent across a sample type this

is not consistent for all substrate/lacquer types. The TCCT 2019 samples displayed a difference of only 6N across the ~7-13% strain range. These results confirm that there is no consistency between uniaxial and biaxial strain and as such uniaxial strain cannot reflect biaxial strain accurately. It can also be concluded that biaxial strain induces a larger reduction in adhesion compared with uniaxial strain.

The increase in uniaxial strain performance of TCCT 2021 compared with TCCT 2019 shows an improvement in the substrate. Despite this the biaxial performance of the substrate types remain similar. This indicates that perhaps the 2021 substrate has been optimised for uniaxial strain performance but not biaxial strain. It is evident that there are different mechanisms of deformation for biaxial strain versus uniaxial strain. Optimising material performance based on uniaxial strain performance is misleading and does not optimise it for biaxial strain or the can making process.

6.4 Biaxial Strain

6.4.1 Dry Adhesion

The biaxially strained samples were analysed as dry, pre-retort samples and post-retort in DI water and 0.1% NaCl. It should be noted that an attempt was made to use 1% NaCl and 0.5% NaCl solutions but the resulting failure force values were outside the measuring range of the hardness pen.

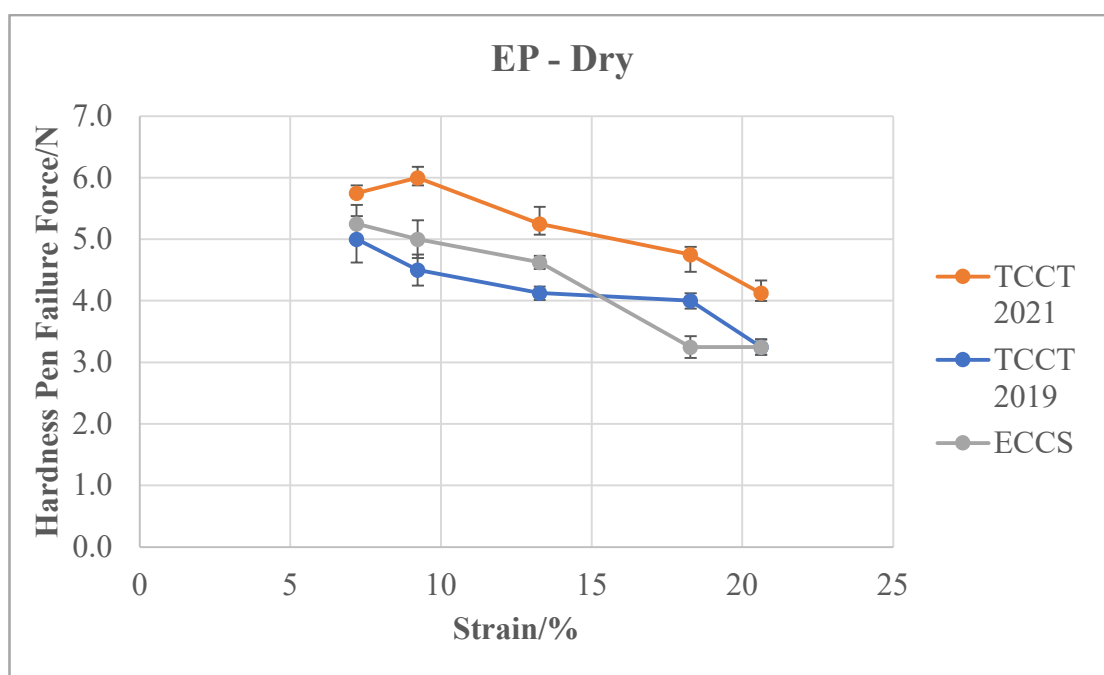


Figure 6.10 Biaxial strain versus failure force for EP coated TCCT and ECCS samples under dry conditions

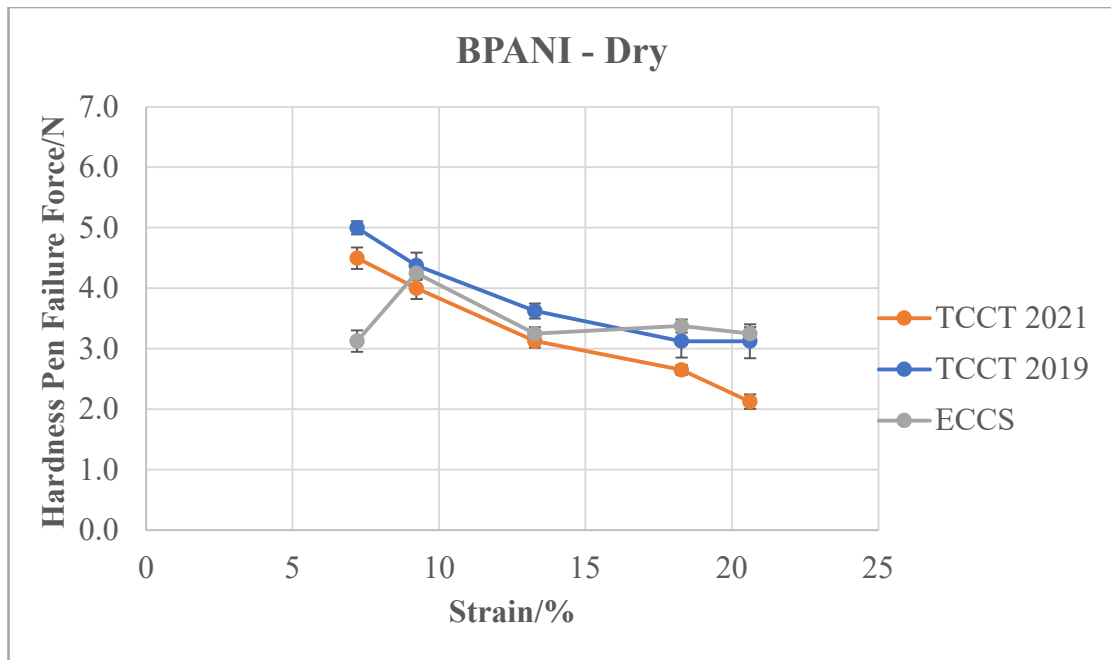


Figure 6.11 Biaxial strain versus failure force for BPANI coated TCCT and ECCS samples under dry conditions

Figure 6.10 and Figure 6.11 demonstrate the changes in adhesion of biaxially strained EP and BPANI coated samples that have not been subjected to the retort process. The results of the failure force indicate the influence that the strain has on the samples without any other factors. It is evident from Figure 6.10 and Figure 6.11 that the performance of the EP lacquer is better than the BPANI lacquer, this is what has been observed throughout this research. The change in failure force as strain is increased from 7 – 20% is around 2.5 N which is consistent for all sample and lacquer types. The EP lacquer failure forces are consistently higher by approximately 1N, this remains the case even once the samples are strained. The resolution of the force when the 0-10N range spring is used is $\pm 0.5\text{N}$, meaning the difference between the EP and BPANI failure forces can be considered almost insignificant. Even though the failure forces for BPANI are lower, its performance remains consistent even under strain.

Despite the difference in lacquer performance, the different substrates perform similarly and there is no notable correlation between the substrate type/generation and the failure force suggesting that all of the substrates are suitable for use as an alternative to the commercially available ECCS substrate if the systems were to be considered only in the dry state.

6.4.2 Lacquer Adhesion Post-Retort in DI Water

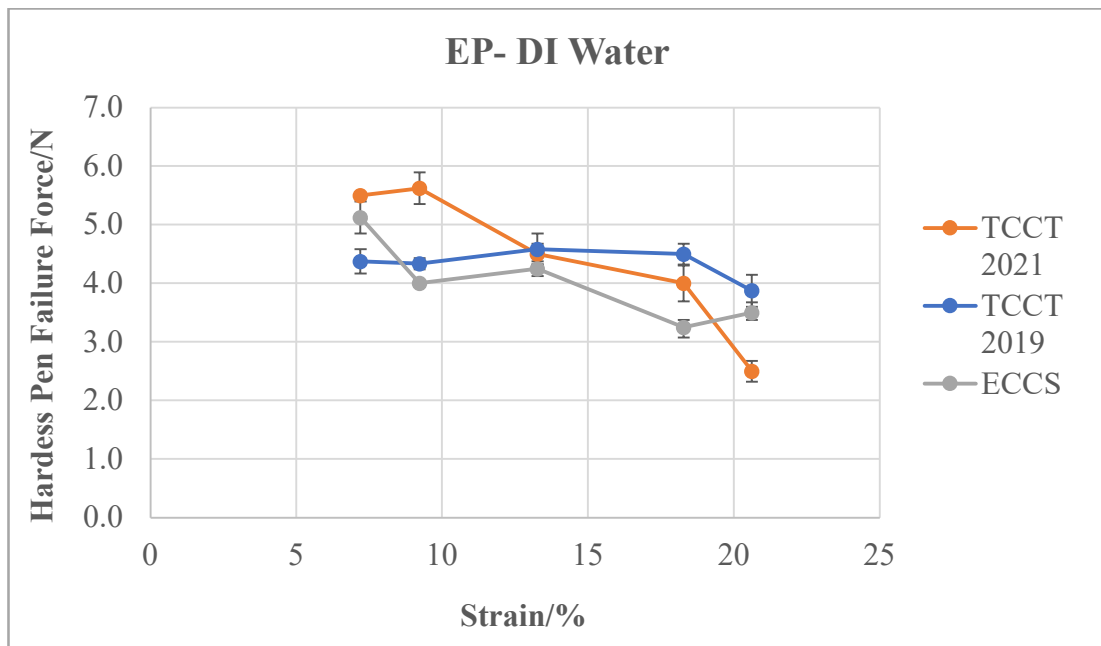


Figure 6.12 A graph of biaxial strain versus failure force for EP coated TCCT and ECCS samples retorted in DI Water

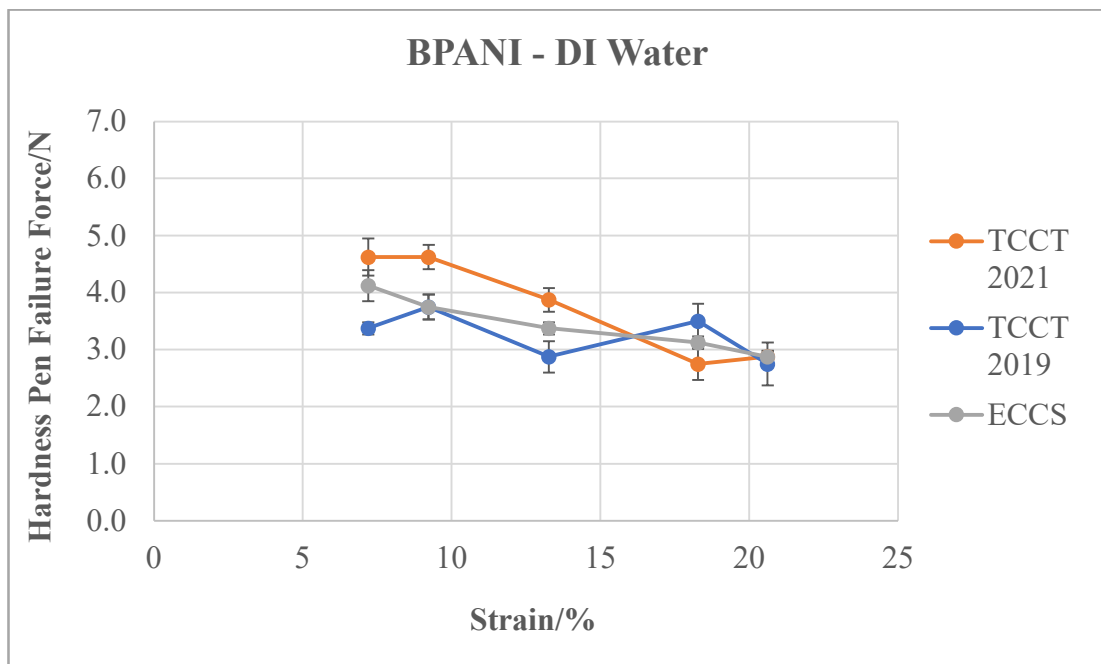


Figure 6.13 A graph of biaxial strain versus failure force for BPANI coated TCCT and ECCS samples retorted in DI Water

Figure 6.12 and Figure 6.13 displayed similar trends for the failure forces for both EP and BPANI lacquers when adhesion tested after retort in DI water. The failure forces are higher by ~1N more for EP than BPANI with a gradual drop in failure force observed as strain is increased. Both lacquers demonstrate the same behaviour in the changes in failure force and all converge to a similar value of around 3N at 20% strain regardless of the lacquer/substrate combination. The greater drop in failure force seen for EP than BPANI suggests that the bonding of EP lacquer is disrupted more by straining the BPANI. This implies a greater change in the number of OH bonding sites as a strain is increase resulted in a great change in lacquer adhesion. As a result, it can be assumed that the adhesion between the CrOx layer and EP is stronger initially than that of CrOx and BPANI. Since the final strain values are comparable for EP/BPANI for TCCT 2021 and ECCS this suggested TCCT is a suitable replacement for ECCS if water is the only constituent of the liquid being retorted.

6.4.3 Lacquer Adhesion Post-Retort in 0.1% NaCl

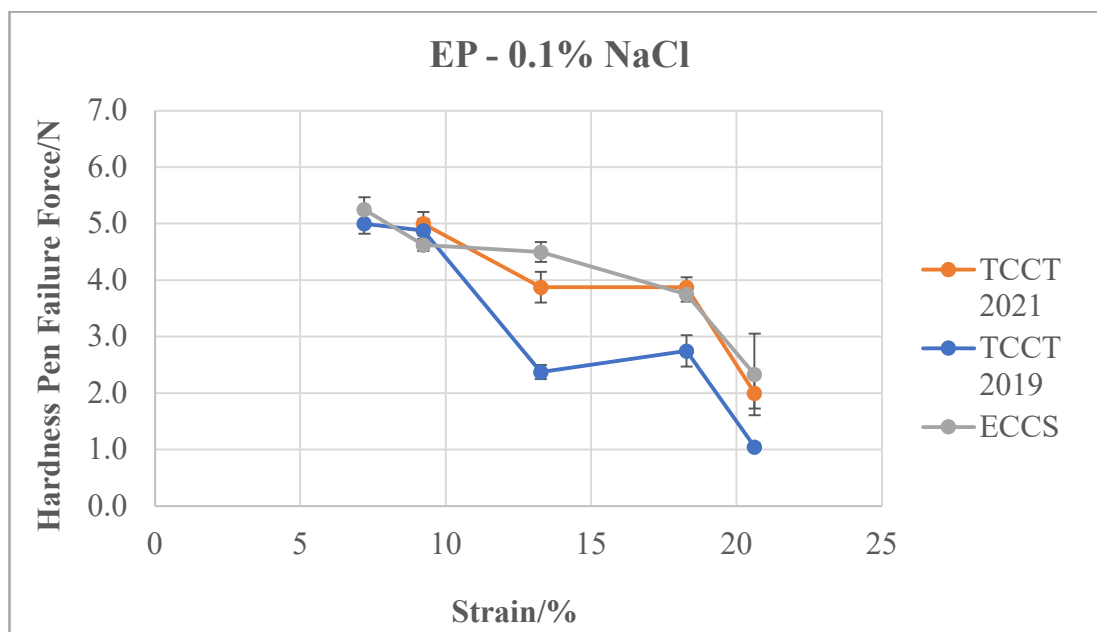


Figure 6.14 Biaxial strain versus failure force for EP coated TCCT and ECCS samples retorted in 0.1% NaCl

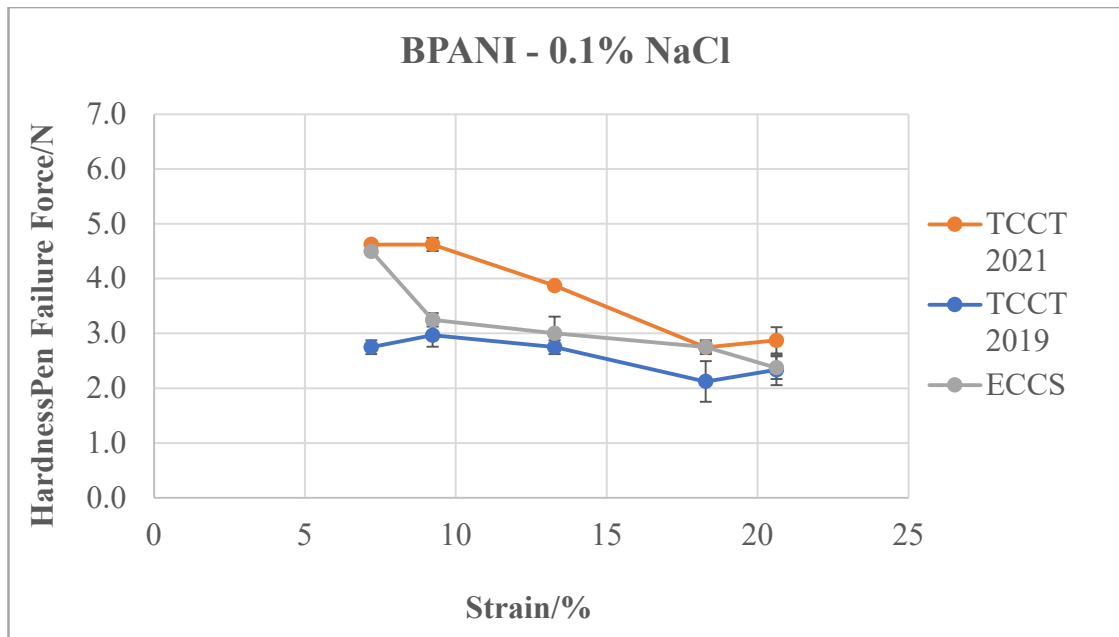


Figure 6.15 Biaxial strain versus failure force for BPANI coated TCCT and ECCS samples retorted in 0.1% NaCl

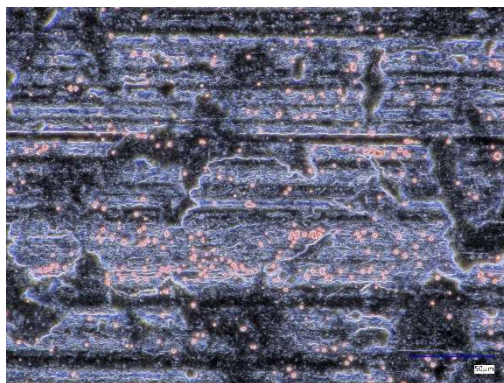
It has been demonstrated in previous work using NaCl as a food simulant that it has a greater destructive effect on the CrOx layer of TCCT 2019 compared with TCCT 2021/ECCS. The same trend is observed for biaxially strained samples with both EP and BPANI as seen in *Figure 6.14* and *Figure 6.15*. The TCCT 2019 substrate exhibits a failure force approximately 2N lower than TCCT 2021/ECCS at low strain values. Suggesting the CrOx layer has more of an influence over the lacquer adhesion than the simulant at low strain. The difference in performance of TCCT 2019 compared with ECCS/TCCT 2021 at higher strain values is only 0.5 to 1N suggesting the influence of strain dominates at higher values. This confirms earlier findings in *Section 5.2.2* that the Cr/CrOx layers on older generations of TCCT are less uniform compared with similar CrOx weight TCCT 2021 and ECCS substrates. The lower adhesion resulting from this non-uniform layer is due to more free iron/chromium being exposed (8,9,136). The amount of which increases with increasing strain. More free iron/chromium means less CrOx so less OH bonding sites for the lacquer to adhere to and as such a reduction in failure force.

Conversely at higher strain values the performance of all substrates converge to similar values suggesting that strain and simulant have a greater influence on the substrate at these values of around 20%. This indicates that the surface of all substrates become similar once strained as more iron or chromium is then exposed on samples of ECCS and TCCT 2021 despite being more homogenous than TCCT 2019 initially. This reconfirms the findings from uniaxial strain studies in *Section 5.2.2*. Despite the reduction in failure forces seen the similar final failure forces of TCCT and ECCS substrates deem TCCT as a suitable replacement for ECCS.

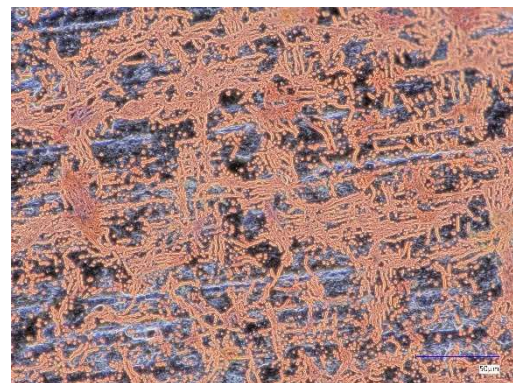
6.5 Oxide Pin Hole Identification using a Preece Test as a Way to Quantify Free Iron and Chromium on a Substrate Surface

An oxide pin hole identification technique was employed in an attempt to quantify and compare the amount of free iron/chromium present on unlacquered ECCS and TCCT substrate surfaces after straining. Since this method (*Section 3.6*) was adapted from work conducted by Dodd, confirmatory analysis of the copper deposits had already been conducted for these substrate types and as such it was not repeated (120).

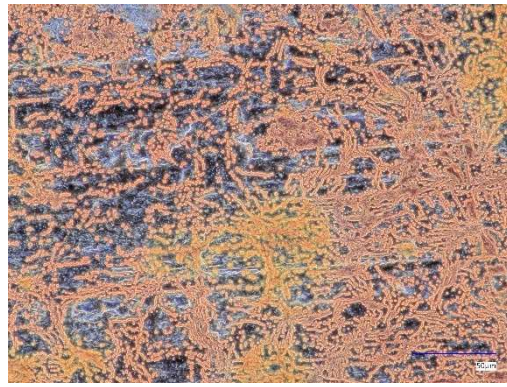
6.5.1 Keyence Imaging and Area analysis



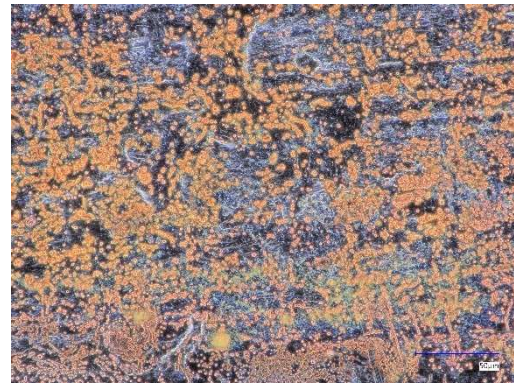
a) IE 0 mm, 0% Strain



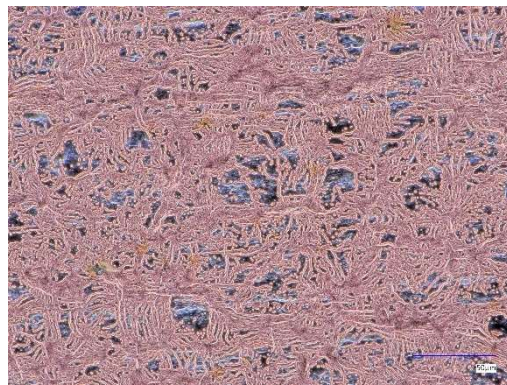
b) IE 1 mm, 7% Strain



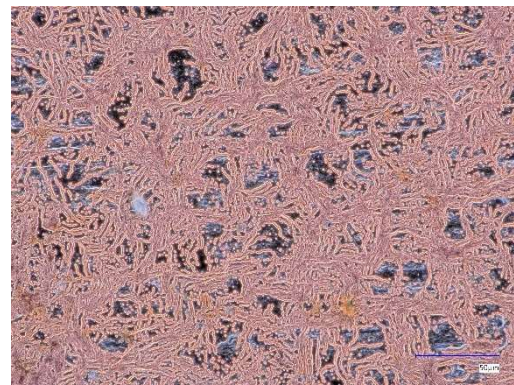
c) IE 2 mm, 9% Strain



d) IE 3 mm, 13% Strain



e) IE 4 mm, 18% Strain



f) IE 5 mm, 21% Strain

Figure 6.16 a) to f) Keyence images of copper deposits on biaxially strained samples of unlacquered TCCT

The Keyence images in *Figure 6.16* show how a visible increase in the amount of deposited copper as the dome height of biaxially strained samples is increased from 0-5mm (0-21% strain). It is clear from these images that there is a significant amount of free iron/chromium exposed on the material surface once the sample is subjected to strain. This implies that the CrOx layer is brittle and cracks upon straining. This is significant as it weakens the material by exposing it to corrosion and chemical attack. Depositing a lacquer onto the unstrained substrate may fill part of the cracks in the surface, however, the lacquer is not ductile enough to withstand being strained and therefore will not hold the CrOx surface together.

Copper deposits onto the surface in a mushroom shape and as such the amount of copper does not equate to the amount of iron/chromium present. Despite this, CuSO₄ dipping enables a comparison to be made between sample types as the amount of copper is relative to the amount of free iron/chromium present so an increase in copper correlates with an increase in iron/chromium.

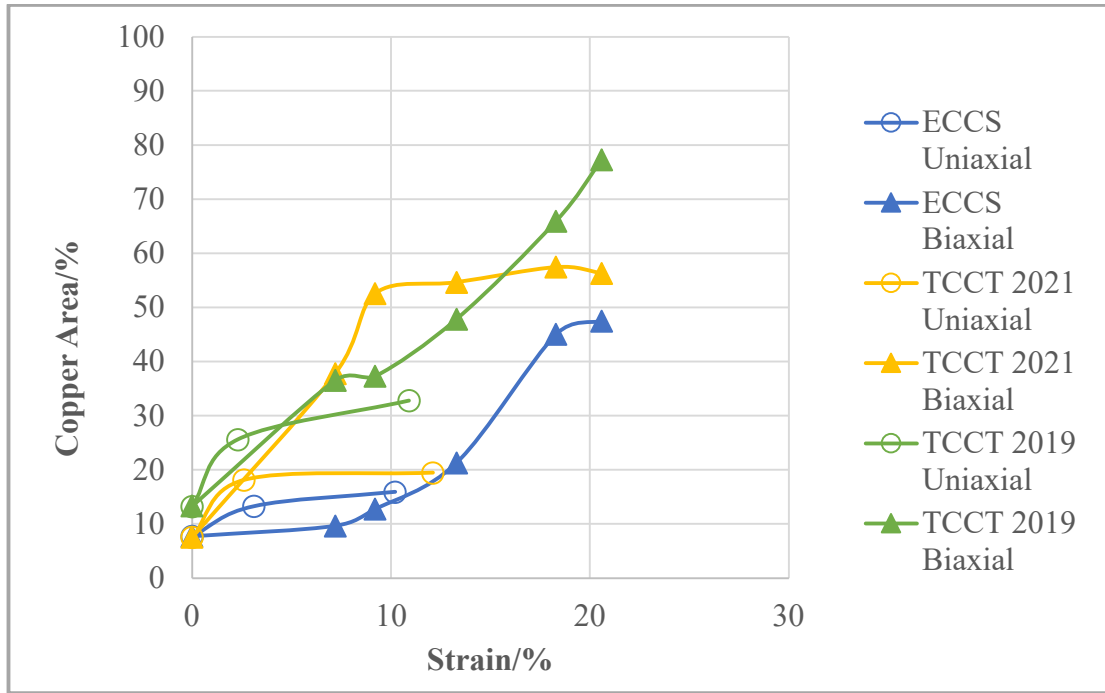


Figure 6.17 The percentage area of copper deposits on a substrate surface at different strain values on various TCCT and ECCS substrates

It is surmised, based on previous adhesion studies, that straining a sample will form cracks in the CrOx surface and expose more of the chromium and iron beneath the surface. The oxide pin hole identification study results shown in *Figure 6.17* demonstrate that an increase in strain increases the amount of free metal that is exposed. It should be noted that biaxially strained samples showed more copper deposits than their uniaxial counterpart of the same substrate. For example, at 15% strain biaxially strained samples of TCCT 2021 showed 35% more copper deposits than the uniaxially strained sample. This is significant as it indicates that introducing another axis of strain has significant effect on the material. This also supports the numerical failure forces seen in *Figure 6.8* where the uniaxial strained samples showed much higher failure forces than the biaxially strained samples did at the same strain values.

The ECCS samples showed the lowest overall amounts of copper which is consistent with previous results that support the theory of the CrOx layer on the ECCS substrate being more homogenous than the CrOx layer of TCCT. In addition to this, at the highest strain value of 21% there is a difference in surface copper of around 20%

between TCCT 2021 and TCCT 2019. This suggests that the newer generations of TCCT substrates have more homogenous surfaces with less defects than their older generation counterparts.

6.5.2 Failure Force and Non-CrOx Coated Area

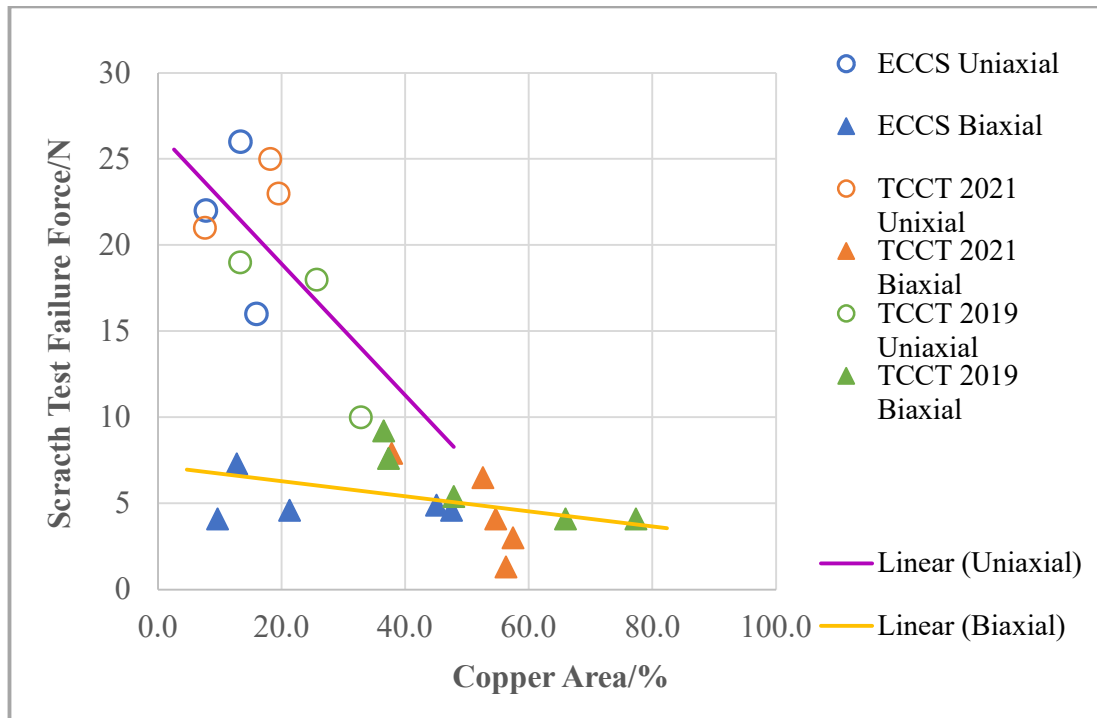


Figure 6.18 Failure Force versus Copper% for BPANI Coated TCCT and ECCS Substrates

The trendlines in *Figure 6.18* demonstrate that there is a general trend in the data set that as copper percentage increases the failure force decreases. The findings from this section of research have also demonstrated a correlation between strain and the amount of CuSO_4 that was subsequently deposited. It is proposed that since this correlation exists it could be a useful QC control to do quick checks on samples to see if they pass or fail. If necessary, the data set could be expanded to encompass different CrOx weights to get a broader range of QC limits making the method more widely applicable and ensuring that a higher CrOx weight does not pass based on the higher copper percentage set by a lower CrOx weight substrate. A CuSO_4 area limit could be set for a specific strain percentage to determine whether each batch of substrate is suitable for a can making application. This would result in significant time saved as straining, dipping and imaging a sample would take minutes compared with the several hours required to coat, strain, retort and scratch test samples.

6.6 Theory of Coating Inhomogeneity

It is proposed, based on the findings of this research and previous work (73,120) that there are inhomogeneities in the Cr/CrOx surfaces of packaging steels. Findings in *Sections 5.2* and *6.4* of this research demonstrated that straining samples exacerbates this inhomogeneity exposing free iron or chromium beneath the Cr/CrOx surface. This in turn has the effect of reducing lacquer adhesion by exposing the substrates to corrosion and chemical attack. The diagrams shown in *Figure 6.19* are two proposed mechanisms as to what is happening on a microscopic level on the surface of the substrate. The two proposed scenarios are:

1. The chromium layer does not yield under strain and cracks like the CrOx layer exposing the iron beneath the surface
2. The chromium layer is more formable than the CrOx layer and when subjected to strain the CrOx layer cracks, but the Cr layer yields under strain. This would leave the chromium layer exposed but the underlying iron layer protected.

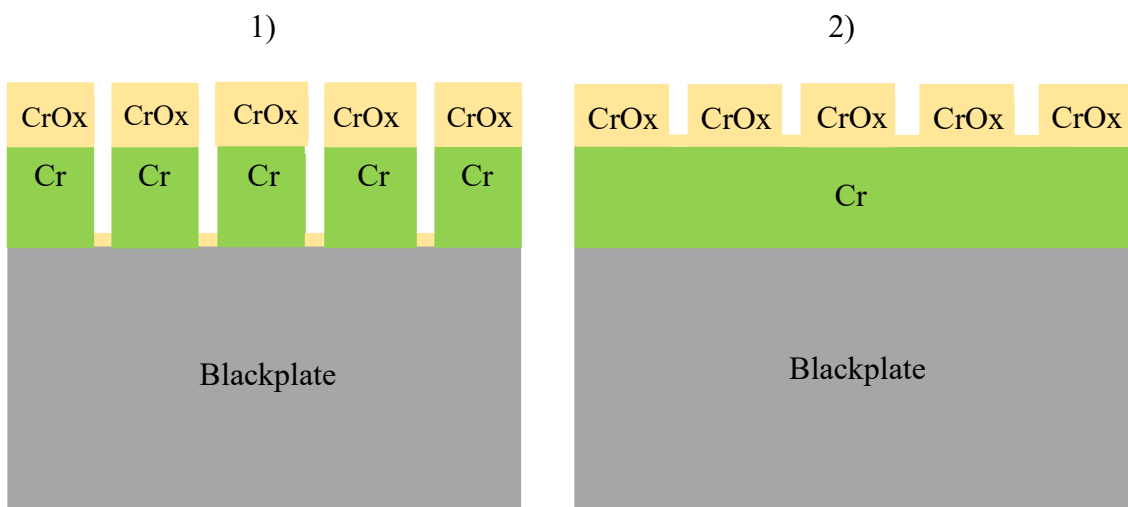


Figure 6.19 Diagrams showing the proposed mechanisms of coating inhomogeneity on steel can making substrates

The layer of chromium that is deposited in both ECCS and TCCT is approximately 20 nm thick. Due to the narrow gauge of the layer then it is plausible this should yield under strain. Aside from this it is not known whether the Cr-CrOx bond is strong enough to withstand deformation enabling the layers to remain bonded and split

together or whether the formability of the Cr layer is good enough to favour the Cr-CrOx bond being broken.

It is well understood that during the chromium deposition process for TCCT there is significant hydrogen evolution occurring at the surface due to the high currents needed for a sufficient layer of metal to be deposited (21). This in turn can result in poor deposition of the chromium coating and as such defects will be present which are not sufficiently covered by the thin layer of CrOx that is subsequently deposited. This means a reduction in the available OH bonding sites for the lacquer and in turn poorer adhesion and low failure forces. The lacquer may fill some of the cracks and cover the exposed iron, but some may remain. This is then intensified when the sample is strained, and the protective layers are thinned. It is also worth noting that due to the deposition of the chromium and CrOx layers being separate processes it is feasible that CrOx could be deposited even when Cr is not present. This is due to the electroplating process for TCCT being a two-bath process where Cr deposition occurs first and CrOx deposition occurs second. It is plausible that the bath containing chromium salts used for depositing the CrOx layer would enable a CrOx layer to be deposited without the presence of a metallic chromium layer. This would give less protection to the surface as the Cr layer is required for hardness and wear resistance and the CrOx layer provides chemical stability and improved corrosion resistance for the steel substrate. (18) .

Unlike with TCCT, the process for producing ECCS is well established and as such is much more controlled. It also differs in how the CrOx layer is produced by which the Cr layer is deposited and the CrOx layer is grown from this rather than being deposited separately (163). As such if there is no Cr, there is no CrOx layer either meaning there is the potential for the organic lacquer to bond to the surface of the steel substrate. This bonding between iron and the lacquer can be difficult to achieve without surface preparation and primers and this could result in areas of the surface with iron exposed where the lacquer has been unable to form bonds with the surface or weak bonds are formed that are easily broken.

It is of importance to note that there is significant literature detailing the formability of the organic coating on ECCS/TCCT but limited research into the formability of the chromium and chromium oxide layers (110,164–166). Adhesion of the lacquer, as well

as its formability, has been thoroughly researched but the literature investigating the changes in surface condition affecting this adhesion has not been characterised on an elemental level (28,44,167–169). It would be useful to understand how the Cr and CrOx layers are affected by straining as they are providing both protection for the steel and bonding sites for lacquer adhesion. Since lacquer adhesion is achieved through hydrogen bonding between the lacquer and the CrOx layer it is vital to understand more about the changes that occur in a strained system.

6.6.1 Validating the Theory of Coating Inhomogeneity

This hypothesis of whether it is free chromium or iron exposed in defects could be tested by various analytical techniques used to map the Cr/CrOx surfaces before and after straining. They could identify defects in the surface post strain and establish whether chromium is present or iron. If chromium is still present post strain, then it yields under strain, if not then it splits with the CrOx layer. Several techniques have been explored that could be used to validate the theory and elementally map the substrate surface providing a distinction between chromium and iron. The non-planar nature of the sample was taken into consideration during the literature research as this will affect the operating parameters of the instruments and make some unsuitable for the application. Additionally, since the Cr layer is between 10 and 20 nm the chosen technique must only analyse at this depth to truly pick up only iron from a defect not the whole steel surface. A summary of key findings from the literature research are summarised in *Table 6.1* this includes the theory and operation of the technique, the advantages and potential issues associated with use of the technique for the application.

Table 6.1 Comparison of Analytical Techniques for Surface Analysis of Chromium Coated Steel Substrates

| Technique | Theory/Operation | Advantages | Potential Issues |
|---|--|--|---|
| XPS (X-Ray Photoelectron Spectroscopy) (170–173) | Qualitative technique for measuring elemental composition of a surface. | Sample height up to 10mm Enables all dome heights within this research to be analysed | Small Surface Area Analysis May be unrepresentative if it hits a defect versus a uniform part of the surface |
| | XPS uses X-rays to bombard the surface of a material, electrons within the material absorb energy from the | Precise Elemental Identification and Quantification Enables each element and compound to be identified and quantified based on peak size | Beam Angle This may be an issue due to the non-planar nature of the sample so it may not hit the top of the dome subsequently not hitting the point with the highest strain which the strain measurement was taken from |
| | X-rays and become excited if the amount of energy absorbed is sufficient to eject the | Surface Analysis only Analysis depth <10 nm means that XPS should not pick up the iron unless it is in an uncoated defect | Surface Contamination Residual solvents, atmospheric gases and contact with the sample can affect measurements and produce additional peaks |

| | | | |
|---|--|---|--|
| | <p>electron from the atom i.e. greater than its binding energy. The kinetic energy of the excited electrons are measured and enable not only elemental mapping of the surface but also individual orbitals and their concentrations.</p> | <p>Sample is Secured The sample is secured with carbon tape in order to make electrical contact – this also prevents it from being affected by the high vacuum</p> | <p>in the spectra which will interfere with the surface analysis. There are several options for removing this contamination which include solvent cleaning, heat treatment and UV cleaning.</p> |
| <p>ToF-SIMS (Time of Flight Secondary Ion Mass Spectroscopy) (9,174,175)</p> | <p>Provides spatially resolved chemical composition of a surface. A pulse of Bi/Ga/Cs ions bombards a</p> | <p>Surface Mapping ToF-SIMS Provides chemical and elemental mapping on a sub-micron scale</p> | <p>Not quantitative The technique cannot provide a full qualitative analysis and is more useful for surface images distinguishing between element types -further analysis would be required</p> |

| | | | |
|--|--|---|--|
| | <p>surface and sputter it. A cloud of molecules and atoms is produced, some of which are ionised. The ions of single polarity are accelerated into a ToF MS and are detected and counted. The lighter ions arrive at the detector before the heavier ones and as such it enables mass selection.</p> | <p>Individual atomic layer profiling</p> <p>Important for this application as want to look at chromium and iron separately and distinguish between the uniform layers and defects</p> | <p>Limited Optical Capabilities</p> <p>ToF-SIMS makes it difficult to find specific areas of interest meaning finding the top of a strained dome may be difficult. This will also be affected by a change in ion data collection mode</p> |
| | | <p>‘Retrospective’ Analysis</p> <p>The software saves data for each molecule on the surface so individual defect analysis can be performed by selecting the spectra for that specific area</p> | <p>Angled Excitation Beam</p> <p>The angled beam may make analysing a domed sample difficult as it may not be directly hitting the most strained part of the sample i.e. the top</p> |
| | | <p>Highly Sensitive</p> <p>Works for trace elements and compounds so could identify differences in small defects</p> | <p>Ultra-High Vacuum</p> <p>May displace the sample and distort analysis of the target area</p> |

| | | | |
|---|---|---|---|
| <p>EIS (Electrochemical Impedance Spectroscopy) (176–178)</p> | <p>EIS can investigate charge-transfer, mass-transfer and diffusion processes. EIS can study material properties or processes that could influence capacitance, resistance or conductance of an electrochemical system.</p> | <p>Sensitive</p> <p>Can detect small fluctuations in impedance. This can indicate corrosion or material degradation is occurring</p> | <p>Limited Spatial Resolution</p> <p>Useful to provide bulk property information but may not be useful for heterogenous surfaces or those with localised defects such as the samples to be analysed here</p> |
| | | <p>Quantitative</p> <p>Will give information about the changes in the coating over time</p> | <p>Complex Data Interpretation</p> <p>Requires mathematical modelling and an understanding of electrochemical principles in order to fit the models to the data</p> |
| | | <p>Discriminative</p> <p>Advantageous over other electrochemical techniques as it can provide information about electrochemical, electrical and physical processes that take place in a real electrochemical system – Would expect to see one curve if the Cr is intact or two if the Cr surface has defects present with iron in it</p> | <p>Potential Barriers</p> <p>Experimental conditions such as temperature and pressure, insufficient sample preparation and electrode polarisation effects can all influence the final result</p> |

6.7 Conclusions

This section of work has established a method for inducing and measuring biaxial strain. It has also utilised a hardness pen to test the adhesion of BPANI/EP coated samples that have been biaxially strained and then retorted in food simulants. This was to simulate the DRD stage of the industrial can making process that these substrates would be subjected to. It has been established that scratch test and hardness pen failure force values can be interconverted using an equation to give values that are comparable to literature and previous research, thus enabling unstrained, uniaxially strained and biaxially strain samples to be compared. There was found to be significantly higher failure forces for uniaxially strained samples compared with biaxially strained samples meaning they cannot be used interchangeably as testing methods.

An extensive sample set was used to produce a calibration curve for samples biaxially strained using an Erichsen cupping apparatus. The working strain range of TCCT and ECCS samples was established to be up to 5 mm dome heights which is equivalent to ~21% strain. Through the use of this calibration curve a biaxial strain study was conducted where it was found that EP and BPANI performance was consistent across all sample types. BPANI coated substrates were found to exhibit failure forces about 1N lower than the EP coated counterpart. A decline in failure force was seen as strain was increased with a difference of 2-3N between the highest and lowest strain values. The highest overall strain values were seen for pre-retort samples with samples post-retort in DI showing similar trends. An attempt was made to retort strained samples in a 1% NaCl salt solution to remain consistent with unstrained and uniaxial strain studies that have been conducted previously. These values were outside of the measuring range of the hardness pen. The same was found for a 0.5% NaCl simulant solution. Samples were retorted in 0.1% NaCl and were found to have lower adhesion values than Dry/DI samples implying that the NaCl is much more detrimental to the substrate, reconfirming findings from previous sections.

Findings from food simulant studies led to hypotheses being formed regarding the uniformity of the substrate surface and the consequences of sample straining. An oxide pin hole identification method was adapted to study surface defects. It showed an increase in the amount of deposited copper as the strain was increased. ECCS substrates, as with previous studies, outperformed TCCT substrates with the newer generation of TCCT showing improvements from the older generation. Copper

percentage was plotted against the failure forces from previous studies and independent trends were found in both the uniaxial and biaxial strain data. Uniaxially strained samples showed less free metal on the surface compared with biaxially strain samples with the same numerical strain. This suggests that not only are the two methods not interchangeable but biaxial strain has a greater influence on the surface condition than uniaxial strain. It is proposed that this method could be a rapid QC tool to establish if a chromium oxide coated sample will fail final stage analysis. Further data acquisition would be required for values outside of the 9-11 mg m⁻² CrOx range used as higher values may pass the QC checks but be unsuitable for other applications.

This research has shown there are defects in the CrOx surface of TCCT and ECCS substrates. It is known that these are either chromium or iron, but they have not been distinguished thus far. Two theories of coating inhomogeneity under strain were proposed, either the chromium layer splits with the CrOx layer or it yields with the steel and only the CrOx layer splits. Several analytical methods have been literature researched as possible ways to investigate this, but they were not performed within this research due to time constraints.

Chapter Seven

Conclusions

7 Conclusions

The REACH legislation banning the use of hexavalent in can making prompted the development of the trivalent chromium coated substrate, TCCT. The added need to remove BPA from food contact materials means that EP lacquers are to be replaced with polyester lacquers, in this instance BPANI is used. The performance of novel TCCT substrates have been investigated under the influence of heat, pressure, chemical environment, humidity, and strain. These have provided a rigorous testing regime to ensure that TCCT can withstand all aspects of the can making, filling, and cooking processes.

The impact of this work is demonstrated in the now thorough understanding that has been gained about the performance of coated TCCT substrates. It is of further importance that the newer TCCT 2021 batches showed improved performance, compared with TCCT 2019 substrates, as these were provided to customers of TATA Steel for trials. This research using different food simulants, various concentrations and different strains has been significant in building a representative testing regime. This more closely reflects the parameters that a substrate is subjected too throughout the can making and food sterilisation processes but on a laboratory scale.

Three main objectives were outlined in the introduction to this research and this section aims to conclude the findings from each chapter of work relevant to each objective.

The aim of chapter four was to establish the degree of influence of food simulant concentration and CrOx weight on lacquer and substrate performance both pre- and post-retort. The key research within this chapter involved the use of various analytical and mechanical techniques to characterise both the lacquers and substrates. Initial multi simulant testing was used to establish the food simulant that was most detrimental to the lacquer and substrate. This was found to be NaCl which was used for varied concentration analysis using adhesion testing. Leading on from this water uptake and corrosion studies were conducted to gain a better understanding of what is happening to the substrate chemically throughout the sterilisation process and during storage.

From initial characterisation studies, it can be concluded that:

- An increase in CrOx weight on the substrate resulted in an increase in failure force, however uniformity of the surface must be considered particularly with earlier generations of TCCT before process improvements were made.
- Varying the concentrations of NaCl simulant solutions confirmed that at low concentrations of NaCl the CrOx weight of the substrate has the greatest influence over the failure force of the lacquer. Conversely at high concentrations of NaCl, the salt had a much greater influence on the failure force independent of the CrOx weight/substrate type.
- Performance of ECCS/EP was consistently better than TCCT/BPANI.
- FTIR studies confirmed that a chemical reaction was not occurring between the polyester lacquer, BPANI, and the salt simulant solution. Mechanical water transport occurring through the porous BPANI lacquer was attributed to the performance that was observed.
- FTIR studies also showed that an increase in CrOx weight correlated with a decrease in the water uptake – due to the thicker and more homogenous CrOx layer it is more difficult for water to diffuse through the lacquer to the substrate
- EP and BPANI provide a sufficient level of corrosion protection for the underlying substrate regardless of the CrOx weight of the substrate
- For PVB coatings higher CrOx weight substrates had smaller areas of FFC supporting the theory that substrate performance and lacquer adhesion is improved at increasing CrOx weights.

The objective of chapter two was to study the impact of uniaxial strain on TCCT and ECCS substrates. Samples of ECCS and TCCT substrates were uniaxially deformed and analysed using scratch testing and SEM imaging. Further analysis of uniaxially strained samples was conducted using an oxide pin hole identification method which is explored in the final chapter. The conclusions from the uniaxial strain studies are:

- ECCS and TCCT 2021 substrates perform better at low strain values compared with older generations of TCCT. As strain was increased these values converged to a similar region.
- At higher salt solution concentrations, the presence of NaCl was the primary influencer over the strain rather than the substrate type in this instance.

- Lüder bands were observed on strained samples. As strain was increased, the number of bands and their depth increased.
- TCCT substrates had more defects on the surface than ECCS. Upon straining the increase in the number of defects on the ECCS surface was greater than the increase for TCCT. This suggests that TCCT substrates are less uniform than ECCS substrates at low strain. At high strain the uniformity of ECCS and TCCT is more similar.
- Several damage mechanisms are proposed due to uniaxial strain of the substrate such as cracking of the CrOx layer and loss of adhesion of the lacquer

The final chapter of work development a method to induce and quantify the strain within the samples whilst also being able to measure the adhesion of the lacquer. Further studies were conducted study the substrate surface of unlacquered TCCT and ECCS which included quantifying any defects in the surface. The chapter is concluded by a literature study which explores methods for elemental surface analysis.

- Comparative analysis of uniaxially and biaxially strained failure force showed that the adhesive failure forces of lacquered uniaxially strained samples were higher than that of biaxially strained samples at the same nominal strain value meaning they cannot be used interchangeably as testing methods.
- A biaxial strain study demonstrated that the performance of EP and BPANI coated substrates were consistent across all samples types. BPANI coated samples exhibited consistently lower failure forces compared with EP coated samples of the same substrate
- Pre-retort samples had the highest strain values with samples post-retort in DI water exhibiting similar trends - this remains consistent for with the outcomes of unstrained and uniaxial strain studies
- Samples retort in NaCl solution had lower adhesion values, reconfirming the detrimental effect that NaCl has on the substrate and lacquer as with previous chapters.
- The oxide pin hole identification method which adopted a Preece test demonstrated an increase in free metal on the substrate surface as strain was increased, this inference stands for all substrate types.

- TCCT 2021 performed better than TCCT 2019. All TCCT substrates were outperformed by ECCS.
- Uniaxial samples had less free metal on the surface than biaxial samples at the same numerical strain value meaning the methods are not interchangeable and biaxial strain has more of an influence on the surface than uniaxial strain – this correlates with the measured lacquer failure forces discussed previously where uniaxially strained samples exhibited higher lacquer failure forces than biaxially strained samples
- Defects are present on the surface of TCCT and ECCS but it is still not known whether these are chromium or iron.
- Two theories of Cr/CrOx coating homogeneity were proposed and literature research identified potential methods for investigating these theories, with the key aim being the ability to distinguish between chromium and iron on the substrate surface.

This research has demonstrated the suitability of novel TCCT substrates as an alternative to commercially available ECCS substrates. This is conditional, as the CrOx layer must be sufficient such that the substrate surface is homogenous and there are sufficient sites for lacquer adhesion. BPANI lacquers, as an alternative for EP lacquers show promise, however, they require improvements since their adhesion performance is consistently poorer, particularly when harsh food simulants are present.

Chapter Eight

Future Work

8 Recommendations for Future Work

The work conducted as part of this research has been examined and areas where further research would benefit and compliment the work that has already been completed were identified. Some of these suggestions are outlined below:

- 4.3 How the performance of the citric acid/NaCl would be altered if the free iron was not present on the surface of substrate – Ensure a defect free surface before conducting retort studies.
- 4.3 CrOx weight variation and its effect on lacquer adhesion have been studied in depth – how would the performances of TCCT substrates compare if the line speed/deposition current was altered and the CrOx weight kept constant.
- 4.4.2 Further work is required to understand how the different generations of TCCT substrates vary and what changes have been made to the surface to improve the performance of the material.
- 4.4.2 Study the surface roughness of newer generation TCCT substrates using techniques such as Atomic Force Microscopy or White Light Interferometry (120,179).
- 4.4 To achieve a truer reflection of the processes occurring within a food can this research could be repeated using the actual foodstuffs. Actual foodstuffs have a much more complex combination of chemicals some of which may counteract the effects of each other and reduce the impact this has on the lacquer adhesion and other material properties.
- 4.5 Quantify the water uptake in BPANI lacquer using methods such as Thermogravimetric Analysis or Atomic Force Microscopy Infrared Spectroscopy– trend this with CrOx weight - balance between production cost of thicker layer and performance (180,181)
- 4.6 FFC – cathodic delamination study to consider all factors influencing the substrate/lacquer
- 4.6 Repeat 0.01M FFC study with a lower humidity for clearer FFC worm like features
- 4.7 Establish the diffusion coefficients of the EP and BPANI lacquers using techniques such as EIS (182).

- 5.2 Use techniques such as XPS to study the strained surface and the surface chemistry changes that during straining when the CrOx layer cracks (172)
- 5.3 Study on depth of Lüder bands for strained samples using techniques such as Digital Image Correlation – is depth similar for ECCS and TCCT for higher strain values where their failure forces are similar (183).
- 6 Repeat work with actual food cans – no exposed edges so may find a reduction in water ingress for NaCl samples. May also find that if the strains were plotted on figure 6.8 that they may not correlate with the biaxial data and would take the research one step further in terms of accuracy. – not possible to do this in this research as sample supply is limited, sample sheets are too small, no can punch apparatus at the university
- 6.3 Biaxial strain study with Cr layer only – would give an understanding of whether the Cu nodule growth was only occurring on iron or chromium too
- 6.4 Future work on localised, high strain samples with hardness pen with samples more similar in shape to a traditional food can
- 6.5 The hypothesis of free Cr or Fe could be tested using large area XPS/TOF SIMS/EIS which can map areas up to a few mm² at a time– it could be used to map the Cr/CrOx surfaces before and after straining. It could identify defects in the surface post strain and establish whether Cr is present or Fe. If Cr is still present post strain, then it yields under strain if not then it splits with the CrOx (184).

Chapter Nine

Publications

9 Appendix 1 - Publications

1. Performance Assessment of Chromium Coated Packaging Steel Manufactured via a Cr(III) Processing Route

M. Dodd, E. Holding, C. Griffiths, E. Bluett, A. Mescall, K. Lammers, A. deVoosy, N. Wint, E. Jewell

RSC Applied Interfaces

(Submitted – In Review)

Chapter Ten

References

10 References

1. Mordor Intelligence. Metal Packaging Market Size & Share Analysis - Growth Trends & Forecasts (2024 - 2029) [Internet]. 2024. Available from: <https://www.mordorintelligence.com/industry-reports/metal-packaging-market>
2. Tikkanen A. Canning [Internet]. Encyclopaedia Britannica. 2019 [cited 2020 Apr 9]. p. 1–2. Available from: <https://www.britannica.com/topic/canning-food-processing>
3. Statista Research Department. Distribution of packaging demand worldwide in 2019, by material type. 2023.
4. Chen S. The coating layer structure of commercial chrome plates. *J Electron Spectros Relat Phenomena* [Internet]. 2015;202:1–6. Available from: <http://dx.doi.org/10.1016/j.elspec.2015.01.006>
5. Izzard CF, Müller DB. Tracking the devil's metal: Historical global and contemporary U.S. tin cycles. *Resour Conserv Recycl* [Internet]. 2010;54(12):1436–41. Available from: <http://dx.doi.org/10.1016/j.resconrec.2010.06.008>
6. Petry T, Knowles R, Meads R. An analysis of the proposed REACH regulation. *Regul Toxicol Pharmacol*. 2006;44(1):24–32.
7. Bott J, Störmer A, Albers P. Investigation into the release of nanomaterials from can coatings into food. *Food Packag Shelf Life* [Internet]. 2018;16(October 2017):112–21. Available from: <https://doi.org/10.1016/j.fpsl.2018.03.004>
8. Melvin C, Jewell E, de Vooy A, Lammers K, Murray NM. Surface and Adhesion Characteristics of Current and Next Generation Steel Packaging Materials. *J Packag Technol Res*. 2018;2(2):93–103.
9. Allman A, Jewell E, de Vooy A, Hayes R, McMurray HN. Food packaging simulant failure mechanisms in next generation steel packaging. *Packag Technol Sci*. 2019;1–15.
10. Allman, A., Jewell, E., de Vooy, A. & Hayes R. Inter-layer Adhesion Performance of Steel Packaging Materials for Food Cans Under Retort Conditions. *J Packag Technol Res* [Internet]. 2018;2:115–24. Available from: <http://cronfa.swan.ac.uk/Record/cronfa39600>
11. Paseiro-Cerrato R, Noonan GO, Begley TH. Evaluation of Long-Term Migration Testing from Can Coatings into Food Simulants: Polyester Coatings. *J Agric Food Chem*. 2016;64(11):2377–85.
12. Allman AM. Understanding and Improving the Post Retort Adhesion of BPANI Lacquers on Cr(III) Electroplated Steel. Swansea University; 2019.
13. Emblem, A. Emblem H. *Packaging Technology : Fundamentals, Materials and Processes*. 1st ed. Emblem A, Emblem H, editors. 2012. 1–600 p.
14. D'yakonov AA, Moleva ON, Mel'nikov YA, Nikiforov MA, Vakil'ev AF. Improving tinplate production. *Steel Transl*. 2012;42(3):253–4.

15. RPA. Environmental Risk Reduction Strategy and Analysis of Advantages and Drawbacks for Hexavalent Chromium Under Framework Contract: CPEC 24. 2005;(October):348.
16. Verdonck T, Verpoort P, De Strycker J, De Cleene A, Banerjee D, Nockemann P, et al. Chromium(iii) in deep eutectic solvents: Towards a sustainable chromium(vi)-free steel plating process. *Green Chem.* 2019;21(13):3637–50.
17. Aluminium Federation. Hexavalent Chromate/Chromium Trioxide EU Authorisation expires on 21/9/24 [Internet]. 2023 [cited 2024 Mar 19]. Available from: <https://alfed.org.uk/hexavalent-chromate-chromium-trioxide-eu-authorisation-expires-on-21-9-23/#:~:text=The existing Hexavalent Chromate%2FChromium,by a GB-held authorisation.>
18. Protsenko VS, Danilov FI. Chromium electroplating from trivalent chromium baths as an environmentally friendly alternative to hazardous hexavalent chromium baths: Comparative study on advantages and disadvantages. *Clean Technol Environ Policy.* 2014;16(6):1201–6.
19. LaKind JS. Can coatings for foods and beverages: Issues and options. *Int J Technol Policy Manag.* 2013;13(1):80–95.
20. Katz SA, Salem H. The toxicology of chromium with respect to its chemical speciation: A review. *J Appl Toxicol.* 1993;13(3):217–24.
21. Wijenberg JHOJ, Steegh M, Aarnts MP, Lammers KR, Mol JMC. Electrodeposition of mixed chromium metal-carbide-oxide coatings from a trivalent chromium-formate electrolyte without a buffering agent. *Electrochim Acta* [Internet]. 2015;173:819–26. Available from: <http://dx.doi.org/10.1016/j.electacta.2015.05.121>
22. Wint N, de Vooy ACA, McMurray HN. The corrosion of chromium based coatings for packaging steel. *Electrochim Acta.* 2016;203:326–36.
23. European Food Safety Authority. Scientific Opinion on the risks to public health related to the presence of bisphenol A (BPA) in foodstuffs. *Eur Food Saf Auth J.* 2015;13(1):3978.
24. Xia DH, Song SZ, Wang JH, Bi HC, Jiang YX, Han ZW. Corrosion behavior of tinplate in NaCl solution. *Trans Nonferrous Met Soc China (English Ed)* [Internet]. 2012;22(3):717–24. Available from: [http://dx.doi.org/10.1016/S1003-6326\(11\)61236-3](http://dx.doi.org/10.1016/S1003-6326(11)61236-3)
25. G. L. Robertson. *Food packaging: principles and practice.* 3rd ed. Boca Raton: Taylor & Francis; 2012. 195 p.
26. Morgan E. Tinplate Manufacture. In: *Tinplate & Modern Canmaking Technology.* 1st ed. 1985. p. 5–73.
27. Catalá R, Cabañes JM, Bastidas JM. An impedance study on the corrosion properties of lacquered tinplate cans in contact with tuna and mussels in pickled sauce. *Corros Sci.* 1998;40(9):1455–67.
28. Azzerri N, Splendorini L. Composition, Structure and Properties of Passivation Layers on Tinplate. [Internet]. *Thin Films Science and*

Technology. Elsevier B.V.; 1983. 707–712 p. Available from:
<http://dx.doi.org/10.1016/B978-0-444-42252-1.50109-0>

29. Yfantis D. A new, chrome-free passivation method of tinplate used in the canning industry. *Corrosion*. 2000;56(7):700–8.
30. Cova Caiazzo F, Brambilla L, Montanari A, Mischler S. Chemical and morphological characterization of commercial tinplate for food packaging. *Surf Interface Anal*. 2018;50(4):430–40.
31. Joseph JHO. Patent Application Publication Pub . No .: US 2016/0271610 A1. Vol. 1. 14/899,241, 2016. p. 1–7.
32. Chen YS, Huang C, Liu PY, Yen HW, Niu R, Burr P, et al. Hydrogen trapping and embrittlement in metals – A review. *Int J Hydrogen Energy*. 2024;1–33.
33. Melvin C, Jewell E, Miedema J, Lammers K, de Vooys A, Allman A, et al. Identifying interlayer surface adhesion failure mechanisms in tinplate packaging steels. *Packag Technol Sci*. 2019;32(7):345–55.
34. Fellows PJ. Part III. Processing by Application of Heat. In: Fellows PJ, editor. *Food Processing Technology: Principles and Practice*,. 4th ed. Woodhead Publishing Ltd.; 2017. p. 513–4.
35. Baral A, Engelken R. Modeling, Optimization, and Comparative Analysis of Trivalent Chromium Electrodeposition from Aqueous Glycine and Formic Acid Baths. *J Electrochem Soc*. 2005;152(7):C504.
36. Song YB, Chin DT. Current efficiency and polarization behavior of trivalent chromium electrodeposition process. *Electrochim Acta*. 2002;48(4):349–56.
37. Vykhodtseva LN, Edigaryan AA, Lubnin EN, Polukarov YM, Safonov VA. Composition, structure, and corrosion-electrochemical properties of chromium coatings deposited from chromium(III) electrolytes containing formic acid and its derivatives. *Russ J Electrochem*. 2004;40(4):387–93.
38. Survilienė S, Nivinskienė O, Češunienė A, Selskis A. Effect of Cr(III) solution chemistry on electrodeposition of chromium. *J Appl Electrochem*. 2006;36(6):649–54.
39. Khani H, Brennecke JF. Hard chromium composite electroplating on high-strength stainless steel from a Cr(III)-ionic liquid solution. *Electrochem commun [Internet]*. 2019;107(September):106537. Available from: <https://doi.org/10.1016/j.elecom.2019.106537>
40. Mohan S, Saravanan G, Renganathan NG. Comparison of chromium coatings and electrochemical behaviour with direct current and pulse current deposition in trivalent chromium formate urea bath as alternative to conventional Cr coatings. *Surf Eng*. 2011;27(10):775–83.
41. TATA Steel. Food [Internet]. 2021 [cited 2021 Jan 23]. Available from: <https://www.tatasteeleurope.com/ts/packaging/applications/food>
42. TATA Steel. TCCT® Trivalent chromium-coating technology [Internet]. 2021 [cited 2021 Jan 23]. Available from:

<https://www.tatasteeleurope.com/ts/packaging/products/tcct>

43. Ninčević A, Pezzani A, Squitieri G. Characterisation of different types of lacquers used in food packaging: Lacquer adhesion tests. *Acta Aliment.* 2007;36(1):27–37.
44. Manfredi LB, Ginés MJL, Benítez GJ, Egli WA, Rissone H, Vázquez A. Use of epoxy-phenolic lacquers in food can coatings: Characterization of lacquers and cured films. *J Appl Polym Sci.* 2005;95(6):1448–58.
45. Pilato LA. Phenolic Resins: A Century of Progress. In: Pilato LA, editor. *Phenolic Resins: A Century of Progress.* Heidelberg: Springer; 2010. p. 41–93.
46. Gardziella A, Pilato LA, Knop A. Phenolic Resins: Chemistry, Reactions, Mechanism. In: *Phenolic Resins.* Heidelberg: Springer Berlin; 2000. p. 24–82.
47. Geueke B. Dossier – Can coatings. *Food Packag Forum.* 2016;(December):1–10.
48. Barilli F, Fragni R, Gelati S, Montanari A. Study on the adhesion of different types of lacquers used in food packaging. *Prog Org Coatings.* 2003;46(2):91–6.
49. Zhao Y, Xu R, Xiao Y, Wang H, Zhang W, Zhang G. Mechanical Performances of Phenolic Modified Epoxy Resins at Room and High Temperatures. *Coatings.* 2022;12(643):1 to 12.
50. Miszczyk A, Darowicki K. Water uptake in protective organic coatings and its reflection in measured coating impedance. *Prog Org Coatings* [Internet]. 2018;124(February):296–302. Available from: <https://doi.org/10.1016/j.porgcoat.2018.03.002>
51. Clark J. Polyesters [Internet]. *Chemistry Libre Texts.* 2019 [cited 2020 Apr 5]. p. 1. Available from: [https://chem.libretexts.org/Bookshelves/Organic_Chemistry/Supplemental_Modules_\(Organic_Chemistry\)/Esters/Reactivity_of_Esters/Polyesters](https://chem.libretexts.org/Bookshelves/Organic_Chemistry/Supplemental_Modules_(Organic_Chemistry)/Esters/Reactivity_of_Esters/Polyesters)
52. Murthy N, Wilson S, Sy JC. Biodegradation of Polymers. In: Matyjaszewski K, Möller M, editors. *Polymer Science: a Comprehensive Reference: Volume 1-10.* Elsevier; 2012. p. 547–60.
53. Farag AA. Applications of nanomaterials in corrosion protection coatings and inhibitors. *Corros Rev.* 2020;38(1):67–86.
54. Lestido-cardama A, Sendón R, Bustos J, Quirós AR De, Nieto MT. Food and beverage can coatings : A review on chemical analysis, migration, and risk assessment. *Compr Rev Food Sci Food Saf.* 2022;(January):1–54.
55. Turner TA. Coating technologies and application methods. In: *Canmaking.* Boston: Springer US; 1998. p. 82–131.
56. The International Tin Association. DI and DRD Tin Cans [Internet]. 2020 [cited 2024 Nov 7]. Available from: <https://www.worldofsteel.com/pages/di-and-drd-tin-cans/#:~:text=Line speeds for DRD are,ratio of the container required>.

57. Page B. Rigid metal packaging. In: Emblem A, Emblem H, editors. *Packaging Technology: Fundamentals, Materials and Processes*. Woodhead Publishing Ltd.; 2012. p. 122–62.
58. Simal-Gándara J. Selection of can coatings for different applications. *Food Rev Int*. 1999;15(1):121–37.
59. Shantou Light Industrial Machinery Factory Co. L. Three-Piece Can Production Line [Internet]. 2024 [cited 2024 Nov 7]. Available from: <http://canbodymakingline.com/three-piece-can-production-line.html#:~:text=Currently%2C a can-body combined,maximum speed of 500 CPM.>
60. Morgan E. Canmaking Processes. In: *Tinplate & Modern Canmaking Technology* [Internet]. 1985. p. 107–45. Available from: <https://doi.org/10.1016/B978-0-08-028680-8.50011-47>
61. Ebnesajjad S, Ebnesajjad S. Chapter 5 – Theories of Adhesion. In: *Surface Treatment of Materials for Adhesive Bonding* [Internet]. 2014. p. 77–91. Available from: <http://dx.doi.org/10.1016/B978-0-323-26435-8.00005-8>
62. Petrie EM. Plastics and Elastomers in Adhesives. In: Harper CA, editor. *Handbook of Plastics, Elastomers, and Composites*. 4th ed. The McGraw-Hill Companies; 2002.
63. Wypych G. Mechanisms of Adhesion. In: *Handbook of Adhesion Promoters*. 1st ed. ChemTec Publishing; 2018. p. 5–44.
64. Packham DE. Surface energy, surface topography and adhesion. *Int J Adhes Adhes*. 2003;23(6):437–48.
65. Bishop CA. Adhesion and Adhesion Tests. In: *Vacuum Deposition Onto Webs, Films and Foils*. 3rd ed. William Andrew; 2015. p. 197–208.
66. Jagannadham K, Marcinkowski MJ. Relationship between surface tension and energy, interfacial energy and lattice friction. *J Mater Sci*. 1979;14(7):1717–32.
67. Deák T. Food Technologies: Sterilization. *Encycl Food Saf*. 2014;3:245–52.
68. Deflorian F, Rossi S. The role of ions diffusion in the cathodic delamination rate of polyester coated phosphatized steel. *J Adhes Sci Technol*. 2003;17(2):291–306.
69. Roy S, Xu WX, Park SJ, Liechti KM. Anomalous Moisture Diffusion in Viscoelastic Polymers : Modeling. *J Appl Mech*. 2000;67(June):391–6.
70. Marais S, Metayer M, Labbe M. Water Diffusion in Unsaturated Polyester Films . Effect of Plasticization on the Glass Transition. *Polym Eng Scince*. 1999;39(8):1508–16.
71. Tomachuk CR, Elsner CI, Di Sarli AR, Ferraz OB. Corrosion resistance of Cr(III) conversion treatments applied on electrogalvanised steel and subjected to chloride containing media. *Mater Chem Phys*. 2010;119(1–2):19–29.
72. Lewis, P. L. Kolody MC, J. Alternative to Nitric Acid for Passivation of

- Stainless Steel Alloys. *J Chem Inf Model*. 2013;53(9):1689–99.
73. Boelen B, Den Hartog H, Van der Weijde H. Product performance of polymer coated packaging steel, study of the mechanism of defect growth in cans. *Prog Org Coatings*. 2004;50(1):40–6.
 74. Ganjeh M, Jafari SM, Amanjani M, Katouzian I. Modeling corrosion trends in tin-free steel and tinplate cans containing tomato paste via adaptive-network-based fuzzy inference system. *J Food Process Eng*. 2017;40(6):1–8.
 75. Bellido-González V, Stefanopoulos N, Deguilhen F. Friction monitored scratch adhesion testing. *Surf Coatings Technol*. 1995;74–75(PART 2):884–9.
 76. BSI. BS EN ISO 1518-1:2023 Paints and varnishes. Determination of scratch resistance. Constant-loading method. 2023.
 77. Laugier M. The development of the scratch test technique for the determination of the adhesion of coatings. *Thin Solid Films*. 1981;76(3):289–94.
 78. Sekler J, Steinmann PA, Hintermann HE. The scratch test: Different critical load determination techniques. *Surf Coatings Technol*. 1988;36(1–2):519–29.
 79. Burnett PJ, Rickerby DS. The scratch adhesion test: An elastic-plastic indentation analysis. *Thin Solid Films*. 1988;157(2):233–54.
 80. BSI. BS EN ISO 22557:2020 Paints and varnishes. Scratch test using a spring-loaded pen. 2021.
 81. TQC Sheen. TQC Hardness test. 2024.
 82. ASTM. Standard Test Methods for Measuring Adhesion by Tape Test. 2012. p. 1–8.
 83. Lausmann GA. Electrolytically deposited hardchrome. *Surf Coatings Technol*. 1996;86–87:814–20.
 84. ISO. Metallic materials — Rockwell hardness test — Part 1: Test method [Internet]. ISO 6508-1:2016. 2016 [cited 2020 Apr 24]. p. 32. Available from: <https://www.iso.org/obp/ui/#iso:std:iso:6508:-1:ed-4:v1:en>
 85. Hosford WF. Stress and Strain. In: *Fundamentals of Engineering Plasticity* [Internet]. Cambridge University Press; 2013. p. 11–9. Available from: <https://ebookcentral.proquest.com/lib/swansea-ebooks/detail.action?docID=1139751>.
 86. Liang A, Ni L, Liu Q, Zhang J. Structure characterization and tribological properties of thick chromium coating electrodeposited from a Cr(III) electrolyte. *Surf Coatings Technol* [Internet]. 2013;218(1):23–9. Available from: <http://dx.doi.org/10.1016/j.surfcoat.2012.12.021>
 87. Hodgkinson JM. Testing the strength and stiffness of polymer matrix composites. In: Robinson P, Greenhalgh E, Pinho S, editors. *Failure Mechanisms in Polymer Matrix Composites*. Woodhead Publishing Ltd.; 2012. p. 129–82.
 88. Brown DW, Bourke MAM, Clausen B, Holden TM, Tomé CN, Varma R. A

neutron diffraction and modeling study of uniaxial deformation in polycrystalline beryllium. *Metall Mater Trans A Phys Metall Mater Sci.* 2003;34 A(7):1439–49.

89. Pineau A. Fatigue (Multiaxial) Testing. In: *Encyclopedia of Materials: Science and Technology*. Elsevier Science Ltd.; 2001. p. 2944–6.
90. Quaak G. Biaxial testing of sheet metal : An experimental-numerical analysis. *Eng Thesis Committe.* 2008;23–8.
91. Kang J, Wilkinson DS, Bruhis M, Jain M, Wu PD, Embury JD, et al. Shear localization and damage in AA5754 aluminum alloy sheets. *J Mater Eng Perform.* 2008;17(3):395–401.
92. Sorce FS, Ngo S, Lowe C, Taylor AC. Quantification of coating surface strains in Erichsen cupping tests. *J Mater Sci [Internet].* 2019;54(10):7997–8009. Available from: <https://doi.org/10.1007/s10853-019-03392-0>
93. Xiao R. A Review of Cruciform Biaxial Tensile Testing of Sheet Metals. *Exp Tech.* 2019;43(5):501–20.
94. Carrado, A. Sprauel, J. Barrallier, L. Lodini A. Residual Stress Measurements at the Metal/Ceramic Interface Using Modelling of Neutron Diffraction Spectrometer. In: *Recent Advances in Experimental Mechanics [Internet]*. Dordrecht: Springer; 2002. p. 487–94. Available from: https://doi.org/10.1007/0-306-48410-2_46
95. Bunn JR, Penumadu D, Lou X, Hubbard CR. Effect of multi-axial loading on residual strain tensor for 12114 steel alloy. *Metall Mater Trans A Phys Metall Mater Sci.* 2014;45(9):3806–13.
96. Sprauel JM. Stress evaluation by neutron diffraction: Modelling of a two-axis spectrometer. *J Neutron Res.* 2001;9(2–4):449–57.
97. Davydov V, Lukáš P, Strunz P, Kužel R. Evolution of internal stresses in the plain ferritic steel studied by neutron diffraction in situ upon tensile straining. *J Phys Condens Matter.* 2009;21(9).
98. Ghadbeigi H, Pinna C, Celotto S. Quantitative Strain Analysis of the Large Deformation at the Scale of Microstructure: Comparison between Digital Image Correlation and Microgrid Techniques. *Exp Mech.* 2012;52(9):1483–92.
99. Delaire F, Raphanel JL, Rey C. Plastic heterogeneities of a copper multicrystal deformed in uniaxial tension: Experimental study and finite element simulations. *Acta Mater.* 2000;48(5):1075–87.
100. M. Obata, Shimada H, Kawasaki A. Fine-grid method for large-strain analysis near a notch Tip. *Exp Mech.* 1983;23:146–51.
101. Boone PM. NDT Techniques : Laser-based. In: *Encyclopedia of Materials: Science and Technology*. 2001. p. 6018–21.
102. Mohan NK, Rastogi P. Recent developments in digital speckle pattern interferometry. *Opt Lasers Eng.* 2003;40:439–45.

103. Almeida E, Costa MR, De Cristofaro N, Mora N, Catalá R, Puente JM, et al. Titanium passivated lacquered tinplate cans in contact with foods. *Corros Eng Sci Technol*. 2005;40(2):158–64.
104. McMurray HN, Williams G, Emeraldine EB. 2.14 Under Film/Coating Corrosion. In: Cottis B, Graham M, Lindsay R, Lyon S, Richardson T, Scantlebury D, et al., editors. *Shreir's Corrosion* [Internet]. 2nd ed. Elsevier B.V.; 2010. p. 988–1004. Available from: 10.1016/B978-044452787-5.00040-8
105. Koehler EL. The Influence of Contaminants on the Failure of Protective Organic Coatings on Steel. *Corrosion*. 1977;33(6):209–17.
106. Bautista A. Filiform corrosion in polymer-coated metals. *Prog Org Coatings*. 1996;28:49–58.
107. Ruggeri RT, Beck TR. Analysis of Mass Transfer in Filiform Corrosion. *Corrosion*. 1983;39(11):452–65.
108. Vacandio F, Massiani Y, Gravier P, Rossi S, Bonora PL, Fedrizzi L. New knowledge on localized corrosion obtained from local measuring techniques. *Electrochim Acta*. 2001;46(24–25):3641–50.
109. Grassino AN, Grabarić Z, Pezzani A, Squitieri G, Berković K. Corrosion inhibition with different protective layers in tinplate cans for food preservation. *J Sci Food Agric*. 2010;90(14):2419–26.
110. Melvin C. *Fundamentals of Adhesion for Steel*. Swansea University; 2017.
111. Man CMD. Food storage trials. In: *The Stability and Shelf Life of Food* [Internet]. 2nd ed. Elsevier Ltd; 2016. p. 171–98. Available from: <http://dx.doi.org/10.1016/B978-0-08-100435-7.00006-X>
112. Newswire PR, York N, York N. *Global Food and Beverage Metal Can Market*. 2020;20–2.
113. Deshwal GK, Panjagari NR. Review on metal packaging: materials, forms, food applications, safety and recyclability. *J Food Sci Technol* [Internet]. 2020;57(7):2377–92. Available from: <https://doi.org/10.1007/s13197-019-04172-z>
114. Canned Food UK. Recycling [Internet]. 2024 [cited 2024 Mar 19]. Available from: <https://www.cannedfood.co.uk/recycling/>
115. Recycle More. Recycling Facts [Internet]. 2024 [cited 2024 Mar 19]. Available from: <https://www.recycle-more.co.uk/what-can-i-recycle/recycling-facts>
116. Güvenç O, Lizarde R, Tasan CC. Solid-state steelmaking by scrap consolidation: A processing pathway with minimal energy and CO₂ burdens. *J Clean Prod* [Internet]. 2024;452(August 2023):1–14. Available from: <https://doi.org/10.1016/j.jclepro.2024.141976>
117. Ossberger M. Food migration testing for food contact materials. Baughan JS, editor. *Global Legislation for Food Contact Materials: Processing, Storage and Packaging*. Elsevier Science Ltd.; 2015. 4–41 p.

118. Whiteside J, Vooy's ACA De, Sackett E, McMurray HN. Influence of Uniaxial Deformation on Surface Morphology and Corrosion Performance of Trivalent Chromium Based Coatings for Packaging Steels. *Corros Sci* [Internet]. 2021;(March):109662. Available from: <https://doi.org/10.1016/j.corsci.2021.109662>
119. Pro Plate. What role does current density play in determining and controlling the thickness of coatings in electroplating? [Internet]. [cited 2024 Jul 20]. Available from: <https://www.proplate.com/what-role-does-current-density-play-in-determining-and-controlling-the-thickness-of-coatings-in-electroplating/#:~:text=The current density is one,concentration of the electrolyte solution.>
120. Dodd M. The Adhesion of Protective Coatings to Novel REACH Compliant Packaging Steel Substrates. Swansea University; 2023.
121. R K Print-Coat Instruments Ltd. K Control Coater. Prod Data Sheet [Internet]. 2012;1–4. Available from: <http://www.rkprint.com/pdfs/kcontrolcoater.pdf>
122. Holo East. Meyer Rod Coating [Internet]. Adhesive Coating Equipment. 20204 [cited 2024 Feb 16]. Available from: <https://www.holoeast.com/machines/coating/adhesive-coating-Meyer-Bar.html>
123. Kopeliovich D. Adhesion Tests [Internet]. 2014 [cited 2023 Mar 31]. Available from: https://www.substech.com/dokuwiki/doku.php?id=adhesion_tests
124. Costa M, Santos M, Diamantino T. FTIR, a powerful technique in organic coatings failure diagnosis. *Eur Corros Congr*. 2011;30(2):57–64.
125. Kawagoe M, Hashimoto S, Nomiya M, Morita M, Qiu J, Mizuno W, et al. Effect of water absorption and desorption on the interfacial degradation in a model composite of an aramid fibre and unsaturated polyester evaluated by Raman and FT infra-red microspectroscopy. *J Raman Spectrosc*. 1999;30(10):913–8.
126. Morsch S, Lyon S, Gibbon SR. The degradation mechanism of an epoxy-phenolic can coating. *Prog Org Coatings*. 2017;102:37–43.
127. Mitchell G, France F, Nordon A, Tang PL, Gibson LT. Assessment of historical polymers using attenuated total reflectance-Fourier transform infrared spectroscopy with principal component analysis. *Herit Sci*. 2013;1(1):1–10.
128. Agilent. ATR-FTIR Spectroscopy [Internet]. 2024 [cited 2024 Feb 17]. Available from: <https://www.agilent.com/en/product/molecular-spectroscopy/ftir-spectroscopy/atr-ftir-spectroscopy#:~:text=In ATR sampling%2C the infrared,where it can be absorbed.>
129. Wikipedia. Attenuated Total Reflectance [Internet]. 2023 [cited 2024 Jul 1]. Available from: https://en.wikipedia.org/wiki/Attenuated_total_reflectance
130. Hayes PA, Vahur S, Leito I. ATR-FTIR spectroscopy and quantitative multivariate analysis of paints and coating materials. *Spectrochim Acta - Part*

- A Mol Biomol Spectrosc [Internet]. 2014;133:207–13. Available from: <http://dx.doi.org/10.1016/j.saa.2014.05.058>
131. Wint N, Eaves D, Williams G, McMurray HN. The effect of composition and thickness on the mechanism and kinetics of filiform corrosion occurring on zinc-aluminium-magnesium coated steel. Corros Sci [Internet]. 2021;179(September 2020):109168. Available from: <https://doi.org/10.1016/j.corsci.2020.109168>
 132. Slabaugh, W. H. Grotheer M. Mechanism of Filiform Corrosion. Ind Eng Chem. 1954;46(5):1014–6.
 133. Williams G, McMurray HN. The mechanism of group (I) chloride initiated filiform corrosion on iron. Electrochem commun. 2003;5:871–7.
 134. ISO. BS EN ISO 6892-1:2019 Metallic materials. Tensile testing. Method of test at room temperature. 2020.
 135. Kamiura T, Takahashi S. Study on effect of strain rate on elongation in advanced high strength steel. Procedia Eng [Internet]. 2017;207:1988–93. Available from: <https://doi.org/10.1016/j.proeng.2017.10.1097>
 136. Zhang X, Boelen B, Beentjes P, Mol JMC, Terryn H, de Wit JHW. Influence of uniaxial deformation on the corrosion performance of pre-coated packaging steel. Prog Org Coatings. 2007;60(4):335–42.
 137. Groesbeck EC, Walkup HH. Preece Test (Copper-Sulphate Dip) For Zinc Coatings. Bur Stand J Res. 1934;12:785–802.
 138. Morsch S, Lyon S, Smith SD, Gibbon SR. Mapping water uptake in an epoxy-phenolic coating. Prog Org Coatings [Internet]. 2015;86:173–80. Available from: <http://dx.doi.org/10.1016/j.porgcoat.2015.05.017>
 139. Allman A, Whiteside J, Jewell E, Griffiths C, McMurray N, de Vooy A. Surface modification of Cr(III) packaging substrates for enhanced adhesion via citric acid processing. Surfaces and Interfaces. 2020;20:1–9.
 140. Yaro AS, Khadom AA, Wael RK. Apricot juice as green corrosion inhibitor of mild steel in phosphoric acid. Alexandria Eng J [Internet]. 2013;52(1):129–35. Available from: <http://dx.doi.org/10.1016/j.aej.2012.11.001>
 141. Nouha M, Veys-renaux D, Rocca E, Ioannou I. Corrosion inhibition of carbon steel in acidic medium by orange peel extract and its main antioxidant compounds. Eval Program Plann [Internet]. 2020;102(2016):55–62. Available from: <http://dx.doi.org/10.1016/j.corsci.2015.09.017>
 142. Clark J. 15.9 Hydrolysis of Esters [Internet]. Chemistry Libre Texts. 2021. p. 9–11. Available from: <https://chem.libretexts.org/@go/page/68163>
 143. Sammon C, Yarwood J, Everall N. FT-IR study of the effect of hydrolytic degradation on the structure of thin PET films. Polym Degrad Stab. 2000;67(1):149–58.
 144. Jung JH, Ree M, Kim H. Acid- and base-catalyzed hydrolyses of aliphatic polycarbonates and polyesters. Catal Today. 2006;115(1–4):283–7.

145. Cheong Z, Sorce FS, Ngo S, Lowe C, Taylor AC. The effect of substrate material properties on the failure behaviour of coatings in the Erichsen cupping test. *Prog Org Coatings* [Internet]. 2021;151(June 2020):106087. Available from: <https://doi.org/10.1016/j.porgcoat.2020.106087>
146. Choi J, Cho M, Choi J, Cho M. Computational IR spectroscopy of water : OH stretch frequencies , transition dipoles , and intermolecular vibrational coupling constants Computational IR spectroscopy of water : OH stretch frequencies , transition dipoles , and intermolecular vibrational. *J Chem Phys*. 2013;138(17).
147. Brubach J, Mermet A, Filabozzi A, Gerschel A, Roy P. Signatures of the hydrogen bonding in the infrared bands of water. *J Chem Phys*. 2005;122(18).
148. Daimay Lin-Vien, Norman B. Colthup, William G. Fateley JGG. Compounds Containing the Carbonyl Group. In: *The Handbook of Infrared and Raman Characteristic Frequencies of Organic Molecules*. 1900. p. 117–54.
149. Parekh VJ, Rathod VK, Pandit AB, Technology C. Substrate Hydrolysis : Methods , Mechanism , and Industrial Applications of Substrate Hydrolysis. In: *Comprehensive Biotechnology* [Internet]. Second Edi. Elsevier B.V.; 2011. p. 103–18. Available from: <http://dx.doi.org/10.1016/B978-0-08-088504-9.00094-5>
150. Edy JE, McMurray HN, Lammers KR, Arnoud CA. Kinetics of corrosion-driven cathodic disbondment on organic coated trivalent chromium metal-oxide-carbide coatings on steel. *Corros Sci* [Internet]. 2019;157(January):51–61. Available from: <https://doi.org/10.1016/j.corsci.2019.04.037>
151. Cambier SM, Frankel GS. Filiform Corrosion of Polyvinyl Butyral- and Bisphenol A-Based Epoxy-Coated Steel After Standard Laboratory Exposures. *Corrosion*. 2014;70(12):1230–7.
152. Arauz-Moreno C, Piroird K, Lorenceau E. Water Clustering in Polyvinyl Butyral (PVB): Evidenced by Diffusion and Sorption Experiments. *J Phys Chem*. 2023;127:11064–73.
153. Hall EO. Yield Point Phenomena and their Theoretical Background. In: *Yield Point Phenomena in Metals and Alloys*. 1970. p. 1–64.
154. Danilov VI, Gorbatenko V V., Zuev LB, Orlova D V., Danilova L V. Luders deformation of low-carbon steel. *Steel Transl*. 2017;47(10):662–8.
155. Gikas J. Lüders Bands Phenomenon in ASTM E8 Tensile Testing [Internet]. 2019 [cited 2024 Mar 11]. Available from: <https://www.admet.com/blog/luders-bands-phenomenon-in-astm-e8-tensile-testing/>
156. Wu Y, Recklin V, Groche P. Strain induced surface change in sheet metal forming: Numerical prediction, influence on friction and tool wear. *J Manuf Mater Process*. 2021;5(2).
157. Brlić T, Rešković S, Jandrlić I, Skender F. Influence of strain rate on stress changes during Lüders bands formation and propagation. *IOP Conf Ser Mater Sci Eng*. 2018;461(1).

158. Corrosionpedia. Surface Defects [Internet]. 2021 [cited 2024 Jan 19]. Available from: <https://www.corrosionpedia.com/definition/1614/surface-defects#:~:text=Surface defects may cause corrosion,corrosion resistance and mechanical properties.>
159. Singh J, Kim MS, Lee SE, Kim EY, Kang JH, Park JH, et al. Heterogeneity in deformation and twinning behaviors through the thickness direction in E-form Mg alloy sheets during an Erichsen test. *Mater Sci Eng A* [Internet]. 2018;729(May):370–84. Available from: <https://doi.org/10.1016/j.msea.2018.05.072>
160. Erichsen. Erichsen Cupping Test [Internet]. 2024 [cited 2024 May 9]. Available from: <https://www.erichsen.de/en-gb/service/test-methods/sheet-metal-testing/erichsen-cupping-test>
161. BSOL. BS EN ISO 20482:2013 Metallic materials. Sheet and strip. Erichsen cupping test. BSI; 2013.
162. BSI. BS EN ISO 20482:2003 Metallic Materials - Sheet and Strip - Erichsen Cupping Test. 2003. p. 1–8.
163. Słowik M, Cępa P, CZAPLA K, Zabiński P. Steel packaging production process and a review of new trends. *Arch Metall Mater*. 2021;66(1):135–43.
164. Zumelzu E, Rull F, Boettcher AA. Deformation and fracture of polymer coated metal sheets: Characterisation and degradation. *Surf Eng*. 2006;22(6):432–8.
165. Van Der Aa MAH, Schreurs PJG, Baaijens FPT. Modelling of the wall ironing process of polymer coated sheet metal. *Mech Mater*. 2001;33(10):555–72.
166. Reinhart W. Formability of Polymer-Coated Metals. Swansea University; 2021.
167. Leng, A. Streckel, H. Stratmann M. The delamination of polymeric coatings from steel. *Corros Sci*. 1999;41:579–97.
168. Curtzweiler GW, Williams EB, Maples AL, Wand SW, Rawlins JW. Understanding the influence of water hydrogen bonding on the cathodic delamination rate of coated steel substrates from pre-exposure characterization. *Corros Sci* [Internet]. 2019;151(January):198–205. Available from: <https://doi.org/10.1016/j.corsci.2019.01.026>
169. Zumelzu E, de Melo HG, Di Sarli AR, Tomachuk CR. Effect of passivation treatment on adhesion and protective properties of steel coated with polymeric film. *Mater Sci Forum*. 2018;930 MSF:422–7.
170. Stevie FA, Donley CL. Introduction to x-ray photoelectron spectroscopy. *J Vac Sci Technol A*. 2020;38(6).
171. Moulder JF, Stickle WF, Sobol PE, Bomben KD. Handbook of X-ray Photoelectron Spectroscopy. Chastain J, editor. Minnesota: Perkin-Elmer Corporation; 1992. p. 1–29.
172. Krishna DNG, Philip J. Review on surface-characterization applications of X-

- ray photoelectron spectroscopy (XPS): Recent developments and challenges. Appl Surf Sci Adv [Internet]. 2022;12(June). Available from: <https://doi.org/10.1016/j.apsadv.2022.100332>
173. Fadley CS. X-Ray Photoelectron Spectroscopy. Prog Surf Sci. 2010;85(7–8):293–330.
 174. Mogawak DW. Time-of-Flight Secondary Ion Mass Spectrometry (ToF-SIMS) [Internet]. Instruments and Methods Common to Nanotechnology. 2024 [cited 2024 Mar 14]. Available from: [https://serc.carleton.edu/msu_nanotech/methods/ToF-SIMS.html#:~:text=Fundamental Principles of Time-of,Mass Spectrometry \(ToF-SIMS\)&text=ToF-SIMS uses a focused,ions \(positive or negative\).](https://serc.carleton.edu/msu_nanotech/methods/ToF-SIMS.html#:~:text=Fundamental Principles of Time-of,Mass Spectrometry (ToF-SIMS)&text=ToF-SIMS uses a focused,ions (positive or negative).)
 175. Benninghoven A, Powell CJ, Rauh RD. Secondary Ion Mass Spectrometry: Basic Concepts, Instrumental Aspects, Applications and Trends. New York: John Wiley and Sons; 1987.
 176. Lazanas AC, Prodromidis MI. Electrochemical Impedance Spectroscopy - A Tutorial. ACS Meas Sci. 2023;3:162–93.
 177. Magar HS, Hasaan RYA, Mulchandani A. Electrochemical Impedance Spectroscopy (EIS): Principles, Construction, and Biosensing Applications. Sensors. 2021;21(6578).
 178. Bard AJ, Faulkner LR. Electrochemical Methods: Fundamentals and Applications. 2nd ed. Wiley; 2001.
 179. Smith JR, Breakspear S, Campbell SA. AFM in Surface Finishing: Part II. Surface Roughness. Trans IMF. 2017;81(3):55–8.
 180. Morsch S, Lyon S, Greensmith P, Smith SD, Gibbon SR. Mapping water uptake in organic coatings using AFM-IR. Faraday Discuss [Internet]. 2015;180:527–42. Available from: <http://dx.doi.org/10.1039/C4FD00229F>
 181. Son A, Causse N, Musiani M, Orazem ME, Pébère N, Tribollet B, et al. Determination of water uptake in organic coatings deposited on 2024 aluminium alloy : Comparison between impedance measurements and gravimetry. Prog Org Coatings [Internet]. 2024;112(June 2017):93–100. Available from: <http://dx.doi.org/10.1016/j.porgcoat.2017.07.004>
 182. Nguyen TQ, Breitenkopf C. Determination of Diffusion Coefficients Using Impedance Spectroscopy Data. J Electrochem Soc. 2018;165:826–31.
 183. Qiu H, Inoue T, Ueji R. Experimental measurement of the variables of Lüders deformation in hot-rolled steel via digital image correlation. Mater Sci Eng A [Internet]. 2020;790(April):139756. Available from: <https://doi.org/10.1016/j.msea.2020.139756>
 184. Krishna DNG, Philip J. Review on surface-characterization applications of X-ray photoelectron spectroscopy (XPS): Recent developments and challenges. Appl Surf Sci Adv [Internet]. 2022;12(June):100332. Available from: <https://doi.org/10.1016/j.apsadv.2022.100332>